Seasonal cold hardiness, deacclimation kinetics, and dormancy completion in cold-climate hybrid grapevine

By

Michael Geiger North

A dissertation submitted in partial fulfillment of
the requirements for the degree of

Doctor of Philosophy
(Horticulture)

at the
UNIVERSITY OF WISCONSIN-MADISON
2021

Date of final oral examination: 06/29/2021

The dissertation is approved by the following members of the Final Oral Committee:
Amaya Atuchua, Professor, Horticulture
Jiwan Palta, Professor, Horticulture
Paul Bethke, Professor, Horticulture
Katherine McCulloh, Professor, Botany

to the grapevines
and their future students

Acknowledgements

First and foremost, thanks to Amaya Atucha for supporting my graduate work, introducing me to the study of plant cold hardiness, and inspiring my interests to wander and grow as much as the grapevines I studied. A huge thank you to my committee, Jiwan Palta, Paul Bethke, and Kate McCulloh for the knowledge, time, and guidance you have shared with me. Special thanks to Jiwan Palta for waiting until 2018 to host the International Plant Cold Hardiness Seminar in a glorious and convenient city. Thanks to the wonderful administrative staff in the Horticulture Department, Tricia Check, Ellen Anlauf, Natalie Ben-Zikri, Thomas Frank, and Kathryn Jones. Your patience and positive energy are stunning, especially in light of my many questions over the years. Thank you to Janet Hedtcke, Rodney Denu, and the West Madison Agricultural Research Station staff. You cultivated a welcoming and inspiring work environment. Thank you to all the members of the Fruit Crops Research and Extension Lab, past and present. Sincere thanks to Beth Workmaster for braving the vineyard in snow and ice no matter how cold it was, for all the thought-provoking conversations, and especially for listening when I needed to share. And to Camilo Villouta for your comradery and "let's do this" attitude. A generous thank you to Maria Kamenetsky for sharing your statistical expertise, teaching me coding tricks, taking time for meaningful check-ins, and for googling on occasion. I would also like to thank Sara Patterson. I would not be where I am today without all the yeses you shared with me. A special thank you to Abbey Thompson and the entire SciMed Graduate Research Scholars community. I could always count on being energized by my SciMed peers. Thank you to my all my friends and family near and far. I am continuously grateful for your unwavering love and support. To Maple and Luna for reminding me to be present and to get outside. Most importantly, thank you Kim and Linden, you ground me in happiness always and in all ways.

Table of Contents

Dedication ..... **i**

Acknowledgements ..... **ii**

Table of Contents ..... **iii**

Thesis abstract ..... **v**

Chapter 1: Literature review **1**

Grapevines 1
Dormancy in woody perennials 2
Freezing and freeze injury 6
Survival strategies 8
Understanding and measuring deep supercooling 9
Seasonal changes of cold hardiness 12
Literature Cited 14

Chapter 2: Cold hardiness of cold-climate interspecific hybrid grapevines grown in a cold-climate region **22**

Abstract 23
Introduction 24
Materials and Methods 26
Results 33
Discussion 37
Conclusion 42
Literature Cited 44
Tables 44
Figures 52

Chapter 3: The effect of ambient temperature and chill unit accumulation on deacclimation kinetics **56**

Abstract 56
Introduction 57
Materials and Methods 60
Results 66
Discussion 68
Conclusion 75
Literature Cited 78
Tables 78
Figures 88

Chapter 4: Dormancy completion in cold-climate hybrid grapevines: considering the role of freezing temperatures and contextual implications of cold hardiness evaluation **95**

Abstract....95
Introduction....97
Materials and Methods....99
Results....103
Discussion....105
Conclusion....110
Literature Cited....112
Tables....116
Figures....119

Chapter 5: General conclusions....126

Appendix A: Supplemental material – Chapter 3....130

Appendix B: Imaging callose at plasmodesmata in the apex of dormant bud meristems with confocal microscopy....134

Background....134
Materials and Methods....135
Summary....137
Literature Cited....138
Figures....139

Thesis abstract

Dormancy and cold hardiness are critical adaptations for temperate woody perennial species to survive winter freezing stress. Grapevine (*Vitis* spp.) buds avoid freeze injury by supercooling water in their buds, which is a seasonally dynamic process and is related to dormancy mechanisms. There is high variability in traits related to dormancy and cold hardiness across grapevine species. Grapevine breeders have developed interspecific hybrid grapevine cultivars that combine desirable fruit quality and cold hardiness traits. These hybrids, referred to as cold-climate cultivars, have propelled the expansion of grapevine production into regions that were previously limited by annual low temperatures. However, cold-climate cultivars are still susceptible to freeze injury. Moreover, climate change predictions indicate new winter challenges, such as erratic and extreme weather events and generally warmer winter weather. Therefore, more information regarding cold hardiness and dormancy traits in cold-climate cultivars is needed. The research targeted in this dissertation aimed to characterize important dormancy and cold hardiness traits in five cold-climate cultivars.

The lower temperature limit for bud cold hardiness changes across the seasons. Continuous, time-series cold hardiness data were collected to establish a foundation for cold hardiness abilities in individual cold-climate cultivars. The research presented in Chapter 2 characterized changes in bud cold hardiness for five cold-climate cultivars to identify relative risk for freeze injury throughout the dormant period and the factors regulating cold hardiness changes. This research also optimized and evaluated a bud cold hardiness prediction model for the same cultivars grown in a cold-climate region. We determined ambient temperature is the most important factor that regulates hybrid grapevine cold hardiness changes, and cultivars respond to temperature signals at varying degrees. We also calculated highly accurate cold

hardiness predictions after reparametrizing a prediction model for each cold-climate cultivar. This information can guide cultivar selection decisions for particular growing regions and provides a framework for future studies concerning the physiological and mechanistic processes of grapevine cold hardiness. In addition, this work can strengthen decision making for improved bud cold hardiness protection, especially in cold-climate growing regions.

The loss of cold hardiness i.e., deacclimation during spring is one of the most critical causes of freeze injury and is a determinant of budbreak phenology. Research presented in Chapter 3 evaluated the effect of chill unit accumulation and ambient temperature on dormancy status, deacclimation responses, and budbreak in five cold-climate cultivars grown in a cold climate region. In addition, this research validated a method for quantifying the contribution of chill unit accumulation to dormancy transitions. We observed deacclimation responses that increased continuously as chill units accumulated. This continuum of deacclimation responses was quantified as a rate ratio, referred to as deacclimation potential. Deacclimation potential provides an advantageous alternative method to assess dormancy status by quantifying a bud growth phenotype that is linked to growth but proceeds externally visible bud enlargement/elongation. We also observed a logistic trend between deacclimation rates and ambient temperature, referred to as the relative thermal contribution. Within an optimal temperature range, higher temperatures triggered higher deacclimation rates. However, changes in temperature have diminishing effects on deacclimation rates above and below that optimal range. Furthermore, deacclimation occurred at low temperatures, as low as 0°C. Relative thermal contribution can inform adjustments to base temperatures and patterns of temperature effects in models predicting phenological development and cold hardiness changes, especially for species that deacclimate at low temperatures. Finally, the effects of both chill unit accumulation and

ambient temperature were combined in a predictive model that accurately describes deacclimation kinetics across the dormant period.

Prolonged exposure to chilling temperature is needed to overcome endodormancy and the duration of endodormancy can be quantified as a chilling requirement. Research presented in Chapter 4 evaluated freezing temperature contribution towards endodormancy completion and aimed to determine chilling requirements for five cold-climate cultivars. We suspect freezing temperatures were effective in promoting endodormancy completion for hybrid grapevine cultivars. Therefore, chill models will need to be adapted to include freezing temperatures for more accurate estimation of chill requirements. Furthermore, we observed budbreak at a similar number of days and within the endodormancy threshold for buds exposed to different chill treatments, while their cold hardiness levels differed by approximately twofold. Cultivar-specific chilling requirements reported in this study do not represent an absolute chill requirement that is transferrable across regions or from year-to-year. Instead, estimated chill requirements likely represent a combination of traits involved in both dormancy status and deacclimation capacity. Therefore, future research that characterizes endodormancy completion should complement bud forcing assays with cold hardiness evaluation and/or deacclimation potential to verify dormancy status interpretations.

Chapter 1: Literature review

Grapevines

Grapevines (*Vitis* spp.) are deciduous woody perennials that are among the five most produced fruit crops in the world (FAO-OIV 2016). In 2019, an estimated seven million hectares worldwide were cultivated with grapevines. The top producers around the world include China, Italy, United States, Spain, and France (USDA-NASS 2018). In the United States, approximately 375,000 hectares are cultivated. This production is largely centered in California and Washington. However, there is interest in developing other growing regions for economic opportunity (Tuck et al. 2017), climate change pressures (Wanyama et al. 2020), and sociocultural significance (Myles and Filan 2019).

Grapevines exhibit a climbing growth habit, which allows them to maximize leaf area and shoot growth rate while minimizing investment in supporting stem structure (Ichihashi and Tateno 2015). In natural ecosystems, grapevines use trees for support whereas a trellis system is necessary in agricultural settings (Gladstone and Dokoozlian 2003). Grapevine form is highly manipulable, which has led to many types of trellis and training systems used in grapevine production. All training systems maintain a portion of the vine as a permanent structure, which generally includes roots, trunks, and often cordons (horizontal trunks). Shoots grow from the vine's permanent structure in each growing season to create the leaf canopy. Axillary buds, some of which contain inflorescence primordia, also form on these shoots. In the following growing season, axillary buds will grow to produce flowers and fruit. Therefore, bud survival through winter determines a grapevine's ability to sexually reproduce and yield potential.

Species in the *Vitis* genus are native to temperate and subtropical climate zones in the Northern Hemisphere (Mullins et al. 1992). *Vitis* contains more than 60 species, spread mostly

throughout continental Eurasia and North America (Alleweldt and Possingham 1988, Wan et al. 2008). The most commonly produced grapevine cultivars today stem from the Eurasian species *Vitis vinifera* because of its desirable fruit quality traits. However, *V. vinifera* lacks some valuable agronomic traits, including resistance to diseases present in North America and many abiotic stresses. Among these abiotic stresses, *V. vinifera* production is most constrained by climactic zone and/or seasonal low temperatures (Parker 1963). In contrast, common North American *Vitis* species have high disease resistance, can survive low freezing temperatures but lack desirable fruit quality traits.

Members of the *Vitis* genus likely have a relatively recent common ancestor because all species can readily interbreed to form fertile interspecific crosses called hybrids (Gerrath et al. 2015). Within the last century, grapevine breeders have developed interspecific hybrid cultivars that combine desirable fruit quality traits (from *V. vinifera*) with cold hardiness traits (from North American *Vitis* spp.) (Luby and Fennell 2006). These hybrids, referred to as cold-climate cultivars, have established opportunities to advance grapevine production in regions that were previously limited by low temperature. However, cold hardiness is a complex trait with several contributing factors. It is also a dynamic process that changes with time. While cold-climate hybrid grapevine cultivars survive harsher winter climates, many aspects of their cold hardiness are unknown.

Dormancy in woody perennials

While the origins of the term dormant (Latin *dormire* = to sleep) in biology are unresolved (Considine and Considine 2016), the underlying phenomena have captured the curiosities of scientists for at least several hundred years (van Leeuwenhoek 1702). Including

contemplation of dormancy in temperate woody perennials (Knight 1801, Müller-Thurgau 1885). This has led to an extensive body of literature concerning many aspects of dormancy. By the mid 1900s, the framework of our current understanding for dormancy in woody perennials had come together (Doorenbos 1953, Samish 1954, Vegis 1964). However, as of today, a comprehensive understanding of dormancy at the whole-plant and cellular level still remains unclear.

There are many reviews of various dormancy aspects and processes related to woody plant dormancy. Topics covered in these reviews, include dormancy terminology (Considine and Considine 2016), experimental approaches in dormancy research (Fadón and Rodrigo 2018), signals regulating dormancy induction and release (Arora et al. 2003, Cooke et al. 2012, Faust et al. 1997, Horvath et al. 2003, Maurya and Bhalerao 2017, Tanino et al. 2010), hormonal orchestration of dormancy (Liu and Sherif 2019), reactive oxygen species activity in dormancy (Beauvieux et al. 2018), proteins related to dormancy (Rowland and Arora 1997), transcriptomics in dormancy (Lloret et al. 2018), genetic regulation of dormancy (Falavigna et al. 2019), epigenetic regulation of dormancy (Campoy et al. 2011, Lloret et al. 2018, Luedeling et al. 2011), apical shoot meristem organization (Paul et al. 2014, Rinne et al. 2010), embolism repair (Brodersen and McElrone 2013), and conceptual overview of seasonal dormancy cycle (Fadón et al. 2020, Rohde and Bhalerao 2007, Saure 1985). This is not a comprehensive list, but these important reviews summarize the complexity of the dormant period and share insights into the historical progression of what is understood about dormancy today.

There are also several definitions for dormancy that have been suggested over the years. At the most fundamental level, dormancy is defined as the inability of a meristem to resume growth under favorable conditions (Rohde and Bhalerao 2007). Dormancy is a condition specifically of the meristem in this regard. In tree research, dormancy is often defined as absence

of visible growth in plant structures containing meristems (Lang 1987). This definition has been criticized for some of its shortcomings (Rohde and Bhalerao 2007). For example, meristem growth is not readily 'visible' since meristems are concealed within organs. In addition, absence of growth is ambiguous and does not distinguish a lack of growth from an inability to grow. The more fundamental definition is often preferred for these reasons, especially for research at the cellular level. That being said, Lang's (1987) dormancy description in tree research is used widely despite its shortcomings. This is likely because it represents an ecological viewpoint of dormancy and considers factors regulating dormancy rather than focusing on the states of dormancy exhibited by the meristem itself (Cooke et al. 2012). This is especially useful for research exploring seasonal progression of dormancy for the whole-plant.

Within the dormant period, three consecutive phases were distinguished including para-, endo-, and ecodormancy (Lang et al. 1987). These phases are divided based on the mechanism associated with growth inhibition. Paradormancy occurs during the growing season. Paradormant bud growth is inhibited by signals from within the plant but outside the bud (e.g., apical dominance; Cline 1997). Buds transition from paradormancy into endodormancy in response to environmental cues including decreasing photoperiod and ambient temperatures (Tanino et al. 2010). In endodormancy, growth suspension signals originate from within the meristem itself. Buds gradually overcome endodormancy through prolonged exposure to cool (i.e., chilling) temperatures (Coville 1920). Buds require certain amounts (i.e., chill requirement) of chilling temperatures to fully eliminate physiological growth inhibitors and transition to ecodormancy (Arora et al. 2003, Rowland and Arora 1997). Ecodormant buds have the capacity to grow but are suspended due to unfavorable environmental conditions. With enough time in warm temperatures, ecodormant buds will resume growth and development. To specify a brief

digression, paradormancy and ecodormancy are not considered “true” dormancy statuses under the fundamental definition for dormancy since the meristem has the capacity to grow but is inhibited by external factors.

There are several examples of proposed mechanisms that regulate dormancy in woody perennials. Some research suggests that endodormancy release may occur after 1,3-β-d-glucan plugs at plasmodesmata are removed and symplastic cell-to-cell communication is opened thereby restoring the supply of growth-promoting signals in the shoot apical meristem (van der Schoot and Rinne 2011). Prolonged exposed to chilling temperatures have been show to open plasmodesmata (Rinne et al. 2011). However, one of the main knowledge gaps in understanding woody plant dormancy concerns the mechanisms whereby plants perceive temperature during dormancy. There is also research that describes molecular mechanisms resembling oxidative stress conditions involved in endodormancy release. Molecules associated with oxidative stress conditions might integrate environmental cues and metabolic processes that regulate plant growth and development (Beauvieux et al. 2018). Finally, some research suggests epigenetic mechanisms that modify gene expression patterns without any changes to DNA sequence might be involved in regulating endodormancy release (Ríos et al. 2014).

Dormancy status has traditionally been assessed with bud forcing assays (Saure 1985). The pattern of budbreak under optimal growing conditions is observed to measure two related criteria, percent budbreak and time to (50%) budbreak. Different plant materials have been used in bud forcing assays including whole plants, large cuttings, or single-node cuttings (Biggs 1966, Couvillon et al. 1975, Vitasse et al. 2014a). In general, low percentages of buds will grow after longer periods of forcing during endodormancy. Whereas high percentages of buds will grow with short (relative to endodormancy) periods of forcing during ecodormancy. These methods

have been criticized for several limitations and are difficult to standardize (Cooke et al. 2012, Dennis 2003, Saure 1985). However, there are currently no validated molecular markers or non-destructive physiological markers to define dormancy status (Cooke et al. 2012). Therefore, many experimental studies have relied on bud forcing assays to assess dormancy.

Experiments using bud forcing assays have focused on phenology modeling, relating temperature to phenological events to identify the most effective temperature range to overcome dormancy (Chuine and Régnière 2017). This has led to the development of temperature-based mathematical models to estimate the chilling requirement (i.e., duration of endodormancy) for several species and cultivars aiming to forecast bloom dates. There are many of these models described in the literature (Pertille et al. 2019). Some examples that are used widely include the Chilling Hours model (Weinberger 1950), the Utah model (Richardson et al. 1974), the North Carolina model (Shaltout and Unrath 1983), and the Dynamic model (Erez et al. 1990, Fishman et al. 1987a, 1987b). All chill models use only temperature data as an input. In addition, all models assume the efficiency of each temperature in stimulating dormancy release is constant throughout the dormancy period. Chill models are known to produce mixed results across regions (Saure 1985), and some experiments aim to adapt models to fit specific regions (Linsley-Noakes et al. 1994, Lu et al. 2012).

Freezing and freeze injury

Freezing is a phase transition where a liquid turns into a solid when its temperature is lowered below its freezing point. Water will readily freeze below 0°C when foreign substances nucleate ice formation (i.e., heterogeneous freezing; Bigg 1953, Langham and Mason 1958). These foreign substances are referred to as ice nucleation active substances and are extremely

prevalent (Wilson et al. 2003). Pure water molecules can also cluster in ice-like patterns, which will self-nucleate ice formation at -40°C (i.e., homogeneous freezing; Bigg 1953, Langham and Mason 1958). Once an ice nucleation event has occurred, ice crystals grow as surrounding water molecules join the ice crystal lattice according to the rate of heat transfer (Fernandez and Barduhn 1967).

Plants can be injured when freezing occurs in their tissues depending on the location of ice nucleation and rate of ice growth (Wisniewski et al. 2004). The process for freeze injury in plants was originally thought to be explained by a "rupture theory" (Goodale 1985, Levitt 1980, West and Edlefsen 1917). This theory suggested that plant tissues expand while freezing and ultimately rupture because of that expansion, which was based on observing freeze splitting in trees combined with the physical fact that freezing water expands. However, microscopic analysis after cell freezing repeatedly contradicted any cell rupture processes (Göppert 1830). The rupture theory was eventually considered unfounded by the discovery that tissues actually contract while freezing. This was determined through observing ice formation outside cells (in extracellular spaces) as opposed to inside cells (in intracellular spaces; Caspary 1857).

Ice forms extracellularly in plants because extracellular fluid contains heterogeneous ice-nucleation agents and has a higher freezing point than intracellular solutions (Ashworth 1992). Water is then pulled from inside the cell to the extracellular ice. This is because ice has a lower vapor pressure than liquid water at a given subfreezing temperature (Feistel and Wagner 2007, Wexler 1977). Consequently, cells contract as ice crystals grow in large masses. This is termed "cytorrhysis" if the cell is irreparably damaged. If cellular water diffuses as fast as extracellular ice forms while temperatures decrease, the cell is in "equilibrium freezing" (Ashworth 1992). Under this scenario, extracellular freezing can be tolerated so far as a plant tissue can tolerate

dehydration (i.e., freeze-desiccation; Arora 2018). There is a general consensus that ice does not form intracellularly under naturally freezing conditions (aside from the major exception of supercooled cells freezing, which is discussed in the following section), but ice can form intracellularly under artificially imposed freezing conditions. With that in mind, it is worth noting, ice that forms intracellularly always leads to lethal injury (Levitt 1980).

Survival strategies

Woody plants have evolved several strategies to survive freeze injury (Burke et al. 1976). These strategies have been organized into two main categories: (1) freezing tolerance and (2) freezing avoidance (Levitt 1980).

Tissues that exhibit freeze tolerance respond to freezing temperatures by formation of extracellular ice (as described above) followed by withdrawal of water from cells in order to come into chemical equilibrium with the external ice (Wisniewski and Arora 2000). The amount of water that is lost from a cell is directly dependent on the vapor pressure (and therefore temperature) of the surrounding ice (Wisniewski et al. 2003). In this way, freeze tolerance strategies also involve a form of dehydration stress.

In contrast, tissues that exhibit freezing avoidance survive freezing temperatures by deep supercooling. Deep supercooling is a process that retains cellular water in a liquid phase at low, subfreezing temperatures by compartmentalizing heterogeneous ice nucleating substances and/or water (Burke and Stushnoff 1979). The phenomena have been termed “deep” supercooling to distinguish it from the small amount of supercooling (-1 to -4°C) that often occurs before extracellular ice nucleation in plants. Supercooled cellular water is thermodynamically metastable and becomes increasingly likely to form ice by a heterogeneous ice nucleating event

as temperature decrease towards -40°C. If a heterogeneous freezing event does not occur, water will self-nucleate and homogenously freeze at approximately -40°C (Fletcher 1970, Quamme et al. 1995).

Both freeze tolerance and freeze avoidance adaptations aim to prevent the formation of intracellular ice because it will lethally injure cells, which leads to death of that tissue (Burke et al. 1976). A plant that survives in freezing temperatures by preventing intracellular ice is cold hardy or has cold hardiness. In woody species, it is common for different tissues (e.g., bark versus xylem and buds) within the same plant to use mechanisms from either category when exposed to freezing temperatures (Sakai and Larcher 1987). Deep supercooling is discussed in more detail in the following section because it is the adaptation grapevine buds use to survive freeze injury.

Understanding and measuring deep supercooling

The ability for woody plant tissue to avoid freezing by deep supercooling has been described and contemplated since the early 1900s (Scarth and Levitt 1937, Wiegand 1906). Deep supercooling has been observed in xylem ray parenchyma cells of deciduous hardwoods (George et al. 1974, George and Burke 1977a, Pierquet et al. 1977, Quamme 1976) and overwintering reproductive buds of many woody perennials (George and Burke 1977b, Ishikawa and Sakai 1981, Pierquet et al. 1977). While the supercooling of water and avoidance of freeze injury are common features of xylem tissues and buds, these two tissues respond differently to freezing temperature stress and so are often discussed separately. Deep supercooling in xylem tissues is reviewed by Wisniewski (1995) and in buds is reviewed by Quamme (1995). This review is confined to the deep supercooling in buds.

There is consensus that two conditions are necessary for tissues to deep supercool: (a) the bud tissues must be free of heterogeneous nucleating agents; and (b) ice must be prevented from propagating through the bud axis into the supercooled flowers or apical meristem (Wisniewski et al. 2014). Regarding the first condition, heterogeneous nucleators are substances that act as a template to make it easier for water molecules to begin to take on a crystalline arrangement, referred to as an ice nucleus (Chen et al. 2006, Franks and Jones 1985). Once a core of water molecules has formed an ice nucleus, they act as a catalyst to induce the freezing of the surrounding water molecules. Heterogeneous nucleators can be extrinsic or intrinsic, the former representing a foreign substance while the latter representing a natural component of the plant (Ashworth 1992). Previous research suggests that deep supercooling tissues prevent ice nucleation by excluding heterogenous nucleators (Wisniewski and Arora 2000) and/or restricting the activity of heterogeneous nucleators (Kasuga et al. 2006). Regarding the second condition, many dormant buds have a zone of adapted tissue that creates an ice barrier. Some proposed models for preventing ice propagation by the ice barrier include decreased pore structure (Ashworth and Abeles 1984), high amounts of impermeable, suberin-based molecules (Chalker-Scott 1992), and/or increased dehydration in the tissue at the base of the bud (Quamme 1978). It is likely that the nature of ice nucleation barriers differs among species and tissues that deep supercool. Understanding the role and source of heterogeneous nucleators as well as development of ice barriers in plants is extremely important because it could guide development of methods for regulating their activity and, in turn, limiting freezing injury to deep supercooling plants (Wisniewski and Fuller, 1999). However, despite many studies of deep supercooling in numerous species, it is not known how buds maintain a supercooled state or how freezing of supercooled buds is initiated (Quamme 1995).

The critical nucleating temperature for supercooled water can be determined by differential thermal analysis (DTA), which measures the latent heat released by water in tissues as they freeze (Quamme et al. 1982). Differential thermal analysis has demonstrated two distinct freezing events occur when buds freeze (Burke et al. 1976). The first freezing event, referred to as the high temperature exotherm (HTE), corresponds to extracellular ice formation (between -5 and -10 °C) and is not considered injurious. The HTE is followed by one or more freezing events, referred to as the low temperature exotherm(s) (LTE), which correspond with freezing of supercooled water within shoot primordium and/or flower(s) of the bud. The low temperature exotherm has been correlated with lethal injury in a tissue (Andrews et al. 1984, Quamme 1986).

A standard DTA method has been developed for determining the extent of grapevine bud deep supercooling (Mills et al. 2006). This method uses a programmable freezer to lower temperatures at a pre-determined, slow rate. Excised buds are loaded onto thermoelectric modules (TEMs) that generate an electrical signal when heated by the exothermic reaction of water freezing. Thermocouples are used to simultaneously measure ambient air temperature. The temperature where HTE and (lethal) LTEs occurred can then be determined by plotting the electrical signal from TEMs across temperature measured by thermocouples.

Grapevine buds are compound and contain primary, secondary, and tertiary buds, each of which may contain an apical meristem and flowers. Up to three LTEs are detected below the HTE, which are thought to correspond to the freezing of each bud type (Andrews et al. 1984, Pierquet and Stushnoff 1980, Quamme 1986, Wolf and Pool 1987). The LTEs occur at progressively lower temperature and are progressively smaller in size. Therefore, the signal size of the LTE is thought to be related to bud size.

Seasonal changes of cold hardiness

A plant's cold hardiness (e.g., ability for a bud to deep supercool) changes on a seasonal basis. The progression of bud cold hardiness in woody species can be separated into three phases: acclimation, maintenance, and deacclimation (Wisniewski et al. 2003). Plants have evolved to synchronize bud cold hardiness with the annual rhythm of seasons in order to survive in climates where freezing occurs.

In fall, active growth stops in response to decreasing daylength and, in some cases, decreasing ambient temperature (Fennell and Hoover 1991, Tanino et al. 2010, Wake and Fennell 2000). This process of growth cessation is a prerequisite for initiation of bud cold hardiness (Fuchigami et al. 1971, Weiser 1970). Once bud cold hardiness mechanisms are established, buds acclimate (LTEs occur at lower temperatures) mainly in response to decreasing temperature or the combination of decreasing temperature and short days (Schnabel and Wample 1987). The change in LTE is associated with a change in internal water balance and external water loss (Ishikawa and Sakai 1981, Johnston 1922). After buds have acclimated, the cold hardiness maintenance phase begins. This generally spans throughout winter when low freezing temperatures commonly occur. Buds deacclimate in spring in response to increasing temperature.

Seasonal cold hardiness changes are dependent on dormancy mechanisms, among other factors. Buds do not deacclimate during endodormancy. The physiological rationale for this is not well understood but several known endodormancy conditions are non-conducive to deacclimation biochemistry, including: symplastic-isolation of shoot meristems due to down-regulated cell-to-cell communication (Paul et al. 2014, Rinne et al. 2011); reduced water content and water mobility (low free to bound water ratio, Fennell and Line 2001; lower aquaporin activity/expression, Yooyongwech et al. 2008); and high levels of accumulated abscisic acid

(Tanino 2004). Buds are physiologically primed for deacclimation in ecodormancy. Buds will deacclimate under conducive temperatures (Kalberer et al. 2006). In this way, the timing of dormancy transitions is an important factor related to the potential for freeze injury risks throughout winter (Kovaleski et al. 2018a).

Literature Cited

Alleweldt G, Possingham J V. 1988. Progress in grapevine breeding. Theor Appl Genet 75:669–673.

Andrews P, Sandidge III C, Toyoma T. 1984. Deep supercooling of dormant and deacclimating Vitis buds. Am J Enol Vitic 35:175–177.

Arora R. 2018. Mechanism of freeze-thaw injury and recovery: A cool retrospective and warming up to new ideas. Plant Sci 270:301–313.

Arora R, Rowland LJ, Tanino K. 2003. Induction and release of bud dormancy in woody perennials: A science comes of age. HortScience 38:911–921.

Ashworth EN. 1992. Formation and Spread of Ice in Plant Tissues.

Ashworth EN, Abeles FB. 1984. Freezing behavior of water in small pores and the possible role in the freezing of plant tissues. Plant Physiol 76:201–204.

Beauvieux R, Wenden B, Dirlewanger E. 2018. Bud dormancy in perennial fruit tree species: A pivotal role for oxidative cues. Front Plant Sci 9:1–13.

Bigg EK. 1953. The supercooling of water. Proc Phys Soc Sect B 66:688–694.

Biggs RH. 1966. Screening chemicals for the capacity to modify bud dormancy of peaches. Proc Fla State Hort Sci 79:3383–386.

Brodersen CR, McElrone AJ. 2013. Maintenance of xylem network transport capacity: A review of embolism repair in vascular plants. Front Plant Sci 4:1–11.

Burke MJ, Stushnoff C. 1979. Frost hardiness: A discussion of possible molecular causes of injury with particular reference to deep supercooling of water. Stress Physiol Crop plants:197–215.

Burke MJ, Gusta L V, Quamme HA, Weiser CJ, Li PH. 1976. Freezing and Injury in Plants. Annu Rev Plant Physiol 27:507–528.

Campoy JA, Ruiz D, Egea J. 2011. Dormancy in temperate fruit trees in a global warming context: A review. Sci Hortic (Amsterdam) 130:357–372.

Caspary R. 1857. Bewirkt die Sonne Risse in Rinde und Holze der Bäume? Bot Zeitung 15:153–156, 329–371.

Chalker-Scott L. 1992. Disruption of an Ice-nucleation Barrier in Cold Hardy Azalea Buds by Sublethal Heat Stress. Ann Bot 70:409–418.

Chen SH, Mallamace F, Mou CY, Broccio M, Corsaro C, Faraone A, Liu L. 2006. The violation of the Stokes-Einstein relation in supercooled water. Proc Natl Acad Sci U S A

103:12974–12978.

Chuine I, Régnière J. 2017. Process-Based Models of Phenology for Plants and Animals. Annu Rev Ecol Evol Syst 48:159–182.

Cline MG. 1997. Concepts and terminology of apical dominance. Am J Bot 84:1064–1069.

Considine MJ, Considine JA. 2016. On the language and physiology of dormancy and quiescence in plants. J Exp Bot 67:3189–3203.

Cooke JEK, Eriksson ME, Junttila O. 2012. The dynamic nature of bud dormancy in trees: Environmental control and molecular mechanisms. Plant, Cell Environ 35:1707–1728.

Couvillon GA, Moore CM, Bush P. 1975. Obtaining small peach plants containing all bud types for "rest" and dormancy studies. HortScience 10:78–79.

Coville F. 1920. The influence of cold in stimulating the growth of plants. Proc Natl Acad Sci USA 6:434–435.

Dennis FG. 2003. Problems in standardizing methods for evaluating the chilling requirements for the breaking of dormancy in buds of woody plants. HortScience 38:347–350.

Doorenbos J. 1953. Review of the literature on dormancy in buds of woody plants. Meded Landbouwhogesch Wagening Ned 53:1–24.

Erez A, Fishman S, Linsley-Noakes GC, Allan P. 1990. the Dynamic Model for Rest Completion in Peach Buds. Acta Hortic:165–174.

Fadón E, Rodrigo J. 2018. Unveiling winter dormancy through empirical experiments. Environ Exp Bot 152:28–36.

Fadón E, Fernandez E, Behn H, Luedeling E. 2020. A conceptual framework for winter dormancy in deciduous trees. Agronomy 10.

Falavigna V da S, Guitton B, Costes E, Andrés F. 2019. I want to (Bud) break free: The potential role of DAM and SVP-like genes in regulating dormancy cycle in temperate fruit trees. Front Plant Sci 9:1–17.

FAO-OIV. 2016. Table and Dried Grapes. FAO-OIV Focus 2016:1–64.

Faust M, Erez A, Rowland LJ, Wang SY, Norman HA. 1997. Bud dormancy in perennial fruit trees. HortScience 32:623–629.

Feistel R, Wagner W. 2007. Sublimation pressure and sublimation enthalpy of H2O ice Ih between 0 and 273.16 K. Geochim Cosmochim Acta 71:36–45.

Fennell A, Hoover E. 1991. Photoperiod influences growth, bud dormancy, and cold acclimation in Vitis labruscana and V. riparia. J Am Soc Hortic Sci 116:270–273.

Fennell A, Line MJ. 2001. Identifying differential tissue response in grape (Vitis riparia) during induction of endodormancy using nuclear magnetic resonance imaging. J Am Soc Hortic Sci 126:681–688.

Fernandez R, Barduhn AJ. 1967. The growth rate of ice crystals. Desalination 3:330–342.

Fishman S, Erez A, Couvillon GA. 1987a. The temperature dependence of dormancy breaking in plants: Computer simulation of processes studied under controlled temperatures. J Theor Biol 126:309–321.

Fishman S, Erez A, Couvillon GA. 1987b. The Temperature Dependence of Dormancy Breaking in Plants: Mathematical Analysis of a Two-Step Model Involving a Cooperative Transition. J Theor Biol 124:473–483.

Fletcher NH. 1970. Liquid water and freezing. *In* The chemical physics of ice. pp. 73–103. Cambridge University Press, Cambridge, England.

Franks F, Jones M. 1985. Biophysics and biochemistry at low temperatures. FEBS Lett 220.

Fuchigami LH, Weiser CJ, Evert DR. 1971. Induction of Cold Acclimation in Cornus stolonifera Michx. . Plant Physiol 47:98–103.

George M, Burke M, Pellett H, Johnson A. 1974. Low Temperature Exotherms and Woody Plant Distribution. HortScience 9:519–522.

George MF, Burke MJ. 1977a. Cold Hardiness and Deep Supercooling in Xylem of Shagbark Hickory. Plant Physiol 59:319–325.

George MF, Burke MJ. 1977b. Supercooling in Overwintering Azalea Flower Buds. Plant Physiol 59:326–328.

Gerrath J, Posluszny U, Melville L. 2015. Taming the Wild Grape: Botany and Horticulture in the Vitaceae. Springer International Publishing, Switzerland.

Gladstone EA, Dokoozlian NK. 2003. Influence of leaf area density and trellis/training system on the light microclimate within grapevine canopies. Vitis 42:123–131.

Goodale G. 1985. Gray's Botanical Textbook, vol. 2: Physiological Botany. Ivison, Blakeman, Taylor, New York.

Göppert H. 1830. Über die Wärme-Entwickelung in den Pflanzen, deren Gefrieren und die Schützmittel gegen dasselbe. Max Comp Berlin.

Horvath DP, Anderson J V., Chao WS, Foley ME. 2003. Knowing when to grow: Signals regulating bud dormancy. Trends Plant Sci 8:534–540.

Ichihashi R, Tateno M. 2015. Biomass allocation and long-term growth patterns of temperate lianas in comparison with trees. New Phytol 207:604–612.

Ishikawa M, Sakai A. 1981. Freezing avoidance mechanisms by supercooling in some rhododendron flower buds with reference to water relations. Plant Cell Physiol 22:953–967.

Johnston ES. 1922. Moisture Content of Peach Buds in Relation to Temperature Evaluations. Bot Gaz 74:314–319.

Kalberer SR, Wisniewski M, Arora R. 2006. Deacclimation and reacclimation of cold-hardy plants: Current understanding and emerging concepts. Plant Sci 171:3–16.

Kasuga J, Mizuno K, Miyaji N, Arakawa K, Fujikawa S. 2006. Role of intracellular contents to facilitate supercooling capability in beech (Fagus crenata) xylem parenchyma cells. Cryo-Letters 27:305–310.

Knight A. 1801. Account of some Experiments on the Ascent of the Sap in Tree. Philos Trans R Soc Lond 91:333–353.

Kovaleski AP, Reisch BI, Londo JP. 2018. Deacclimation kinetics as a quantitative phenotype for delineating the dormancy transition and thermal efficiency for budbreak in Vitis species. AoB Plants 10:1–12.

Lang GA. 1987. Dormancy: A New Universal Terminology. HortScience 22:817–820.

Lang GA, Early JD, Martin GC, Darnell RL. 1987. Endo-, para-, and Ecodormancy: Physiological Terminology and Classification for Dormancy Research. HortScience 22:371–377.

Langham EJ, Mason BJ. 1958. The heterogeneous and homogeneous nucleation of supercooled water. Proc Roy Soc A 247:493–504.

van Leeuwenhoek A. 1702. On certain animalcules found in the sendiment in gutters of the roofs of houses. *In* Hoole, S. The select works of Antony van Leeuwenhoek: containing his microscopical discoveries in many of the works of nature. pp. 207–213. London: The Philanthropic Society.

Levitt J. 1980. Responses of Plants to Environmental Stresses: Chilling, Freezing, and High Temperature Stresses. Academic Press. New York, New York.

Linsley-Noakes GC, Allan P, Matthee G. 1994. Modification of rest completion prediction models for improved accuracy in south african stone fruit orchards. J South African Soc Hortic Sci 4:13–15.

Liu J, Sherif SM. 2019. Hormonal Orchestration of Bud Dormancy Cycle in Deciduous Woody Perennials. Front Plant Sci 10:1–21.

Lloret A, Badenes ML, Ríos G. 2018. Modulation of dormancy and growth responses in reproductive buds of temperate trees. Front Plant Sci 9:1–12.

Lu M Te, Song CW, Ou SK, Chena CL. 2012. A model for estimating chilling requirement of

very low-chill peaches in Taiwan. Acta Hortic 962:245–252.

Luby J, Fennell A. 2006. Fruit breeding for the northern great plains at the University of Minnesota and South Dakota State University. HortScience 41:25–26.

Luedeling E, Girvetz EH, Semenov MA, Brown PH. 2011. Climate change affects winter chill for temperate fruit and nut trees. PLoS One 6.

Maurya JP, Bhalerao RP. 2017. Photoperiod- and temperature-mediated control of growth cessation and dormancy in trees: A molecular perspective. Ann Bot 120:351–360.

Mills LJ, Ferguson JC, Keller M. 2006. Cold-hardiness evaluation of grapevine buds and cane tissues. Am J Enol Vitic 57:194–200.

Müller-Thurgau H. 1885. Beitrag zur Erklärung der Ruheperioden der Pflanzen. Landw Jahrb 14:851–907.

Mullins MG, Bouquet A, Williams LE. 1992. Biology of the grapevine. Cambridge : Cambridge University Press.

Myles CC, Filan TR. 2019. Making (a) place: wine, society and environment in California's Sierra Nevada foothills. Reg Stud Reg Sci 6:157–167.

Parker J. 1963. Cold Resistance in Woody Plants. Bot Rev 29.

Paul LK, Rinne PLH, Van der Schoot C. 2014. Shoot meristems of deciduous woody perennials: Self-organization and morphogenetic transitions. Curr Opin Plant Biol 17:86–95.

Pertille RH, Sachet MR, Guerrezi MT, Citadin I. 2019. An R package to quantify different chilling and heat models for temperate fruit trees. Comput Electron Agric 167:105067.

Pierquet P, Stushnoff C. 1980. Relationship of Low Temperature Exotherms to Cold Injury in Vitis Riaria Michx. Am J Enol Vitic 31:1–6.

Pierquet P, Stushnoff C, Burke M. 1977. Low Temperature Exotherms in Stem and Bud Tissues of Vitis riparia Michx. J Am Soc Hortic Sci 102:54–55.

Quamme HA. 1976. Relationship of the Low Temperature Exotherm To Apple and Pear Production in North America. Can J Plant Sci 56:493–500.

Quamme HA. 1986. Use of thermal analysis to measure freezing resistance of grape buds. Can J Plant Sci 66:945–952.

Quamme HA. 1995. Deep Supercooling in Buds of Woody Plants. *In* Biological Ice Nucleation and its Applications. pp. 183–199. American Phytopathological Society-St. Paul, USA.

Quamme HA, Chen PM, Gusta LV. 1982. Relationship of Deep Supercooling and Dehydration Resistance to Freezing Injury in Dormant Stem Tissues of "Starkrimson Delicious" Apple

and “Siberian C” Peach. J Am Soc Hortic Sci 107:299–304.

Quamme HA, Su Wei Ai, Veto LJ. 1995. Anatomical features facilitating supercooling of the flower within the dormant peach flower bud. J Am Soc Hortic Sci 120:814–822.

Richardson EA, Sceley SD, Walker DR. 1974. A Model for Estimating the Completion of Rest for “Redhaven” and “Elberta” Peach Trees. HortScience 9:331–332.

Rinne PLH, Welling A, van der Schoot C. 2010. Perennial Life Style of Populus: Dormancy Cycling and Overwintering. *In* Genetics and Genomics of Populus. S Jansson, R Bhalerao, and A Groover (eds.), pp. 171–200. Springer New York, New York, NY.

Rinne PLH, Welling A, Vahala J, Ripel L, Ruonala R, Kangasjärvi J, van der Schoot C. 2011. Chilling of dormant buds hyperinduces FLOWERING LOCUS T and recruits GA-inducible 1,3-β-glucanases to reopen signal conduits and release dormancy in Populus. Plant Cell 23:130–146.

Ríos G, Leida C, Conejero A, Badenes ML. 2014. Epigenetic regulation of bud dormancy events in perennial plants. Front Plant Sci 5:1–6.

Rohde A, Bhalerao RP. 2007. Plant dormancy in the perennial context. Trends Plant Sci 12:217–223.

Rowland LJ, Arora R. 1997. Proteins related to endodormancy (rest) in woody perennials. Plant Sci 126:119–144.

Sakai A, Larcher W. 1987. Frost survival of plants: responses and adaptation to freezing stress. Springer-Verlag, Berlin.

Samish RM. 1954. Dormancy in Woody Plants. Annu Rev Plant Physiol:183–204.

Saure MC. 1985. Dormancy Release in Deciduous Fruit Trees. Hortic Rev (Am Soc Hortic Sci) 7:239–300.

Scarth GW, Levitt J. 1937. The frost-hardening mechanism of plant cells. Plant Physiol 12:51–78.

Schnabel B, Wample R. 1987. Dormancy and cold hardiness in Vitis vinifera L. cv. White Riesling as influenced by photoperiod and temperature. Am J Enol Vitic 38:265–272.

van der Schoot C, Rinne PLH. 2011. Dormancy cycling at the shoot apical meristem: Transitioning between self-organization and self-arrest. Plant Sci 180:120–131.

Shaltout AD, Unrath CR. 1983. Rest Completion Prediction Model for “Starkrimson Delicious” Apples. J Am Soc Hortic Sci 108:957–961.

Tanino KK. 2004. Hormones and endodormancy induction in woody plants. J Crop Improv 10:157–199.

Tanino KK, Kalcsits L, Silim S, Kendall E, Gray GR. 2010. Temperature-driven plasticity in growth cessation and dormancy development in deciduous woody plants: A working hypothesis suggesting how molecular and cellular function is affected by temperature during dormancy induction. Plant Mol Biol 73:49–65.

Tuck B, Gartner W, Appiah G. 2017. Economic Contribution of Vineyards and Wineries of the North, 2015. University of Minnesota Extension.

USDA-NASS. 2018. Noncitrus Fruits and Nuts 2020 Summary.

Vegis A. 1964. Dormancy in Higher Plants. Annu Rev Plant Physiol 15:185–224.

Vitasse Y, Basler D, Way D. 2014. Is the use of cuttings a good proxy to explore phenological responses of temperate forests in warming and photoperiod experiments? Tree Physiol 34:174–183.

Wake CMF, Fennell A. 2000. Morphological, physiological and dormancy responses of three Vitis genotypes to short photoperiod. Physiol Plant 109:203–210.

Wan Y, Wang Y, Li D, He P. 2008. Evaluation of agronomic traits in Chinese wild grapes and screening superior accessions for use in a breeding program. Vitis 47:153–158.

Wanyama D, Bunting EL, Goodwin R, Weil N, Sabbatini P, Andresen JA. 2020. Modeling land suitability for Vitis vinifera in Michigan using advanced geospatial data and methods. Atmosphere (Basel) 11.

Weinberger JH. 1950. Chilling Requirements of Peach Varieties. Proc Amer Soc Hort Sci 56:122–128.

Weiser C. 1970. Cold Resistance and Injury in Woody Plants. 169:1269–1278.

West F, Edlefsen N. 1917. Freezing of fruit buds. Utah Agr Expt Sta Bull 151:1–24.

Wexler A. 1977. Vapor Pressure Formulation for Ice. J Res Natl Bur Stand Sect A Phys Chem 81A:5–20.

Wiegand KM. 1906. The occurence of ice in plant tissue. The Plant World 9:25–39.

Wilson PW, Heneghan AF, Haymet ADJ. 2003. Ice nucleation in nature: Supercooling point (SCP) measurements and the role of heterogeneous nucleation. Cryobiology 46:88–98.

Wisniewski M. 1995. Deep Supercooling in Woody Plants and the Role of Cell Wall Structure. *In* Biological Ice Nucleation and its Applications. pp. 163–181. American Phytopathological Society-St. Paul, USA.

Wisniewski M, Arora R. 2000. Structural and Biochemical Aspecets of Cold Hardiness in Woody Plants. *In* Molecular Biology of Woody Plants. pp. 419–437.

Wisniewski M, Bassett C, Gusta LV. 2003. An overview of cold hardiness in woody plants:

Seeing the forest through the trees. HortScience 38:952–959.

Wisniewski M, Fuller M, Palta J, Carter J, Arora R. 2004. Ice nucleation, propagation, and deep supercooling in woody plants. J Crop Improv 10:5–16.

Wisniewski M, Gusta L, Neuner G. 2014. Adaptive mechanisms of freeze avoidance in plants: A brief update. Environ Exp Bot 99:133–140.

Wolf TK, Pool R. 1987. Factors affecting exotherm detection in the differential thermal analysis of grapevine dormant buds. J Am Soc Hortic Sci 112:520–525.

Yooyongwech S, Horigane AK, Yoshida M, Yamaguchi M, Sekozawa Y, Sugaya S, Gemma H. 2008. Changes in aquaporin gene expression and magnetic resonance imaging of water status in peach tree flower buds during dormancy. Physiol Plant 134:522–533.

Chapter 2: Cold hardiness of cold-climate interspecific hybrid grapevines grown in a cold-climate region

Michael North[1], Beth Ann Workmaster[1], Amaya Atucha[1*]

[1]Department of Horticulture, University of Wisconsin-Madison, 1575 Linden Drive, Madison, WI 53706, USA

[*]Corresponding author (atucha@wisc.edu, tel: 608-262-6452, fax: 608-262-4743)

Key words: hybrid grapevine, freezing stress resistance, differential thermal analysis, explanatory model, prediction model

Published in: American Journal of Enology and Viticulture

Abstract

Cold-climate interspecific hybrid grapevines (CCIHG) selected for their superior mid-winter cold hardiness have expanded grape production to cold-climate regions. However, extreme weather events, such as polar vortexes, and high frequency of fall and spring freezes often result in yield and vine losses. The main objective of this study was to evaluate changes in bud cold hardiness of five CCIHG cultivars grown in the upper Midwest in order to identify relative risk for freeze damage throughout the dormant period, and to adapt a bud cold hardiness prediction model to CCIHG cultivars grown in cold-climate regions. Bud cold hardiness was evaluated biweekly throughout the dormant period by measuring lethal temperatures for buds using differential thermal analysis (DTA). CCIHG cultivars in our study had an early acclimation response with increased levels of cold hardiness before the occurrence of freezing temperatures. Maximum levels of hardiness (-28 to -30°C) were observed both years in February, however deeper levels of freezing stress resistance, probably attained by freeze dehydration, were not detected using DTA. CCIHG cultivars had a rapid deacclimation response that was accelerated with additional chilling accumulation during spring. The reparametrizing of a discrete-dynamic cold hardiness prediction model by expanding the range of ecodormant threshold temperatures for CCIHG resulted in predictions with an average RMSE = 1.01. Although CCIHG cultivars have superior mid-winter bud cold hardiness, fast deacclimation responses increase the risk of freeze damage during spring, thus this trait should be evaluated for future CCIHG cultivar release. The development of tools, such as the discrete-dynamic cold hardiness prediction model for CCIHG cultivars, will aid growers in decision-making to minimize damage, as well as yield and vine losses.

Introduction

Extreme low temperature is the most significant constraint for grape production in cold-climate regions. Freeze injury to buds, canes, cordons, and trunks limits yields and increases production costs due to the additional retraining and replacing of damaged vines (Zabadal et al. 2007). Thus, grapevine genotypes with superior cold hardiness are essential for a successful viticulture industry in cold-climate regions.

Cold-climate interspecific hybrid grapevines (CCIHG) have genetic backgrounds that include *Vitis aestivalis*, *V. labrusca*, *V. riparia*, and *V. rupestris*, and *V. vinifera* (Atucha et al. 2018, Smiley and Cochran 2016). The development of CCIHG cultivars has combined high fruit quality traits of *V. vinifera* with the superior mid-winter cold hardiness traits found in wild *Vitis* species, which has propelled the development of a $539.2 million viticulture industry in cold-climate regions, such as the US Midwest (Dami et al. 2005, Luby and Fennell 2006, Tuck et al. 2017). However, extreme and erratic weather events continue to result in substantial freeze damage to CCIHG and, in turn, economic losses. Some recent examples of devastating freezing events that led to unprecedented crop and vine losses include: the Easter freeze of 2007, Mother's Day freeze of 2010, the "killer frost" of 2012, and the polar vortex event of 2014 (Dami and Lewis 2014, Wisniewski et al. 2017). The Easter freeze of 2007 alone was estimated to be nearly $1 billion in economic losses to small fruit crop growers, including grapes, across 21 states (Warmund et al. 2008). Most recently, in 2019, the polar vortex split, in which a portion of the polar vortex separated and traveled southward and resulted in record-setting cold temperatures in many cold-climate regions of the United States ("National Centers for Environmental Information" 2020). The economic consequences of these extreme weather

events highlight the need for more information on CCIHG cold hardiness dynamics to more specifically identify: 1) periods of high risk, 2) the extent of variability among CCIHG cultivars, and 3) potential risk-mitigation practices.

Previous studies have described a U-shaped pattern of grapevine bud cold hardiness that spans the duration of the dormant period (Ferguson et al. 2014, 2011, Londo and Kovaleski 2017, Mills et al. 2006). This pattern begins with acclimation (gain of cold hardiness) in the fall, continues with maintenance of cold hardiness throughout winter, and ends with deacclimation (loss of cold hardiness) in the spring. While this general pattern of seasonal response has been described extensively, there is substantial variability in grapevine cold hardiness across years, genotypes, climates, and cultural practices (Ferguson et al. 2014, Grant and Dami 2015, Londo and Kovaleski 2017, Pierquet and Stushnoff 1980, Williams et al. 1994). The use of explanatory models, such as the one developed by Londo and Kovaleski (2017), characterizes the relationship between cold hardiness and temperature fluctuations during the dormant season by genotype.

While characterizing grapevine cold hardiness changes in response to temperature fluctuations across the dormant period is critical to understand how genotypes will behave in different growing conditions, the need for information on short-term changes in cold hardiness is critical for protection decision making by growers. However, routine assessment of bud cold hardiness is a time-intensive process that requires specialized equipment. One approach to this is the use of discrete-dynamic modelling where continual changes to a system are modeled using arbitrary incremental time steps, such as hours, days, etc. A discrete-dynamic model developed by Ferguson et al. (Ferguson et al. 2014, 2011) predicts daily changes of cold hardiness for twenty-one *V. vinifera* cultivars and two *V. labrusca* cultivars using daily maximum and

minimum temperatures and cultivar-specific parameters. However, this model was developed using cold hardiness data collected in Washington State from primarily *V. vinifera* genotypes. Therefore, in order to extend its utility to CCIHG and the cold-climate regions where they are mostly grown, this model must be reparametrized for these genotypes and evaluated using cold hardiness data collected in these additional relevant growing regions.

The main objective of this study is to evaluate changes in bud cold hardiness of five CCIHG cultivars to identify relative risk for freeze damage throughout the dormant period. The secondary objective is to optimize and evaluate a bud cold hardiness prediction model for the same five CCIHG cultivars grown in a cold-climate region. This information will contribute to cultivar selection for particular regions and inform designs for future research into the physiological and mechanistic processes of grapevine cold hardiness. In addition, this work will promote the testing and refinement of predictive models with independent sets of data and will strengthen grapevine bud cold hardiness protection decision making in cold-climate regions.

Materials and Methods

Site description. This study was conducted over two winters, 2017-2018 (Year 1) and 2018-2019 (Year 2), in a vineyard at the West Madison Agricultural Research Station in Verona, WI (lat. 43° 03’ 37” N, long. 89° 31’ 54” W). The vineyard is in U.S. Department of Agriculture Plant Hardiness Zone 5a (USDA, 2019), and has deep silt Griswold loam soil with 2 to 6% slopes (“Web Soil Survey - USDA NRCS” 2020).

Vineyard design and vine material. The vineyard was established with one-year-old bare root vines. In 2008, Brianna (BR), Frontenac (FR), La Crescent (LC), and Marquette (MQ) were planted and grown on a vertical shoot positioned trellis system with double trunks trained into unilateral cordons one meter above ground. In 2011, Petite Pearl (PP) was planted and trained to a high cordon trellis system with double trunks trained into unilateral cordons 1.5 meters above ground. All vines were spur-pruned to approximately 45 nodes per vine and all cultivars were thinned to 20 shoots per meter-length of trellis. The vineyard is arranged as a randomized complete block design with four replications. Each block includes two rows of vines with six, four-vine panels per row. At the time of the study, seven of the twelve panels within each block contained cultivars that were not included in this study. Rows are oriented north-south with 3.4 meters between rows and 2.1 meters between vines for a total density of 1398 vines/ha (566 vines/acre).

Weather Data. Hourly average, daily maximum, and daily minimum air temperature data were collected from September 1 to April 30, using a Network for Environment and Weather Applications ("NEWA" 2020) participating station (Model MK-III SP running IP-100 software; Rainwise, Trenton, ME) located onsite, 2 m above ground level (lat. 43° 3' 39.6" N, long. 89° 32' 2.4" W, and elevation at 330 m).

Bud collection. Buds were collected in the morning using similar methods as described in Mills et al. (2006), Ferguson et al. (Ferguson et al. 2014), and Londo and Kovaleski (2017). Buds from node positions four to seven were sampled (4 buds per vine) from canes with green phloem and xylem. Buds were sampled evenly across vineyard blocks and across vines within vineyard

blocks (16 vines total), approximately biweekly 15 times in Year 1 and 14 times in Year 2. Canes were cut several centimeters away from the bud. Buds were collected in plastics bags, stored on ice during transportation, and processed immediately upon returning to the lab.

Differential Thermal Analysis (DTA). The DTA equipment used in this study was the same as described by Villouta et al. (2020). Thermoelectric modules (TEMs) (model HP-127-1.4-1.5-74 and model SP-254-1.0-1.3, TE Technology, Traverse City, MI) were used to detect freezing exothermic reactions. TEMs were placed in individual hinged tin-plated steel containers lined with 5 mm thick open-cell foam pieces to reduce effects of freezing chamber air turbulence. Eleven TEM units were evenly spaced and attached to each of four 30x30 cm perforated aluminum sheet pieces (hereafter called "trays") with the leads of each tray wired to a single 24-pin D-sub connector. A copper-constantan (Type T) thermocouple (22 AWG) was positioned on each tray to monitor temperature in proximity to the TEM units. Trays were positioned vertically in a Tenney Model T2C programmable freezing chamber (Thermal Product Solutions, New Columbia, PA) and connected to a Keithley 2700-DAQ-40 multimeter data acquisition system (Keithley Instruments, Cleveland, OH). TEM voltage and thermocouple temperature readings were collected at 6-second intervals via a Keithley add-in in Microsoft Excel (Microsoft Corp., Redmond, WA). The effect of freezing chamber fan turbulence on the TEM units was minimized by covering trays with 13 mm open-cell foam sheets and by installing a removable piece of perforated, corrugated cardboard across the top of the chamber's interior to function as a damper.

To prepare samples for DTA, nodes were pruned out of the canes. Buds, including the bud cushion, were excised from the node using a razor blade. Five buds were arranged with the cut surface up (i.e., bud on bottom) on a small piece of aluminum foil (Reynolds Consumer

Products, Lake Forest, IL). Cut surfaces of the buds were covered with a piece of moistened Kimwipe (Kimberly Clark, Roswell, GA) to provide an extrinsic ice nucleator source and to prevent dehydration prior to bud freezing. The aluminum foil was folded into a packet containing the five buds. Each single aluminum foil packet was randomly assigned to a TEM chamber.

The DTA protocol used a temperature ramp from room temperature to 4 °C over one-hour, a one-hour hold, ramp to 0 °C over one-hour, a one-hour hold, ramp to -44 °C over 11-hours, a 30-minute hold, and then a finishing ramp back to 4 °C over two-hours. The resulting cooling rate was -0.067 °C per minute (or -4 °C per hour). One TEM chamber on each tray was left empty to document baseline background electrical noise. Heat is released with the freezing of each supercooled meristem in the grape compound bud, and this release is referred to as a low temperature exotherm (LTE). A single compound grapevine bud contains primary, secondary, and tertiary meristems. In this experimental setup, a TEM will occasionally record a large peak followed by one or two smaller peaks. The larger peak relates to the freezing of the primary meristem, while the smaller peaks correspond to the freezing of the secondary and tertiary meristems, a reflection of their smaller size and lower water content. Frequently, these peaks are undiscernible. In a given set of DTA run results, up to five bud LTEs were identified and documented for each TEM, corresponding to the freezing of the primary meristems. As only obvious peaks were identified in this way, occasionally fewer than five peaks were documented for some TEMs.

In Year 1, DTA was performed 15 times, approximately biweekly from November 2 to April 30 (40 buds per sampling date per cultivar). In Year 2, DTA was performed 14 times, approximately biweekly from September 26 to April 16 (30 buds per sampling date per cultivar**)**.

Additional DTA runs were performed as part of a temperature conditioning experiment following an extreme cold weather event in late January 2019. Buds were sampled from all cultivars (16 buds per cultivar) on February 12, 2019, less than two weeks after the extreme low temperatures. Excised and prepared buds were conditioned in the TEM chambers. The protocol used a temperature ramp from room temperature to 4 °C over one hour, a one-hour hold, ramp to 0 °C over one-hour, a one-hour hold, ramp to -33 °C over 33-hours (-1 °C/hour), a 30-minute hold, a ramp to -10 °C over 6 hours, ramp to 0 °C over 5 hours, ramp to 4 °C over 2 hours. A freezing experiment was then started with the standard DTA protocol, which cools to a minimum of -44 °C.

Visual bud injury evaluation. Following the extreme cold weather event in January 2019, an additional collection of buds was dissected while visually evaluating freeze injury using an Olympus SZX12 microscope with a 1x objective (Olympus Optical Company, Tokyo, Japan). Forty buds for each cultivar were collected following the same protocol as for DTA. Before dissection, buds were incubated in sealed plastic bags on ice for 24 hours, then at 4 °C for 24 hours, and finally at room temperature for 24 hours. Sequential cross-sections were cut from the buds with a double-edged razor blade until meristems were visible for evaluation. Freezing injury was assessed for primary and secondary meristems in each bud. Oxidative browning (Goffinet 2004) was rated as present (injured) or absent (not injured).

Statistics. For each DTA run, the temperatures at which 10%, 50%, and 90% of the buds froze were determined and referred to respectively as the LT_{10}, LT_{50}, and LT_{90} temperatures. Two models were developed in R (ver. 3.5.2, R Foundation for Statistical Computing, Vienna,

Austria), an explanatory regression model (Londo and Kovaleski 2017) and a predictive discrete-dynamic model (Ferguson et al. 2014, 2011). Symbols and abbreviations used for each model are listed in Table 1. Data from both years of the study were used in the evaluation of each model (more detail below).

Explanatory Model. An explanatory linear regression model was created in R using multiple linear regression and a model selection process based on Londo and Kovaleski (2017). The model was used to determine significant differences among cultivars' seasonal bud cold hardiness and their relative responsiveness to temperature fluctuations and time. The explanatory variables used were Cultivar, Time, Time^2, Year, and a temperature index (σ_T). Cultivar was included as a categorical variable. Time and Time^2 were measured in units of days from September 6. The temperature index σ_T describes shifts in temperature during a time period preceding cold hardiness measurement by DTA and was calculated using the same formulas described by Londo and Kovaleski:

$$T_E = T - T_{base}$$

$$\sigma_T^2 = \sum_{i=1}^{n} (T_E \times |T_E|)_i$$

$$\sigma_T = sign(\sigma_T^2) \times \sqrt{|\sigma_T^2|}$$

where T_E is the temperature experienced by the plant and T is the hourly average temperature. The base temperature, T_{base}, used was 0 °C. The 'n' used was 168 and specifies that σ_T is a sum of the temperature variations experienced during the 168 hours (or 7 days) preceding cold hardiness measurements by DTA. The square of T_E was calculated by multiplying the value of

T_E by its absolute value in order to keep the sign. A similar tactic is used to calculate the square-root of σ_T^2 to keep the sign.

Model selection included a forward-backward stepwise procedure with a Bayesian Information Criterion (BIC). BIC was chosen to avoid overfitting the model and because there is a high number of sampling points. First, a model was selected using data from a single year (Year 1), precluding the use of a year term. For this process, the null model included only the intercept and the full model included all parameters, as well as interactions. Subsequently, a model was selected with the full two-year dataset. This time the null model was the regression model previously found, and the full model included the interaction between the terms in the null model with year. Using this new regression model, data points with studentized residual ≥ 2 or Cook's distance ≥ 0.002 were ranked as outliers and removed from the dataset. Finally, the regression model was re-fit using the non-outlier subset to obtain the final coefficients. Dominance analysis was performed to evaluate the relative contribution of each parameter.

Prediction Model. A predictive discrete-dynamic model with 1-day time steps described in detail by Ferguson et al. (Ferguson et al. 2014, 2011) was created in R. The model generates daily cold hardiness predictions for grapevine buds from September 7 to May 15. A stepwise iterative method was used to identify eleven pre-defined cultivar-specific parameters. We included four more levels (-1, 0, 1, and 2 °C) for the ecodormant temperature threshold parameter, in addition to the five levels (3, 4, 5, 6, and 7 °C) used by Ferguson et al., resulting in a total of 2,976,750 parameter combinations (1,323,000 additional combinations, Table 2). The model was optimized and evaluated with the same 2-year dataset. The parameter combination that minimized the RMSE between predicted and observed LT_{50} was selected and evaluated for

each year. Internal model validity was tested by Pearson correlation analysis of predicted versus observed LT_{50}.

Results

Summary of weather conditions. Winter conditions in the two years of this experiment were distinctly different; therefore, the results for each year are described separately. The first day that air temperatures dropped below 0 °C was October 28 and October 12 for Year 1 and Year 2, respectively, and the last day air temperatures dropped below 0 °C was April 29 and April 28 for Year 1 and Year 2, respectively. In Year 1, between September 1 and April 30, on 62 days the maximum temperature was ≤ 0 °C (180 days > 0 °C). During the same time period, in Year 2, on 78 days the maximum temperature was ≤ 0 °C (164 days > 0 °C). The minimum temperature reached during winter of Year 1 was -25.3 °C on January 1. The minimum temperature reached during winter of Year 2 was -32.9 °C on two days, January 30 and January 31, and was part of the 2019 polar vortex split event. These minimum temperatures in Year 2 were extreme for the area. During this event, temperatures in the vineyard dropped below -25 °C for 37 consecutive hours. The minimum temperature during this time, -32.9 °C, was reached twice, on the evening of January 30 and again in the morning of January 31.

Cold hardiness response of CCIHG. All cultivars exhibited the standard U-shaped cold hardiness curve, with acclimation in the fall/early winter and deacclimation in late winter/spring. Figure 1 illustrates the LT_{50} response for each cultivar in both years tested. There were slight differences among cultivars and years in the LT_{50} temperature. The timing of minimal LT_{50} temperatures occurred nearly unanimously in mid-February. The exception to this was Brianna in Year 1, which

reached its minimal LT_{50} in late December and had a comparable (+0.3 °C) LT_{50} in mid-February. Frontenac and La Crescent had the overall lowest LT_{50} values in both years (respectively, -30.6 and -30.3 °C in Year 1 and -28.4 and -29.7 °C in Year 2).

There were also differences in the range of temperature between LT_{10} and LT_{90} throughout the dormant season. The general trend was a small difference between LT_{10} and LT_{90} in the fall during acclimation, changing to a wide difference in midwinter, and then returning to a small difference in spring during deacclimation. The average LT_{10}-to-LT_{90} range for all cultivars in both years was 3.9 °C. The largest LT_{10}-to-LT_{90} range was 9.5 °C measured in Brianna on December 28 in Year 1. The smallest LT_{10}-to-LT_{90} range was 1.6 °C measured in Petite Pearl on November 15 in Year 1. Across all cultivars, the changes in LT_{90} mimicked changes in LT_{50} and had a similar magnitude of difference (average of 1.5 °C). In contrast, the changes in LT_{10} did not parallel the changes in LT_{50} and were also more distant in magnitude (average of 2.3 °C difference).

Year 1 (2017-18). All cultivars had LT_{50} values lower than -20 °C by November 15. Brianna's maximal hardiness (-29.9 °C) occurred in the end of December, while the maximal hardiness for Frontenac (-30.6 °C), La Crescent (-30.3 °C), Marquette (-29.3 °C), and Petite Pearl (-28.9 °C) occurred in early February. All of the cultivars acclimated through the end of December, followed by a period of fluctuating maximal hardiness until the end of February, before continuously deacclimating for the remainder of the sampling period. The only exception to this pattern was Frontenac, which gained hardiness between February and March. All of the cultivars maintained LT_{50} values lower than the daily minimum air temperatures.

Year 2 (2018-19). All the cultivars had LT_{50} values lower than -20 °C by November 13. The rate of acclimation increased after October 12 (Figure 1). Maximal hardiness was measured in the end of February for all cultivars: Brianna (-27.1 °C), Frontenac (-28.4 °C), La Crescent (-29.7 °C), Marquette (-27.8 °C), and Petite Pearl (-27.9 °C). All of the cultivars acclimated rapidly through December, then continued with slow acclimation through the first part of February, before deacclimating rapidly for the remainder of the sampling period.

The minimum temperature of -32.9 °C on January 30 and 31, 2019, was 6.3-7.7 °C colder than the LT_{50} measured most recently (January 16) for all of the cultivars. Buds from all cultivars tested by DTA on February 1 showed no LTEs. Based on these observations, we expected extensive and severe damage in the vineyard. Buds from all cultivars tested by DTA on February 5 showed the resumption of normal peak patterns.

Visual bud injury evaluation. Following the extreme cold weather event in January 2019, an additional collection of buds was dissected to visually evaluate the extent of damage in the vineyard. While some damage was observed, it was not as widespread as the most recently preceding DTA results had indicated to be likely. A higher rate of injury was visible in primary meristems, as compared to secondary meristems. Specifically, meristem injury was in 12.5% primary and 5.0% secondary for Brianna, 5% primary and 0% secondary for Frontenac, 10% primary and 5.0% secondary for La Crescent, 7.5% primary and 0% secondary for Marquette, and 17.5% primary and 2.5% secondary for Petite Pearl.

Explanatory Model. The final multiple linear regression model selected included four parameters, six interaction terms, and an intercept. The equation selected was:

$$\text{LTE} = Cultivar + \sigma_T + Time^2 + Time + \sigma_T{:}\,Time^2 + \sigma_T{:}\,Time + \sigma_T{:}\,Cultivar + Cultivar{:}\,Time + Cultivar{:}\,Time^2 + Time{:}\,Year$$

Estimates were calculated separately for each cultivar and year dataset separately (Table 3). Parameters with estimates that vary across cultivar interacted with the Cultivar parameter (σ_T, $Time^2$, Time). The Time parameter (in days) is the only parameter that varies between years, as detected by the Time x Year interaction. The overall model selected had a p-value < 0.0001 ($2.2\text{x}10^{-16}$) and adjusted-R^2 = 89.5%. The temperature index parameter, σ_T, had an interaction with cultivar but not with year. Groupings for the significant differences between the estimates for σ_T, Time, and $Time^2$ are listed in Table 3. In addition, overall dominance analysis showed σ_T had the largest relative contribution (50.1%), followed by $Time^2$ (18.0%), and then Time (16.4%) (Table 4).

Prediction Model. Collectively, the optimized model parameters predicted LT_{50} values with an overall r^2 = 0.97 ($r^2_{\text{Year 1}}$ = 0.95 and $r^2_{\text{Year 2}}$ = 0.98) and RMSE = 1.01 °C ($\text{RMSE}_{\text{Year 1}}$ = 1.11 and $\text{RMSE}_{\text{Year 2}}$ = 0.91). For all cultivars, $r^2 \geq 0.93$ by internal validity test, while RMSE varied from 0.65 °C for Brianna in Year 2 to 1.30 °C for La Crescent in Year 1. The optimized model parameters for all cultivars and both years predicted LT_{50} values with an overall bias = 3.13×10^{-4} ($\text{bias}_{\text{Year 1}}$ = 0.21 and $\text{bias}_{\text{Year 2}}$ = -0.21). In general, the model slightly underpredicted LT_{50} values in Year 1 and slightly overpredicted LT_{50} values in Year 2. Individual cultivar parameters are listed in Table 5 and performance is illustrated in Figure 2 and 3.

Discussion

This is the first study to report continuous, time series-based bud cold hardiness measurements for CCIHG cultivars grown in a cold-climate region. The main objective of this study was to evaluate changes in bud cold hardiness of CCIHG cultivars during the dormant period, with the goal of identifying periods of higher risk of incurring freeze damage. Bud cold hardiness patterns observed in CCIHG had a similar U-shaped as those previously reported for *V. vinifera* and wild North American species (Cragin et al. 2017, Fennell 2004, Grant and Dami 2015, Kovács et al. 2003, Mills et al. 2006, Pool et al. 1990, Wolf and Cook 1992). However, CCIHG cultivars present noteworthy differences within the classic U-shaped pattern.

Acclimation

The CCIHG cultivars in this study acclimated before experiencing freezing temperatures. During Year 1, these cultivars had LT_{50} values ranging from -16.7 to -18.6 °C within 5 days of the first frost. During Year 2, these cultivars had LT_{50} values ranging from -10.7 to -14.0 °C on the day of the first frost (Figure 1). This is consistent with reports that gradually decreasing daylengths and photoperiods less than 13 hours promote cold acclimation in *V. labrusca* and *V. riparia*, while these phenomena do not promote acclimation in *V. vinifera* (Fennell 2004, Fennell and Hoover 1991, Wake and Fennell 2000). It is possible that the synergistic effect of shorter photoperiod and cooler, but not freezing, temperatures during the late summer and early fall in our study area promote faster acclimation rates in CCIHG cultivars than in other areas with warmer falls. In Wisconsin, the fast acclimation rate of CCIHG, plus the low incidence of hard freeze events (<-2.2 °C) before mid-October (“Freeze Maps - MRCC” 2020), result in a relatively low risk of freeze damage during fall for these cultivars.

Midwinter cold hardiness

The lowest LT_{50} values for these CCIHG cultivars ranged from -28.9 to -30.6 °C in Year 1 and -27.1 to -29.7 °C in Year 2 and were recorded in both years during midwinter (Figure 1). This is comparable to bud cold hardiness levels reported for wild *Vitis* species in northern North America, including *V. labrusca*, *V. riparia*, and *V. aestivalis*, that are able to withstand temperatures as low as -35 °C (Fennell 2004, Keller 2020, Londo and Kovaleski 2017). This is not surprising given that CCIHG cultivars include wild *Vitis* species in their complex genetic background (Maul et al. 2021), and that the focus of CCIHG breeding programs is to release cultivars to be grown in regions where mid-winter temperatures regularly reach -25 °C and colder.

On January 30 and 31, 2019, minimum temperatures were lower than the LT_{50} measured for all cultivars (most recently tested on January 16), when a polar vortex brought record low temperature across the US Midwest region ("NOAA Online Weather Data" 2020). Temperatures at our study site reached -32.9 °C twice within 48 hours and remained below -25 °C for 37 consecutive hours, including 15 hours below -30 °C. No LTEs were detected from the DTA performed the day after the lowest temperature was recorded (vertical dotted line in Figure 1), which led us to believe buds had been damaged in the field when the temperature was lower than their supercooling capacity. However, there was only 10.5% and 2.5% damage in primary meristems and secondary meristems, respectively found in bud dissections performed on a subset of the buds. It is possible that the long exposure to temperatures below -30 °C resulted in freeze dehydration of the buds, lowering the water content inside the buds, thus leading to an increase in freezing stress resistance. This phenomenon has been described by Kasuga et al. (2020) in

interspecific hybrid grapes grown in northern Japan. In that study, buds conditioned to -15 °C for 12 hours experienced partial dehydration of primordial cells, as revealed by cryo-scanning electron microscopy, resulting in a lowering of the buds' median freezing temperature (Kasuga et al. 2020). Similarly, DTA-based studies of *V. riparia* buds did not produce LTEs following prolonged exposure to extreme cold conditions and low relative humidity, which may indicate the loss of all freezable water (Pierquet and Stushnoff 1980, Pierquet et al. 1977). In our conditioning experiments conducted less than two weeks after the extreme low temperature event, no LTEs were detected in the DTA performed after the conditioning protocol and no visual symptoms of freezing damage were observed in bud dissections after allowing expression of damage symptoms (data not shown). DTA is widely used in the scientific community to assess cold hardiness of grape buds. However, its exclusive use to monitor changes in bud freezing stress resistance of existing and future releases of CCIHG cultivars adapted to cold-climate regions may underestimate their true cold hardiness potential due to their buds' ability to partially dehydrate when exposed to prolonged and extreme cold temperature conditions (e.g., 15 hours below -30 °C). Future studies aiming to quantify the full extent of grapevine midwinter cold hardiness should include controlled freezing tests and visual evaluation of freeze damage in buds (e.g., oxidative browning or water-soaked appearance) to complement DTA (Villouta et al. 2020).

Deacclimation

Grapevines in our study began deacclimating in early February 2018 and March 2019, and from this point, buds lost hardiness (Figure 1). One exception to this general trend was in Year 1 when buds deacclimated in early January but then reacclimated by the time of the first

hardiness evaluation in February (Figure 1). Although many factors can affect deacclimation dynamics (Kalberer et al. 2006), the completion of endodormancy appears to be a key factor influencing the onset of deacclimation (Ferguson et al. 2014, 2011). The fulfilment of chilling requirements marks the transition from endo- to ecodormancy (Lang et al. 1987), and is considered to happen in *V. riparia*, *V. vinifera, V. labrusca* and some interspecific hybrids after exposure to 750-1000 chilling hours (Londo and Johnson 2014). In our study, vines experienced 750 chilling hours by February and January in Year 1 and Year 2, respectively. The attainment of 1000 chilling hours by late March in both years coincided with the onset of deacclimation. However, in unpublished data on chilling requirements for these CCIHG cultivars collected by our research group, endodormancy was complete when 400-500 chilling hours had been accumulated, which typically occurs November - mid December in our region. Potential for deacclimation could begin as early as December for CCIHG cultivars grown in Wisconsin. However, deacclimation does not occur during this point in ecodormancy until vines are exposed to temperatures above freezing.

We also observed an increase in the deacclimation rate from late March throughout April in both years. In Year 1, deacclimation rates increased from 0.12-0.14 °C/day to 0.26-0.83 °C/day during this time period. In Year 2, deacclimation rates increased from 0.38-0.53 °C/day to 0.46-0.63 °C/day. Kovaleski et al. (2018b) established that grapevine bud deacclimation rate increases in a logistic relationship as more chilling is accumulated. During the deacclimation period from late March through April, air temperatures were between 0-7.2 °C about 37% and 55% of the time for Year 1 and Year 2, respectively. This additional chilling accumulated during ecodormancy likely increases deacclimation potential, meaning deacclimation responses happen at cool temperatures above 0 °C.

Cultivar differences

Cultivar differences in cold hardiness responsiveness can be compared using the explanatory model because Cultivar was a significant parameter in the final model (Table 3). Cultivar-specific estimates for a particular parameter quantify differences in aspects of cold hardiness responsiveness across cultivars. Overall, Petite Pearl and Brianna bud cold hardiness had relatively low levels of responsiveness to temperature fluctuations, compared to La Crescent, the cultivar with the highest responsiveness, and to Marquette and Frontenac, which had moderate responses to temperature fluctuation, reflected in their respective σ_T estimates (Table 3). In terms of acclimation and deacclimation responses, La Crescent and Brianna had relatively fast responses, reflected in their high Time and $Time^2$ estimate values, while Petite Pearl and Frontenac had slow acclimation and deacclimation responses, compared to the other cultivars (Table 3).

Grape bud cold hardiness prediction

The secondary objective of this study was to test and adapt the discrete-dynamic cold hardiness prediction model developed by Ferguson et al. (Ferguson et al. 2014, 2011) for CCIHG cultivars grown in cold-climate regions. The ecodormant temperature thresholds above 2 °C in the original version of the model limited the accurate estimation of deacclimation during late winter and early spring for the CCIHG cultivars, and thus over-predicted cold hardiness once deacclimation began. Reparametrizing the model with an expanded range for the ecodormant temperature threshold parameter (including -1, 0, 1, and 2 °C) was critical to improve the performance of the prediction model (Figure 2 and 3). The warmest ecodormant temperature

threshold parametrized was for Brianna and Frontenac (1 °C), the coldest was for Marquette (-1 °C), and an intermediate threshold for La Crescent and Petite Pearl (0 °C). Lower ecodormant temperature thresholds than those used by Ferguson et al. allowed the model to accurately calculate deacclimation during cool spring temperatures (Figure 2). Deacclimation at lower temperatures in preparation for bud break could be an important ecological adaptation by CCIHG to maximize their use of shorter growing seasons. However, it also increases the risk of freezing damage for CCIHG buds throughout spring. After reparametrizing with an expanded range of ecodormant temperature thresholds, the overall performance of the predictive model had a RMSE = 1.01 °C, r^2 = 97%, and bias = 3.13×10^{-4}. While these are exceptional model statistics that provide evidence for the possibility to adapt the discrete-dynamic cold hardiness prediction model for CCIHG cultivars, our results are partially a consequence of the limited number of years in our dataset. This model requires further optimization and testing for CCIHG using longer-term cold hardiness datasets collected in the future.

Conclusion

This is the first study to evaluate continuous changes in bud cold hardiness for CCIHG grown in a cold-climate region. These CCIHG cultivars had an early acclimation response during fall, with increased levels of cold hardiness before the occurrence of freezing temperatures, which reflects the decreased risk of freezing damage during the fall in regions with similar fall conditions to southern Wisconsin. Although these CCIHG cultivars maintained deep levels of cold hardiness throughout midwinter, the higher frequency of extreme weather events due to climate change may increase the risk of freezing damage during midwinter. The highest risk of freezing damage to CCIHG is during spring, due to the rapid deacclimation response once air

temperatures rise above freezing. This trait should be considered when evaluating future releases of CCHIG cultivars for cold-climate regions.

Following an extreme cold weather event during our study, we observed a cold hardiness response that presumably leveraged the mechanisms of both deep supercooling and freeze dehydration, which allowed these hybrids to achieve a deeper level of freeze stress resistance than previously evaluated. Further research to provide direct or further supporting evidence of the physiological mechanism underlying this interplay between deep supercooling and freeze dehydration will provide critical information for the breeding of new CCIHG cultivars.

Finally, our predictive model demonstrates that the discrete-dynamic model can be reparametrized to predict CCIHG cultivars' cold hardiness in a cold-climate region. This model and the CCIHG-specific parameters will be a useful tool in the prediction of CCIHG cold hardiness responses to variable climate scenarios and for the evaluation of new sites before planting vineyards, as well as providing assistance to growers in decision-making to minimize yield and vine losses based on freeze damage risk.

Literature Cited

Atucha A, Hedtcke J, Workmaster BA. 2018. Evaluation of cold-climate interspecific hybrid wine grape cultivars for the upper midwest. J Am Pomol Soc 72:80–93.

Cragin J, Serpe M, Keller M, Shellie K. 2017. Dormancy and cold hardiness transitions in winegrape cultivars chardonnay and cabernet sauvignon. Am J Enol Vitic 68:195–202.

Dami I, Lewis D. 2014. 2014 Grape Winter Damage Survey Report. Ohio State University.

Dami I, Bordelon B, Ferree DC, Brown M, Ellis MA, Williams RN, Doohan D. 2005. Midwest Grape Production Guide. Bulletin 919.

Fennell A. 2004. Freezing tolerance and injury in grapevines. J Crop Improv 10:201–235.

Fennell A, Hoover E. 1991. Photoperiod influences growth, bud dormancy, and cold acclimation in Vitis labruscana and V. riparia. J Am Soc Hortic Sci 116:270–273.

Ferguson JC, Tarara JM, Mills LJ, Grove GG, Keller M. 2011. Dynamic thermal time model of cold hardiness for dormant grapevine buds. Ann Bot 107:389–396.

Ferguson JC, Moyer MM, Mills LJ, Hoogenboom G, Keller M. 2014. Modeling dormant bud cold hardiness and Budbreak in twenty-three Vitis genotypes reveals variation by region of origin. Am J Enol Vitic 65:59–71.

Freeze Maps - MRCC. 2020. (accessed December 29, 2020). as found on the website (https://mrcc.illinois.edu/VIP/frz_maps/area_150.html#frzMaps).

Goffinet MC. 2004. Anatomy of Grapevine Winter Injury and Recovery. Cornell University.

Grant TNL, Dami IE. 2015. Physiological and biochemical seasonal changes in vitis genotypes with contrasting freezing tolerance. Am J Enol Vitic 66:195–203.

Kalberer SR, Wisniewski M, Arora R. 2006. Deacclimation and reacclimation of cold-hardy plants: Current understanding and emerging concepts. Plant Sci 171:3–16.

Kasuga J, Tsumura Y, Kondoh D, Jitsuyama Y, Horiuchi R, Arakawa K. 2020. Cryo-scanning electron microscopy reveals that supercooling of overwintering buds of freezing-resistant interspecific hybrid grape ‘Yamasachi’ is accompanied by partial dehydration. J Plant Physiol 253:1–6.

Keller M. 2020. The Science of Grapevines. Academic Press, an imprint of Elsevier London.

Kovács LG, Byers PL, Kaps ML, Saenz J. 2003. Dormancy, cold hardiness, and spring frost hazard in Vitis amurensis hybrids under continental climatic conditions. Am J Enol Vitic 54:8–14.

Kovaleski AP, Reisch BI, Londo JP. 2018. Deacclimation kinetics as a quantitative phenotype

for delineating the dormancy transition and thermal efficiency for budbreak in Vitis species. AoB Plants 10:1–12.

Lang GA, Early JD, Martin GC, Darnell RL. 1987. Endo-, para-, and Ecodormancy: Physiological Terminology and Classification for Dormancy Research. HortScience 22:371–377.

Londo JP, Johnson LM. 2014. Variation in the chilling requirement and budburst rate of wild Vitis species. Environ Exp Bot 106:138–147.

Londo JP, Kovaleski AP. 2017. Characterization of Wild North American Grapevine Cold Hardiness Using Differential Thermal Analysis. Am J Enol Vitic 68:203–212.

Luby J, Fennell A. 2006. Fruit breeding for the northern great plains at the University of Minnesota and South Dakota State University. HortScience 41:25–26.

Maul E, Töpfer R, Röckel F, Brühl U, Hundemer M, Mahler-Ries A, Walk M, Kecke S, Wolck A, Ganesch A. 2021. Vitis International Variety Catalogue. as found on the website (www.vivc.de).

Mills LJ, Ferguson JC, Keller M. 2006. Cold-hardiness evaluation of grapevine buds and cane tissues. Am J Enol Vitic 57:194–200.

National Centers for Environmental Information. 2020. (accessed December 29, 2020). as found on the website (https://www.ncdc.noaa.gov/).

NEWA. 2020. (accessed December 29, 2020). as found on the website (http://www.newa.cornell.edu/).

NOAA Online Weather Data. 2020. (accessed December 29, 2020):Applied Climate Information System. as found on the website (https://w2.weather.gov/climate/xmacis.php?wfo=mkx).

Pierquet P, Stushnoff C. 1980. Relationship of Low Temperature Exotherms to Cold Injury in Vitis Riaria Michx. Am J Enol Vitic 31:1–6.

Pierquet P, Stushnoff C, Burke M. 1977. Low Temperature Exotherms in Stem and Bud Tissues of Vitis riparia Michx. J Am Soc Hortic Sci 102:54–55.

Pool R, Reisch B, Welser M. 1990. Use of differential thermal analysis to quantify bud cold hardiness of grape selections and clones. Vitis 29:318–329.

Smiley L, Cochran D. 2016. A Review of Cold Climate Grape Cultivars. Iowa State University Extension and Outreach.

Tuck B, Gartner W, Appiah G. 2017. Economic Contribution of Vineyards and Wineries of the North, 2015. University of Minnesota Extension.

Villouta C, Workmaster BA, Bolivar-Medina J, Sinclair S, Atucha A. 2020. Freezing stress

survival mechanisms in Vaccinium macrocarpon Ait. terminal buds. Tree Physiol 40:841–855.

Wake CMF, Fennell A. 2000. Morphological, physiological and dormancy responses of three Vitis genotypes to short photoperiod. Physiol Plant 109:203–210.

Warmund MR, Guinan P, Fernandez G. 2008. Temperatures and cold damage to small fruit crops across the eastern United States associated with the April 2007 freeze. HortScience 43:1643–1647.

Web Soil Survey - USDA NRCS. 2020. (accessed December 29, 2020). as found on the website (https://websoilsurvey.sc.egov.usda.gov/App/WebSoilSurvey.aspx).

Williams L, Dokoozlian N, Wample R. 1994. Grape. *In* Handbook of Environmental Physiology of Fruit Crops, vol. I Temperate Crops. B Schaffer and P Andersen (eds.), pp. 85–133. CRC Press.

Wisniewski M, Willick I, Gusta L V. 2017. Freeze Tolerance and Avoidance in Plants. *In* Plant Stress Physiology. S Shabala (ed.), pp. 279–299. CAB International.

Wolf TK, Cook MK. 1992. Seasonal Deacclimation Patterns of Three Grape Cultivars at Constant, Warm Temperature. Am J Enol Vitic 43:171–179.

Zabadal TJ, Dami IE, Goffinet MC, Martinson TE, Chien ML. 2007. Winter Injury to Grapevines and Methods of Protection. Michigan State Univ Ext:1–44.

Tables

Table 1. Symbols, abbreviations, and units of measurement used in explanatory and predictive models.

Abbreviation	Definition	Unit
B	Bias or mean error	°C
EDB	Ecodormancy boundary, accumulation of chilling degree days required to transition from endo- to ecodormancy	°C
$H_{c,\ initial}$	Initial cold hardiness	°C
$H_{c,\ max}$	Maximum hardiness (most hardy condition)	°C
$H_{c,\ min}$	Minimum hardiness (least hardy condition)	°C
$k_{a,\ eco}$	Acclimation rate during ecodormancy	°C/°C
$k_{a,\ endo}$	Acclimation rate during endodormancy	°C/°C
$k_{d,\ eco}$	Deacclimation rate during ecodormancy	°C/°C
$k_{d,\ endo}$	Deacclimation rate during endodormancy	°C/°C
LT_{10}	Temperature lethal to 10% of buds sampled	°C
LT_{50}	Temperature lethal to 50% of buds sampled	°C
LT_{90}	Temperature lethal to 90% of buds sampled	°C
RMSE	Root mean square error	°C
$T_{th,\ eco}$	Threshold temperature to calculate degree days during ecodormancy relevant to changes in hardiness	°C
$T_{th,\ endo}$	Threshold temperature to calculate degree days during endodormancy relevant to changes in hardiness	°C
θ	Theta exponent in deacclimation logistic equation	dimensionless
σ_T	Sigma-T, temperature index in the explanatory model	°C

Table 2. Parameter levels tested in all combinations stepwise for five cold-climate interspecific hybrid grapevine cultivars to minimize root mean square error (RMSE): endodormant temperature threshold ($T_{th,endo}$), ecodormant temperature threshold ($T_{th,eco}$), endodormant acclimation rate ($k_{a,endo}$), ecodormant acclimation rate ($k_{a,eco}$), endodormant deacclimation rate ($k_{d,endo}$), ecodormant deacclimation rate ($k_{d,eco}$), theta exponent in deacclimation logistic equation (θ), and ecodormancy boundary (EDB). A total of 2,976,750 combinations were tested per cultivar and for two years (2017-18 and 2018-19).

	$T_{th,endo}$ (°C)	$T_{th,eco}$ (°C)	$k_{a,endo}$ (°C/°C)	$k_{a,eco}$ (°C/°C)	$k_{d,endo}$ (°C/°C)	$k_{d,eco}$ (°C/°C)	θ	EDB (°C)
Start	9.0	-1.0	0.04	0.02	0.02	0.04	1.0	-300
Stop	15.0	7.0	0.16	0.10	0.10	0.20	7.0	-800
Step	1.0	1.0	0.02	0.02	0.02	0.02	2.0	100
n	7	9[a]	7	5	5	9	5[b]	6

[a] Levels for $T_{th,eco}$ started at -1.0 as compared to 3.0 in Ferguson et al. (2014).

[b] θ = 1.5 was also tested.

Table 3. Estimates for parameters and interactions for the explanatory linear regression model describing low temperature exotherms for five cold-climate interspecific hybrid grapevine cultivars during two years using the temperature index (σ_T), Time (days), and Time^2 (days^2) as parameters. Parameters separated by a colon represent interactions between two parameters. Different letters within a column denote statistical differences between cultivars using a t-test with $\alpha = 0.05$.

Cultivar	Intercept	σ_T	Time^2	Time	Interaction σ_T:Time^2	Interaction σ_T:Time
Year 1 (2017-18)						
Brianna	-3.4968 ± 0.9976 a	0.0154 ± 0.0032 c	0.0013 ± 0.0001 a	-0.3523 ± 0.0169 a	1.03×10^{-6} ± 1.60×10^{-7}	-1.90×10^{-4} ± 4.06×10^{-5}
Frontenac	-5.9346 ± 0.9943 b	0.0169 ± 0.0032 bc	0.0010 ± 0.0001 c	-0.2964 ± 0.0170 bc		
La Crescent	-5.7240 ± 1.0104 b	0.0218 ± 0.0032 a	0.0011 ± 0.0001 b	-0.3127 ± 0.0173 b		
Marquette	-5.8606 ± 1.0065 b	0.0184 ± 0.0032 b	0.0011 ± 0.0001 b	-0.3054 ± 0.0171 bc		
Petite Pearl	-6.6509 ± 1.0174 b	0.0144 ± 0.0032 c	0.0010 ± 0.0001 c	-0.2838 ± 0.0174 c		
Year 2 (2018-19)						
Brianna	-4.6544 ± 0.9601 a	0.0154 ± 0.0032 c	0.0013 ± 0.0001 a	-0.3369 ± 0.0168 a	1.03×10^{-6} ± 1.60×10^{-7}	-1.90×10^{-4} ± 4.06×10^{-5}
Frontenac	-7.5035 ± 0.9555 bc	0.0169 ± 0.0032 bc	0.0010 ± 0.0001 c	-0.2810 ± 0.0168 bc		
La Crescent	-6.7422 ± 0.9679 b	0.0218 ± 0.0032 a	0.0011 ± 0.0001 b	-0.2973 ± 0.0171 b		
Marquette	-8.0404 ± 0.9654 c	0.0184 ± 0.0032 b	0.0011 ± 0.0001 b	-0.2899 ± 0.0169 bc		
Petite Pearl	-7.6518 ± 0.9822 bc	0.0144 ± 0.0032 c	0.0010 ± 0.0001 c	-0.2683 ± 0.0172 c		

Table 4. Relative contribution of parameters in the explanatory linear regression model calculated using dominance analysis. The temperature index is represented by σ_T. Parameters separated by a colon represent interactions between two parameters.

Relative importance:		
σ_T 50.1%	$Time^2$:Year 0.7%	Cultivar 0.3%
$Time^2$ 18.0%	$Time^2$:Cultivar 0.6%	σ_T:Time 0.3%
Time 16.4%	σ_T:Cultivar 0.5%	Cultivar:Year 0.2%
Year 1.8%	σ_T:$Time^2$ 0.4%	

Table 5. Parameter value combinations that minimize root mean square error (RMSE) after reparametrizing the predictive discrete-dynamic model to simulate bud cold hardiness for five cold-climate interspecific hybrid grapevine cultivars. Cold hardiness (H_c) predictions begin at $H_{c,\ initial}$, which is the earliest median low temperature exotherm (LT_{50}) observed. Predictions are bound by lower ($H_{c,\ max}$) and upper ($H_{c,\ min}$) limits. $H_{c,\ max}$ is the lowest LT_{50} observed, while $H_{c,\ min}$ is highest LT_{50} observed. Other parameters include: endodormant temperature threshold ($T_{th,endo}$), ecodormant temperature threshold ($T_{th,eco}$), endodormant acclimation rate ($k_{a,endo}$), ecodormant acclimation rate ($k_{a,eco}$), endodormant deacclimation rate ($k_{d,endo}$), ecodormant deacclimation rate ($k_{d,eco}$), theta exponent in deacclimation logistic equation (θ), and ecodormancy boundary (EDB).

Cultivar	$T_{th,\ endo}$ (°C)	$T_{th,\ eco}$ (°C)	$k_{a,\ endo}$ (°C/°C)	$k_{d,\ endo}$ (°C/°C)	$k_{a,\ eco}$ (°C/°C)	$k_{d,\ eco}$ (°C/°C)	θ	EDB (°C)	$H_{c,\ initial}$ (°C)	$H_{c,\ max}$ (°C)	$H_{c,\ min}$ (°C)
Brianna	9	1	0.10	0.02	0.10	0.16	7	-600	-11.0	-29.9	-9.0
Frontenac	12	1	0.08	0.06	0.10	0.20	1.5	-300	-10.5	-30.6	-10.5
La Crescent	11	0	0.08	0.06	0.10	0.14	3	-600	-9.6	-30.3	-9.6
Marquette	13	-1	0.06	0.06	0.04	0.10	7	-600	-11.5	-29.3	-10.2
Petite Pearl	15	0	0.04	0.08	0.10	0.18	1	-600	-11.4	-28.9	-11.4

Figures

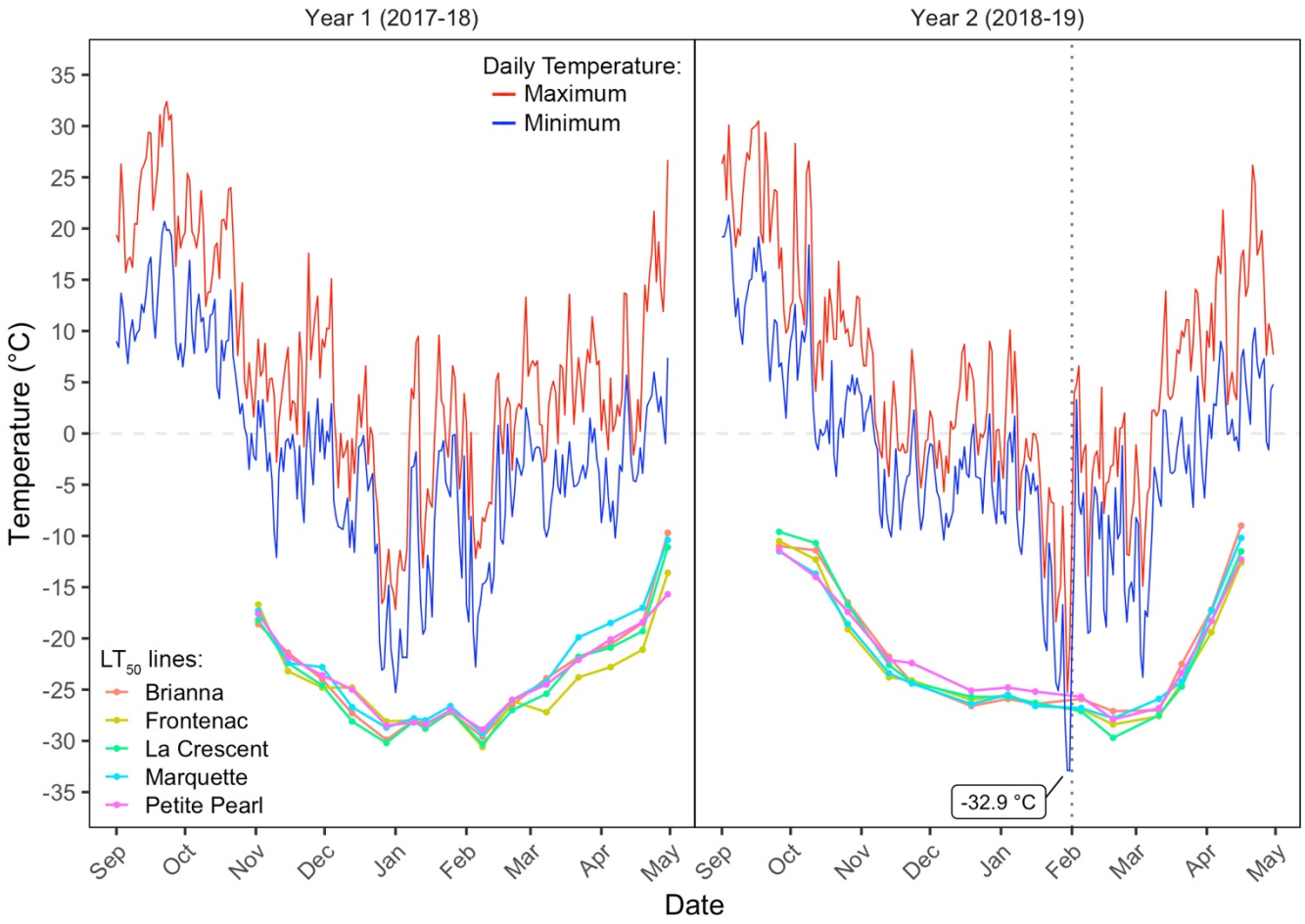

Figure 1. Median low temperature exotherm (LT_{50}) trends plotted for five cold-climate interspecific hybrid grapevine cultivars, with daily maximum (red line) and minimum (blue line) temperatures for 2017-18 and 2018-19. Vertical dotted line identifies the date (February 1, 2019) that buds tested with differential thermal analysis showed no low temperature exotherms.

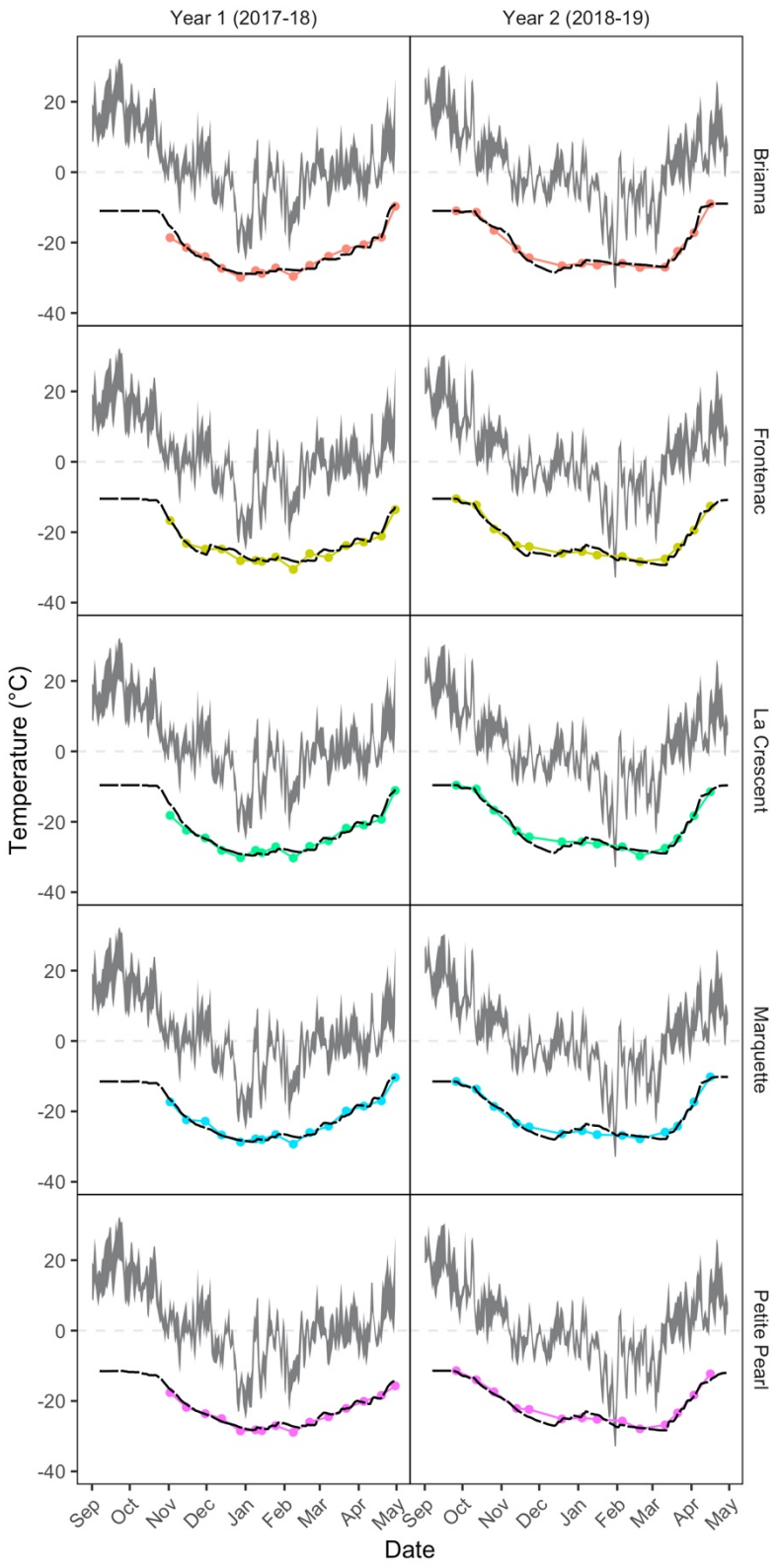

Figure 2. See caption on the follow page.

Figure 2. Predicted bud cold hardiness (black, dashed lines) and observed median low temperature exotherm (LT_{50}) values (colored lines and circles) plotted for five cold-climate interspecific hybrid grapevine cultivars, with daily maximum and minimum temperature ranges for 2017-18 and 2018-19 (gray shaded area). Predictions were generated using the Ferguson et al. (2011, 2014) model reparametrized for each cultivar.

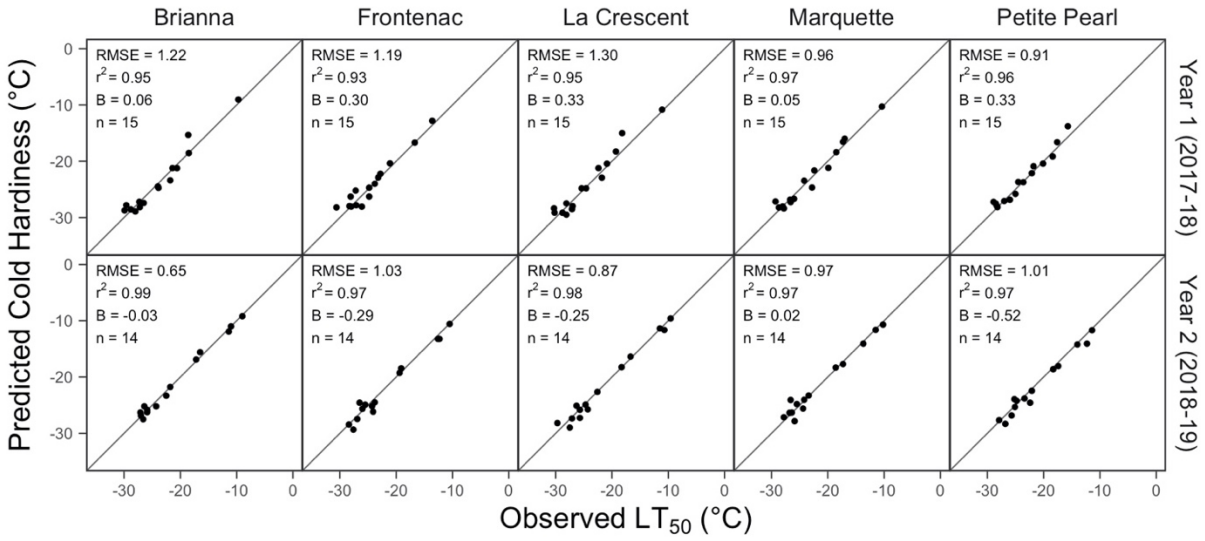

Figure 3. Comparison between predicted and observed bud cold hardiness, expressed as median low temperature exotherm (LT_{50}) for five cold-climate interspecific hybrid grapevine cultivars, including r^2, bias (B), and sample size (n) for each cultivar and year. Predictions were generated using the Ferguson et al. (2011, 2014) model reparametrized for each cultivar.

Chapter 3: The effect of ambient temperature and chill unit accumulation on deacclimation kinetics

Abstract

Woody perennials develop cold hardiness mechanisms in the fall and lose cold hardiness mechanisms in the spring in order to survive freezing winter temperatures. Acquiring and losing cold hardiness are referred to as acclimation and deacclimation, respectively. Previous studies have demonstrated deacclimation responses increase as ambient temperatures increase and between endodormancy and ecodormancy. However, the progression of increasing deacclimation responses across a range of temperatures and throughout the transition from endo- to ecodormancy is not well described. Climate change predictions, such as warmer winters, erratic and extreme winter weather events, and late spring frosts could also disrupt optimal timing of deacclimation. More detailed descriptions of the factors regulating deacclimation are necessary to understand the risks plants may face under climate change scenarios. In this study, we aimed to describe temporal relationships between deacclimation responses and chill unit accumulation at various temperatures. We also aimed to test a quantitative method to determine bud dormancy status using an assessment of deacclimation potential (Ψ_{deacc}). We evaluated cold hardiness loss and budbreak under multiple temperature conditions at multiple levels of chill unit accumulation using differential thermal analysis (DTA) and bud forcing assays. Deacclimation responses increased continuously following logistic trends as chill unit accumulation increased. The cumulative chill unit range where Ψ_{deacc} increased, overlapped with the transition from endo- to ecodormancy. Therefore, deacclimation potential provides an objective and quantitative method

for describing dormancy transitions. Deacclimation responses also increased following a nonlinear trend as ambient temperature increased. There are optimal temperatures where deacclimation rates increased but below and above these temperatures, changes in deacclimation rates diminished. This information will contribute to a clearer understanding of when and how deacclimation might contribute to increased risks by freezing injury. In addition, our descriptions of factors effecting deacclimation could inform improvements to models predicting cold hardiness, dormancy transitions, and phenological development.

Introduction

Perennial plants in temperate climates synchronize development, maintenance, and loss of cold hardiness mechanisms with the annual rhythm of seasonally occurring freezing temperatures in order to survive freezing temperatures (Hänninen and Kramer 2007, Levitt 1980). Properly timed acclimation (e.g., gaining cold hardiness) and deacclimation (e.g., losing cold hardiness) is essential for plants to minimize freeze injury risks while also maximizing opportunities for growth. Early deacclimation increases the risk of freeze injury whereas late deacclimation delays growth resumption and leads to lost opportunity for growth resources (Hanninen 2013). However, climate change predictions, such as warmer winters overall, erratic and extreme winter weather events, and late spring frosts could disrupt the timing of deacclimation and, as a consequence, increase freeze injury risks (Gu et al. 2008, IPCC 2014, Pagter and Arora 2013).

Ambient temperature is a major factor driving deacclimation (Arora and Taulavuori 2016). In general, deacclimation responses increase as ambient temperatures increase (Kalberer

et al. 2006). However, deacclimation cannot be predicted solely based on temperature because deacclimation is also influenced by the dormancy status of a plant (Ferguson et al. 2014, Ögren 2001, Taulavuori et al. 2004, Vitasse et al. 2014b, Vyse et al. 2019). Dormancy is defined as the suspension of visible growth and development in meristem containing structures, such as buds (Lang 1987). There are three main categories of dormancy, which are divided based on the mechanism associated with growth cessation, including: para-, endo- and ecodormancy (Lang et al. 1987). Of particular relevance to deacclimation are endodormancy and ecodormancy. During endodormancy, the signals suspending growth originate from within the meristem itself. Buds overcome endodormancy and transition to ecodormancy upon prolonged exposure to low, non-freezing temperatures, a process referred to as chill unit accumulation (Coville 1920, Junttila and Hänninen 2012, Londo and Johnson 2014). During ecodormancy, growth is suspended due to unfavorable environmental conditions, which means growth and development resumes upon the return of suitable conditions. Buds are resistant to deacclimation during endodormancy whereas buds are considered "physiologically primed" for deacclimation during ecodormancy (Arora and Rowland 2011, Arora and Taulavuori 2016, Kalberer et al. 2006, Litzow and Pellett 1980, Wolf and Cook 1992). Therefore, descriptions of a deacclimation responses require an understanding of dormancy status in addition to considering the effects of ambient temperatures.

How dormancy status effects on deacclimation responses is not well understood. Distinguishing the effects of dormancy status from the effects of ambient temperature on deacclimation is complicated by the fact that mechanisms regulating dormancy are also directly influenced by temperature. More thorough descriptions of the role of dormancy status and temperature in regulating deacclimation are necessary to better understand seasonal rhythms of deacclimation kinetics.

Deacclimation potential (Ψ_{deacc}) is a rate ratio that quantifies deacclimation responses in proportions relative to the maximum observed response (Kovaleski et al. 2018a). Considering dormancy status is a factor regulating deacclimation responses, deacclimation potential can be used to assess dormancy status. Dormancy status is traditionally assessed via bud forcing assays that observe percent budbreak and time to (50%) budbreak under favorable growth conditions. However, deacclimation potential does not rely on an arbitrary assumption, such as the threshold time to 50% budbreak. Deacclimation potential also quantifies a bud growth phenotype that proceeds externally visible bud growth, which is the observation necessary for bud forcing assays. This highlights an important association between deacclimation potential and results from bud forcing assays, that is visible bud growth is only apparent after a bud has deacclimated (Ferguson et al. 2014, Salazar-Gutiérrez et al. 2014). Therefore, a quantitative assessment tool such as deacclimation potential could be an advantageous alternative to bud forcing assays for describing dormancy transitions.

The main objective of this study was to evaluate the effect of chill unit accumulation and temperature on dormancy status, deacclimation responses, and budbreak in five interspecific hybrid grapevine cultivars grown in a cold-climate region. In addition, we aim to test a method that uses deacclimation potential to quantify the contribution of chill unit accumulation to dormancy transitions. This information will contribute to a clearer understanding of when and how climactic conditions might contribute to increased risks by freezing injury. In addition, a more thorough description of factors that effect deacclimation could inform improvements to models predicting cold hardiness, dormancy transitions, and phenological development.

Materials and Methods

Site description. This study was conducted during two winter seasons, 2018-2019 (Year 1), and 2019-2020 (Year 2) in a vineyard at the West Madison Agricultural Research Station in Verona, WI (lat. 43° 03' 37" N, long. 89° 31' 54" W). The vineyard is in U.S. Department of Agriculture Plant Hardiness Zone 5a (USDA, 2019).

Weather data. Weather data were collected from September 1 to April 30 using a Network for Environment and Weather Applications (NEWA; http://www.newa.cornell.edu/) participating station (Model MK-III SP running IP-100 software; Rainwise, Trenton, ME). Hourly weather data were used to compute chill units using the North Carolina ('NC') model (Shaltout and Unrath 1983). Cumulative number of chill units was calculated using different start dates for each season. First, the cumulative chill was calculated starting from September 1. Second, the time after September 1 with the most negative number of chill units was identified and cumulative chill was re-calculated with this as the start date for computing chill unit accumulation. These dates were September 21, 2018, and October 2, 2019.

Bud sampling. The vineyard is arranged as a randomized complete block design with four replications. Each block is comprised of two rows of vines that include six, four-vine panels per row. A maximum of 10 buds per vine were sampled for deacclimation experiments and bud forcing assays from node positions three to ~ten. Buds were sampled evenly across vineyard blocks and vines within vineyard blocks (16 vines total for each cultivar). Canes were cut several centimeters away from the bud. Buds were collected in plastics bags, stored on ice during

transportation, and prepped immediately upon returning to the lab. Sample frequency for bud forcing assays and deacclimation experiments in each year are listed in Table 1.

Bud forcing assays. For each bud forcing assay, 25 single-node cuttings were placed in square 8-cm pots that were arranged in plastic seedling trays filled with deionized water. The trays were maintained at 22±1.5 °C with a 16-hour photoperiod using LED fixtures (Model: HY-MD-D169-S, Roleandro, Shenzhen, China). The LED fixtures include blue (460-465 nm) and red (620-740 nm) lights with 150 µmol $m^{-2}s^{-1}$ photon flux. The growth stage of the bud on each single-node cutting was evaluated every day for up to 60 days, and the date of budbreak was recorded. Budbreak was defined as stage 3 (wooly bud) of the modified E-L system (Coombe 1995). Buds that had no visible change by the end of the assay were dissected with a razor blade to determine if the bud was viable (green) or dead (brown). Dead buds were removed from the sample used for data analysis.

Similar bud forcing assays were conducted in 2019-20 but under four different forcing temperatures conditions (10, 15, 20, 25 °C). Photoperiod and light intensity were the same as in 2018-19. Buds were evaluated daily for up to 120 days and the date of budbreak was recorded. Budbreak was defined as stage 3 (wooly bud) in the modified E-L system (Coombe 1995).

Deacclimation experiments. Canes were cut into single-node cuttings and cuttings were randomized across vines and blocks. The randomized cuttings were then grouped into bundles, wrapped at either end of the bundle with moist paper towels, and sealed in a plastic bag. The bagged bundles were placed in growth chambers programmed to a constant 0, 7, 10, 14, 15, 20, 21, and 25 °C. Within each year, deacclimation experiments were a full factorial design, where

all combinations of factors were tested at once. However, not all cultivars or temperatures were included in each season's experiments (Table 1).

Cold hardiness evaluation. Differential thermal analysis (DTA) was used to estimate the cold hardiness of individual buds by measuring their low temperature exotherms (LTE) (Mills et al. 2006). The DTA equipment and sample preparation used in this study was the same as described in Chapter 2. To summarize, the equipment used includes four trays with thermoelectric modules (TEMs) (model HP-127-1.4-1.5-74 and model SP-254-1.0-1.3, TE Technology, Traverse City, MI) to detect exothermic freezing reactions. A copper-constantan (Type T) thermocouple (22 AWG) was positioned on each tray to monitor temperature. Trays with TEMs and thermocouples were loaded in a Tenney Model T2C programmable freezing chamber (Thermal Product Solutions, New Columbia, PA) connected to a Keithley 2700-DAQ-40 multimeter data acquisition system (Keithley Instruments, Cleveland, OH). TEM voltage and thermocouple temperature readings were collected at 6- or 15-second intervals via a Keithley add-in for Microsoft Excel (Microsoft Corp., Redmond, WA) or Keithley KickStart software.

Each DTA included 15 buds per storage temperature treatment per cultivar. To prepare samples for DTA, buds including the bud cushion were excised from the cane. The cut surface of the bud was covered with a piece of Kimwipe (Kimberly Clark, Roswell, GA) moistened with water to provide an extrinsic ice nucleator source and to prevent dehydration prior to bud freezing. A group of five buds from the same cultivar and temperature treatment was wrapped in aluminum foil and placed on a TEM. The trays were cooled to 4 °C and conditioned for an hour, cooled to 0 °C and conditioned for an hour, then cooled to -44 °C at a rate of -4 °C per hour. Intervals between DTA for deacclimation experiment are listed in Table 1.

Bud forcing data analysis. All data analysis was performed using R (ver. 4.0.5; R Core Team 2021). The relationship between chill unit accumulation and budburst rate was visualized for each cultivar by plotting days to budbreak as box-and-whisker plots for each level of chill unit accumulation. A smoothed line was then fit using the "loess" method of non-parametric regression. Chilling requirements were classified as fulfilled when the fitted regression line crossed 28 days, i.e., 50% of buds reached budbreak within 28 days of exposure to bud forcing assay conditions (Londo and Johnson 2014).

Deacclimation data analysis. Individual deacclimation rates (k_{deacc}) were calculated using linear regression for each temperature and chill unit accumulation as factors (regression results including slopes are available in Appendix A). The regression models were allowed to have varying intercepts for each level of temperature and chill. In addition, data points that had a studentized residual ≥ 3.0 were considered outliers and removed from the data set, and each regression model was re-fit without these outliers (Cook 1977). Rates from each model were used for analysis of the effects of chill unit accumulation, the effects of temperature, and the combined effects of chill unit accumulation and temperature.

Effects of chill unit accumulation. The deacclimation rate at each chill unit accumulation were transformed to a percentage ratio, by normalizing to the mean of the two highest rates. This was done separately for each temperature treatment $(k_{deacc(T)} / [\frac{k_{deacc,(T,max)} + k_{deacc(T,max-1)}}{2}]) \times 100$. The resulting ratio is referred to as deacclimation potential (Ψ_{deacc}). Predictions for Ψ_{deacc} across

the chill continuum were estimated as a logistic curve using the nls() function with the port algorithm, following the equation,

$$\Psi_{deacc} = \frac{1}{1+e^{[b\times(\ln Chill - \ln c)]}} ,$$

where *b* and *c* are parameters estimated by the model and *Chill* is the chill unit accumulation at each prediction. The parameter *c* is the inflection point of the logistic curve and the parameter *b* estimates the steepness of the curve.

To calculate critical chill quantities along the deacclimation potential curve, we applied a mathematical procedure that has been used in other disciplines studying phenomena also described by logistic curves (Deshpande and Jia 2020, McDowall and Dampney 2006). These chill quantities are referred to as chill threshold ($chill_{thr}$), chill saturation ($chill_{sat}$), and *active chill range*. A conceptual illustration and the relevant equations for each of these estimates are described in Figure 1. Briefly, the line tangent to Ψ_{deacc} at its inflection point is fit (this is a straight line with a slope based on the first derivative of Ψ_{deacc} at parameter *b* and parameter *c*). $Chill_{thr}$ is the point where that tangent line is equal to no deacclimation potential ($\Psi_{deacc} = 0$). $Chill_{sat}$ is the point that tangent line is equal to maximum deacclimation potential (Ψ_{deacc} = 100%). The *active chill range* is the difference between $chill_{thr}$ and $chill_{sat}$.

Effects of temperature. Deacclimation rates were analyzed for temperature effects at each level of chill unit accumulation separately. The effect of temperature, referred to as relative thermal contribution (H_{deacc}), was tested for nonlinearity by fitting a linear, quadratic and cubic model with deacclimation rate as the response variable and temperature (°C) as the explanatory variable. A likelihood ratio test was used to compare the linear model with second- and third-

degree polynomials. The effect of temperature was also estimated as a logistic curve. To do this, H_{deacc} was estimated using the nls() function with the port algorithm, following the equation,

$$H_{deacc} = a + \frac{k_{deacc,max}}{1+e^{[g\times(\ln T - \ln h)]}} \ ,$$

where *a, g,* and *h* are estimated parameters and *T* is the temperature in °C. The parameter *a* is the lower limit of the logistic curve, the parameter *c* is the inflection point of the logistic curve and the parameter *b* estimates the steepness of the curve at the inflection point.

Combined effects of chill unit accumulation and temperature. The combined effect of chill unit accumulation and temperature were estimated by a combined logistic curve using the nls() function with the port algorithm, following the equation,

$$k_{deacc(T,Chill)} = \Psi_{deacc} \times H_{deacc} = \frac{1}{1+e^{[b\times(\ln Chill - \ln c)]}} \times \left[a + \frac{k_{deacc,max}}{1+e^{[g\times(\ln T - \ln h)]}}\right] \ ,$$

where Ψ_{deacc} and H_{deacc} are equal to the equations previously described. This combined model estimated all parameters (b, c, a, g, and h) based on *Chill* and *T* (°C) inputs.

The fits of all non-linear curves were tested using Effron's pseudo-R^2 with the Rsq() function in the soilphysics library. A linear model was used with the complete LTE data set to evaluate the accuracy of the combined model's deacclimation predictions. In this model, change in LTE (ΔLTE) is a function of the temperature (T) that a bud was stored at, the quantity of chill units accumulated (*Chill*) before exposure to deacclimation temperatures, and the duration of exposure to deacclimation temperatures (time). The temperature and chill unit accumulation effects are incorporated in the combined model and represented within k_{deacc}. Considering predictions were accurate, the β associated with k_{deacc} was expected to be 1 ($\Delta LTE_{(T,Chill)} = \beta \times k_{deacc} \times time$), meaning there is 1 unit change in ΔLTE for every 1-unit change in k_{deacc}.

Results

Bud forcing assays. The time to 50% budbreak decreased as chill units accumulated (Figure 2). For cultivars included in both years, the chill requirements were lower in Year 1 than in Year 2 according to 50% budbreak within 28 days. Chill requirements ranged from 674-761 ('NC') in Year 1 and from 428-602 ('NC') in Year 2.

For budbreak assays that included multiple forcing temperature treatments, days to 50% budbreak decreased for all temperatures as chill units accumulated (Figure 3). At low chill, buds incubated at warmer temperatures reached 50% budbreak faster than buds incubated at cooler temperatures. As chill increased, warmer temperatures generally still reached 50% budbreak in fewer days but the difference was smaller across temperatures.

Linear regression for deacclimation rates. Deacclimation responses were linear across time at all temperatures regardless of how much chill had accumulated (Supplemental Table in Appendix A). After outliers were removed from multiple linear regression analysis, ≥84% of the observations were kept for each cultivar in both years. The minimum portion of observations kept for each year were 97.6% in Year 1, and 86% in Year 2.

The deacclimation slopes for a given temperature increased as chill units accumulated. However, deacclimation rates for experiments at chill unit accumulation >~1100 ('NC') were slightly lower than the maximum deacclimation rate previously measured. Higher temperatures produced higher deacclimation rates as compared to lower temperatures, regardless of chill unit accumulation. There were two deviations from this trend. First, deacclimation rates were similarly small for 0, 7, and 14°C at 689 ('NC'), or low cumulative chill, in Year 1. Second,

deacclimation rates were comparable for all temperatures tested (10, 15, 20, and 25°C) at 1289 ('NC'), or high cumulative chill, in Year 2.

Effects of chill unit accumulation (Ψ_{deacc}). Deacclimation rates continuously increased as chill units accumulated. The continuum of deacclimation rates was quantified using a rate ratio, referred to as deacclimation potential (Ψ_{deacc}), by normalizing deacclimation rates across chill unit accumulation to an average of the two highest deacclimation rates. Psuedo-R^2 values for Ψ_{deacc} models were between 0.51 and 0.62 in Year 1 and between 0.79 and 0.98 in Year 2 (Table 2). Deacclimation potential followed a logistic curve as chill units accumulated when asymptotic bounds at 0 and 100 were used as inputs for initial and final deacclimation potential, respectively (Figure 4). The period where deacclimation potential increased correlated with chilling requirements estimated by bud forcing assays (Figure 2).

Three critical chill quantities were calculated based on Ψ_{deacc} models, including chill threshold ($chill_{thr}$), chill saturation ($chill_{sat}$), and *active chill range*. There were similar portions of Ψ_{deacc} that correlated with $chill_{thr}$, $chill_{sat}$, and *active chill range* for all cultivars in both years ([e, f, g] in Table 3). In terms of absolute chill units, $chill_{thr}$ and $chill_{sat}$ varied between years, while *active chill range* did not ([b, c, d] in Table 3). For cultivars that were included in both years of the study, values for $chill_{thr}$ in Year 1 were similar to the $chill_{sat}$ values in Year 2. Inflection points for Ψ_{deacc} curves (parameter *c*) also varied between years than across cultivars (Table 2). Inflection points were estimated as 746-890 in Year 1 and as 493-618 in Year 2.

Effects of temperature (H_{deacc}). We observed a nonlinear relationship between temperature and deacclimation responses (Figure 5) as well as growth responses (Figure 3). This relationship is

referred to as relative thermal contribution (H_{deacc}). Cultivars were pooled to evaluate the H_{deacc} because they followed similar trends even though the magnitude of deacclimation rates varied among cultivars. Based on likelihood ratios tests, all linear parameters were significant for describing the H_{deacc}, but quadratic and cubic parameters were significant at higher chill unit accumulation levels. Relative thermal contribution (H_{deacc}) was also fit as a logistic curve that estimated three parameters. The y-intercept for H_{deacc} curves (parameter *a*) were nonzero at all levels of chill except 1289 in Year 2, which is likely due to the absence of data for temperatures <10 °C in Year 2. In the logistic model, both the inflection points (parameter h) and the steepness (parameter g) of H_{deacc} were lower as chill unit accumulation increased. The logistic curve was used in the model for combined effect of chill and temperature because it had the highest fitness of all the temperature effect models (Table 4).

Combined model for effects of chill unit accumulation and temperature. Estimates for the combined chill unit accumulation and temperature effects model are listed in Table 5. The Pseudo-R^2 for all cultivars ranged from 0.815-0.854 in Year 1 and 0.848-0.984 in Year 2. Statistics based on the linear model used to test the accuracy of the combined effects model are listed in Table 6, including the regression coefficient (β), R^2, absolute sample size (N), and proportion of total observations (n).

Discussion

Dormancy, cold hardiness, and budbreak are complex processes dependent on both physiological and environmental factors. Plants synchronize the development and maintenance

of dormancy, changes in cold hardiness, and timing of budbreak with the annual rhythm of seasons in order to survive in temperate climates. The main objective of this study was to evaluate the effect of chill unit accumulation and temperature on dormancy status, deacclimation responses, and budbreak in five interspecific hybrid grapevine cultivars grown in a cold-climate region. In addition, this study aimed to validate a method for quantifying the contribution of chill unit accumulation to dormancy transitions.

Effects of chill unit accumulation

We observed deacclimation responses that increased continuously as chill units accumulated. This continuum of responses is different from the typical characterization of deacclimation responses across winter, which describe a singular "switch" from no response to a full response corresponding with dormancy status. Those descriptions are based on previous studies, which have clearly demonstrated buds are resistant to deacclimation during endodormancy, whereas buds are "physiologically primed" for deacclimation during ecodormancy (Arora and Taulavuori 2016, Kalberer et al. 2006, Litzow and Pellett 1980, Wolf and Cook 1992). However, there are few studies that have evaluated deacclimation at multiple times throughout the entire dormant period (Kovaleski et al. 2018a). Therefore, descriptions of how deacclimation responses change throughout the entire dormant period have not been possible. The continuum of increasing deacclimation responses we observed provides evidence that an endo- versus ecodormant categorization for deacclimation is oversimplified.

We quantified the continuum of increasing deacclimation responses as deacclimation potential (Ψ_{deacc}, %) (Kovaleski et al. 2018a), which represents the potential to deacclimate at any temperature based on the amount of chill units that have accumulated. Deacclimation

potential increased as chill units accumulated following a logistic curve that can be divided into three phases (Figure 4). During the first phase, deacclimation potential is stable at zero potential, meaning deacclimation does not occur at any temperature. This is followed by a phase where deacclimation potential increases rapidly, meaning deacclimation rates become increasingly large as chill accumulates. In the final phase, changes in deacclimation potential slow down and deacclimation potential plateaus at 100% potential. At this point, additional chill unit accumulation does not contribute to larger deacclimation responses. When this pattern is plotted across cumulative chill, deacclimation potential represents the degree of cold hardiness loss that can occur based on chill.

The phase where deacclimation potential increased overlapped the completion of endodormancy as estimated by bud forcing assays. Specifically, the chill requirement estimated by bud forcing assays was slightly lower than the chill quantity where the deacclimation potential curve reached its inflection point ($\Psi_{deacc} = 50\%$). An exception to this was Frontenac and Marquette in Year 2, where chilling requirement estimated by bud forcing was roughly equal to the chill quantity where deacclimation potential began to increase (between the first and second phases of deacclimation potential). Compared to the traditional method, bud forcing assays, deacclimation potential is an advantageous tool for estimating the endo- to ecodormancy transition and for estimating the contribution of chill units to dormancy release. Deacclimation potential provides a quantitative assessment for dormancy status that avoids arbitrary assumptions inherent in bud forcing assays (i.e., the threshold number of days to reach 50% budbreak). Deacclimation potential also quantifies a phenotype that proceeds visually observable growth. Since budbreak occurs after cold hardiness mechanisms are lost (Ferguson et al. 2014, Kovaleski et al. 2018a, Salazar-Gutiérrez et al. 2014), the amount of time needed to reach

budbreak in forcing assays is a combination of the time needed to fully deacclimate and the time needed for deacclimated buds to visibly grow. In other words, results from bud forcing assays are confounded by deacclimation potential. For all of these reasons, deacclimation potential is a useful tool for quantifying dormancy status.

Deacclimation potential along with the parameters, chill threshold ($chill_{thr}$), chill saturation ($chill_{sat}$), and *active chill range* can be used to determine how chilling temperatures contribute to overcoming endodormancy. There were similar portions of Ψ_{deacc} that correlated with $chill_{thr}$, $chill_{sat}$, and *active chill range* for all cultivars in both years ($^{e, f, g}$ in Table 3), which suggests these parameters identify a consistent phenological status. In terms of absolute chill units, $chill_{thr}$ and $chill_{sat}$ varied between years, while *active chill range* did not ($^{b, c, d}$ in Table 3). This annual variation provides evidence that the sub-model estimating chill units is not capturing all of the factors contributing to changes in deacclimation potential and, consequently, dormancy transitions. Even though chilling temperatures are one of the most important environmental factors that regulate dormancy transitions and subsequent phenological development, chill models provide fairly rough mathematical approximations of temperature efficiency toward overcoming endodormancy (Fadón et al. 2020). Variation in $chill_{thr}$, $chill_{sat}$, and *active chill range* could be used in to identify the most effective temperatures that contribute to changes in deacclimation potential and, therefore, dormancy transitions. As a result, Ψ_{deacc}, $chill_{thr}$, $chill_{sat}$, and *active chill range* introduce a valuable opportunity to improve chill models and accordingly, phenology models.

Effects of temperature

Deacclimation rates were greater at higher temperatures as compared to lower temperatures. We refer to this relationship as relative thermal contribution (H_{deacc}). Relative thermal contribution followed a nonlinear trend as temperature increased (Figure 5). A similar pattern across temperature was observed in time to budbreak (Figure 3). We used a logistic curve to describe the relative thermal contribution because a minimum response is reached as temperatures decrease and a maximum response is reached as temperatures increase (Chuine 2000, Guak and Neilsen 2013, Kovaleski et al. 2018a). While we generally observed greater deacclimation rates at higher temperatures as compared to lower temperatures, the logistic relationship accurately captures the range where higher temperatures contribute diminishing increases in deacclimation response. The range where increases in deacclimation rates diminished varied across cultivars but was approximately 10-15 °C and greater. In contrast to a nonlinear relationship, previous literature has used a linear relationship to model the effect of temperature on deacclimation (Ferguson et al. 2014, Lecomte et al. 2003) as well as the effect of temperature on plant development (Cannell and Smith 1983, Clark and Thompson 2010, Linkosalo et al. 2000, Richardson et al. 2018). That choice has been criticized for many years but has been acceptable because there are often only slight departures from linearity within the range of temperatures that many models are concerned with (Arnold 1959). However, the departure from linearity is significant below the minimum and above the optimum temperatures that stimulate plant development and deacclimation. In addition, the choice between linearity and nonlinearity influences how temperature should be integrated into models. A linear relationship implies temperature can be integrated as a change quantity (ΔT), as is often done (Buermann et al. 2018, Ettinger et al. 2020). However, a nonlinear relationship between growth and temperature implies that temperature must be integrated into models in absolute quantities in

order to delineate varying contribution towards a response. Therefore, it is important to recognize the nonlinear relationship between temperature and deacclimation in order to continue deepening our understanding of interdependent factors regulating deacclimation and improve growth and development models.

We observed deacclimation at low temperatures, as low as 0 °C, which was the minimum temperature treatment included in our study. Also, a y-intercept (parameter *a*) was estimated in logistic H_{deacc} models in order predict deacclimation at 0 °C. To our knowledge, no previous studies that examined deacclimation in grapevine have reported deacclimation at 0 °C. The lowest base temperature parametrized in a cold hardiness prediction model for 23 grapevine genotypes grown in Washington was 3 °C (Ferguson et al. 2014). In addition, deacclimation was reported at temperatures as low as 2 °C for four grapevine species grown in New York (Kovaleski et al. 2018a). Neither of these studies included the cold-climate interspecific hybrid cultivars that were featured in our study. In addition, we have demonstrated in a previous study that low base temperatures (-1 to 1 °C) provided the best fits when we reparametrized the Ferguson et al. (2014) cold hardiness prediction model for use with cold-climate interspecific hybrid cultivars (Chapter 2). Accordingly, it is possible that deacclimation at low temperature is a genetically specific trait. While this has been the case, several previous deacclimation studies did not include low temperature treatments in their experimental designs (Arora et al. 2004, Cragin et al. 2017, Slater et al. 1991). Future studies that examine deacclimation and budbreak, in any type of temperate woody plant, should include low temperatures in their experimental designs to determine the range of plants with a propensity to deacclimate at low temperatures. Ultimately, deacclimation at low temperatures demonstrates the importance for integrating possible low temperature contributions toward growth when modeling phenology.

Combined effects of chill unit accumulation and temperature

Deacclimation responses are conditional on both chill unit accumulation and temperature. The following descriptions of the combined effects of chill accumulation and temperature are illustrated in Figure 6. Deacclimation responses increased at all temperatures as chill units accumulated until deacclimation potential reached its maximum, at which point additional chill unit accumulation did not contribute to changes in deacclimation responses. Therefore, low (i.e., chilling) temperatures that occur in spring are not changing the nature of deacclimation responses but are instead directly contributing to deacclimation. The differences in deacclimation rates across temperature were small at low chill unit accumulation. As chill units accumulated, deacclimation rates increased at all temperatures but there were larger increases at high temperatures as compared to low temperatures. In general, changes in deacclimation rates at a given temperature were relative to the maximum rate for that temperature and correspond to increases in deacclimation potential. Therefore, deacclimation potential evenly regulates deacclimation rates for all temperatures. Based on the nonlinear relationship between temperature and deacclimation, there are different but proportional increases in deacclimation rates across temperature as chill accumulates.

We observed an exception to this trend during our low chill, high temperature treatments, which triggered disproportionately large deacclimation responses (top left panel in Figure 5). It is possible that the long duration of a high temperature treatment overcame growth suppression effects associated with endodormancy in place of chill unit accumulation. Previous studies observed deacclimation responses and fewer number of days to budbreak after buds were treated with hot water (Tanino et al. 1989, Wisniewski et al. 1997, Wolf and Cook 1992). It is generally

understood that sublethal stresses are capable of breaking endodormancy even though the specific actions of stress are unclear. While the hot water treatments used in previous studies were much greater than the high temperature treatments in our study, the duration of their treatments was short (1 or 2 hours) as compared to ours (24-120 hours). Both the degree and duration are important aspects for impact of temperature on dormant buds (Arora and Taulavuori 2016). Consequently, the long duration of our high temperature treatment may have prompted a stress response similar to those observed in previous studies, which ultimately led to an inconsistent deacclimation response.

Apart from this exception, the model that combines chilling accumulation and temperature effects accurately represents the overall changes in deacclimation rates. The linear model used to test the combined effects model's accuracy had a regression coefficient (β) ranging from 0.824 to 1.006 across all cultivars in both years (Table 6). This is exceptional considering a β=1 would indicate there is 1 unit change in ΔLTE for every 1-unit change in k_{deacc}. The low R^2 values associated with the 2018-19 models indicates that there was a wide range of LTEs throughout the deacclimation experiments. However, the model still accurately represented the kinetics for changes in deacclimation rates since the regression coefficients are near one. Therefore, the individual effects of chill unit accumulation and temperature on deacclimation can be combined into a single model that quantifies deacclimation kinetics throughout the dormant period and can guide improvements to models predicting cold hardiness fluctuations and phenological development in woody perennials.

Conclusion

Descriptions of the mechanisms by which plants deacclimate, the factors regulating deacclimation, and seasonal rhythm of deacclimation kinetics are necessary to understand the freeze injury risks that perennial plants face in climates where freezing temperatures occur. In this study, we have described the effects of two factors, chill unit accumulation and temperature, on deacclimation responses. Regarding the effect of chill, deacclimation responses increased continuously as chill units accumulated rather than categorically based on dormancy status. This continuum of deacclimation responses was quantified as a rate ratio, referred to as deacclimation potential (Ψ_{deacc}). Future studies aiming to describe dormancy transitions and chilling requirements should include assessment of deacclimation potential in their experimental designs because it provides an advantageous alternative to bud forcing assays for quantifying dormancy transitions. Most importantly, deacclimation potential quantifies a bud growth phenotype that proceeds externally visible bud growth, which is the observation that is necessary in bud forcing assays. In addition, deacclimation potential characterizes a chill range where bud growth responses continuously increase until they reach their maximum potential, which introduces an opportunity to identify the most effective temperatures that contribute to dormancy transition and thereby improve chill models. Regarding the effect of temperature, deacclimation rates increased along a nonlinear trend, referred to as the relative thermal contribution (H_{deacc}), as temperatures increase. Relative thermal contribution demonstrates that temperature, as a variable in predictive models, needs to be integrated in total units rather than units of change (ΔT). Furthermore, deacclimation occurred at low temperatures (as low as 0 °C), which has not been observed in grapevine before. Future studies are necessary to evaluate the potential for deacclimation at low temperatures in other woody plants. This could inform adjustments to base temperatures in models predicting phenological development for plants that deacclimate at low temperatures.

Finally, we have demonstrated that the effects of chill unit accumulation and temperature can be combined in a predictive model that accurately describes changes in deacclimation responses across the dormant period. This deacclimation model can guide development of new cold hardiness prediction models or improvements to existing models.

Literature Cited

Arnold CY. 1959. The determination and significance of the base temperature in a linear heat unit system. Am Soc Hortic Sci 74:430–445.

Arora R, Rowland LJ. 2011. Physiological research on winter-hardiness: Deacclimation resistance, reacclimation ability, photoprotection strategies, and a cold acclimation protocol design. HortScience 46:1070–1078.

Arora R, Taulavuori K. 2016. Increased risk of freeze damage in woody perennials VIS-À-VIS climate change: Importance of deacclimation and dormancy response. Front Environ Sci 4:1–7.

Arora R, Rowland LJ, Ogden EL, Dhanaraj AL, Marian CO, Ehlenfeldt MK, Vinyard B. 2004. Dehardening kinetics, bud development, and dehydrin metabolism in blueberry cultivars during deacclimation at constant, warm temperatures. J Am Soc Hortic Sci 129:667–674.

Buermann W, Forkel M, O'Sullivan M, Sitch S, Friedlingstein P, Haverd V, Jain AK, Kato E, Kautz M, Lienert S, et al. 2018. Widespread seasonal compensation effects of spring warming on northern plant productivity. Nature 562:110–114.

Cannell MGR, Smith RI. 1983. Thermal Time, Chill Days and Prediction of Budburst in Picea sitchensis. J Appl Ecol 20:951–963.

Chuine I. 2000. A unified model for budburst of trees. J Theor Biol 207:337–347.

Clark RM, Thompson R. 2010. Predicting the impact of global warming on the timing of spring flowering. Int J Climatol 30:1599–1613.

Cook RD. 1977. Detection of Influential Observation in Linear Regression Detection of Influential Observation in Linear Regression. Technometrics 19:15–18.

Coombe BG. 1995. Growth Stages of the Grapevine: Adoption of a system for identifying grapevine growth stages. Aust J Grape Wine Res 1:104–110.

Coville F. 1920. The influence of cold in stimulating the growth of plants. Proc Natl Acad Sci USA 6:434–435.

Cragin J, Serpe M, Keller M, Shellie K. 2017. Dormancy and cold hardiness transitions in winegrape cultivars chardonnay and cabernet sauvignon. Am J Enol Vitic 68:195–202.

Deshpande G, Jia H. 2020. Multi-Level Clustering of Dynamic Directional Brain Network Patterns and Their Behavioral Relevance. Front Neurosci 13:1–22.

Ettinger AK, Chamberlain CJ, Morales-Castilla I, Buonaiuto DM, Flynn DFB, Savas T, Samaha JA, Wolkovich EM. 2020. Winter temperatures predominate in spring phenological responses to warming. Nat Clim Chang 10:1137–1142.

Fadón E, Fernandez E, Behn H, Luedeling E. 2020. A conceptual framework for winter dormancy in deciduous trees. Agronomy 10.

Ferguson JC, Moyer MM, Mills LJ, Hoogenboom G, Keller M. 2014. Modeling dormant bud cold hardiness and Budbreak in twenty-three Vitis genotypes reveals variation by region of origin. Am J Enol Vitic 65:59–71.

Gu L, Hanson PJ, Post W Mac, Kaiser DP, Yang B, Nemani R, Pallardy SG, Meyers T. 2008. The 2007 eastern US spring freeze: Increased cold damage in a warming world? Bioscience 58:253–262.

Guak S, Neilsen D. 2013. Chill unit models for predicting dormancy completion of floral buds in apple and sweet cherry. Hortic Environ Biotechnol 54:29–36.

Hanninen H. 2013. Modeling bud dormancy release in trees from cool and temeprate regions. Acta For Fenn 213:47.

Hänninen H, Kramer K. 2007. A framework for modelling the annual cycle of trees in boreal and temperate regions. Silva Fenn 41:167–205.

IPCC. 2014. Climate Change 2013. The physical science basis. Cambridge Cambridge Univ Press.

Junttila O, Hänninen H. 2012. The minimum temperature for budburst in Betula depends on the state of dormancy. Tree Physiol 32:337–345.

Kalberer SR, Wisniewski M, Arora R. 2006. Deacclimation and reacclimation of cold-hardy plants: Current understanding and emerging concepts. Plant Sci 171:3–16.

Kovaleski AP, Reisch BI, Londo JP. 2018. Deacclimation kinetics as a quantitative phenotype for delineating the dormancy transition and thermal efficiency for budbreak in Vitis species. AoB Plants 10:1–12.

Lang GA. 1987. Dormancy: A New Universal Terminology. HortScience 22:817–820.

Lang GA, Early JD, Martin GC, Darnell RL. 1987. Endo-, para-, and Ecodormancy: Physiological Terminology and Classification for Dormancy Research. HortScience 22:371–377.

Lecomte C, Giraud A, Aubert V. 2003. Testing a predicting model for frost resistance of winter wheat under natural conditions. Agronomie 23:51–66.

Levitt J. 1980. Responses of Plants to Environmental Stresses: Chilling, Freezing, and High Temperature Stresses. Academic Press. New York, New York.

Linkosalo T, Carter TR, Hakkinen R, Hari P. 2000. Predicting spring phenology and frost damage risk of Betula spp. under climatic warming: A comparison of two models. Tree Physiol 20:1175–1182.

Litzow M, Pellett H. 1980. Relationship of rest to dehardening in red-osier dogwood. HortScience 15:92–93.

Londo JP, Johnson LM. 2014. Variation in the chilling requirement and budburst rate of wild Vitis species. Environ Exp Bot 106:138–147.

McDowall LM, Dampney RAL. 2006. Calculation of threshold and saturation points of sigmoidal baroreflex function curves. Am J Physiol - Hear Circ Physiol 291:2003–2007.

Mills LJ, Ferguson JC, Keller M. 2006. Cold-hardiness evaluation of grapevine buds and cane tissues. Am J Enol Vitic 57:194–200.

Ögren E. 2001. Effects of climatic warming on cold hardiness of some northern woody plants assessed from simulation experiments. Physiol Plant 112:71–77.

Pagter M, Arora R. 2013. Winter survival and deacclimation of perennials under warming climate: Physiological perspectives. Physiol Plant 147:75–87.

Richardson AD, Hufkens K, Milliman T, Aubrecht DM, Furze ME, Seyednasrollah B, Krassovski MB, Latimer JM, Nettles WR, Heiderman RR, et al. 2018. Ecosystem warming extends vegetation activity but heightens vulnerability to cold temperatures. Nature 560:368–371.

Salazar-Gutiérrez MR, Chaves B, Anothai J, Whiting M, Hoogenboom G. 2014. Variation in cold hardiness of sweet cherry flower buds through different phenological stages. Sci Hortic (Amsterdam) 172:161–167.

Shaltout AD, Unrath CR. 1983. Rest Completion Prediction Model for "Starkrimson Delicious" Apples. J Am Soc Hortic Sci 108:957–961.

Slater J V., Warmund MR, George MF, Ellersieck MR. 1991. Deacclimation of winter hardy "Seyval blanc" grape tissue after exposure to 16°C. Sci Hortic (Amsterdam) 45:273–285.

Tanino KK, Fuchigami LH, Chen THH. 1989. Dormancy-breaking agents on acclimation and deacclimation of dogwood. HortScience 24:353–354.

Taulavuori KMJ, Taulavuori EB, Skre O, Nilsen J, Igeland B, Laine KM. 2004. Dehardening of mountain birch (Betula pubescens ssp. czerepanovii) ecotypes at elevated winter temperatures. New Phytol 162:427–436.

Vitasse Y, Lenz A, Körner C. 2014. The interaction between freezing tolerance and phenology in temperate deciduous trees. Front Plant Sci 5:1–12.

Vyse K, Pagter M, Zuther E, Hincha DK. 2019. Deacclimation after cold acclimation- A crucial, but widely neglected part of plant winter survival. J Exp Bot 70:4595–4604.

Wisniewski M, Sauter J, Fuchigami L, Stepien V. 1997. Effects of near-lethal heat stress on bud break, heat-shock proteins and ubiquitin in dormant poplar (Populus nigra

charkowiensis x P. nigra incrassata). Tree Physiol 17:453–460.

Wolf TK, Cook MK. 1992. Seasonal Deacclimation Patterns of Three Grape Cultivars at Constant, Warm Temperature. Am J Enol Vitic 43:171–179.

Tables

Table 1. Summary of deacclimation experiments and bud forcing assays, including cultivars that were included in 2018-19 and 2019-20. For deacclimation experiments: length specifies the number of days buds were conditioned in treatment temperatures; interval specifies the average number of days between DTA runs. For both experiments, repetitions (n) specify the number of experiments performed each year. In each year, experiments were full factorial design.

	Year	2018-19	2019-20
	Cultivars	Frontenac, Marquette, Petite Pearl	Brianna, Frontenac, La Crescent, Marquette, Petite Pearl
Deacclimation	Temperatures (°C)	0, 7, 14, 21	10, 15, 20, 25
	Length (days)	5	up to 13
	Interval (days)	1.33	~4
	Repetitions (n)	5	3
Bud forcing	Repetitions at 22 °C (n)	7	8
	Repetitions at 10, 15, 20, 25 °C (n)	NA	3

Table 2. Parameters estimated for the deacclimation potential (Ψ_{deacc}) model using the nls() function, including parameter *b* (steepness of curve), parameter *c* (inflection point), and Pseudo-R^2 (fit of the nonlinear curve). Estimates were calculated separately for each cultivar and between years. Parameter *c* is represented in units of chill accumulation.

Deacclimation Potential (Ψ_{deacc})			
Cultivar	*b*	*c*	Pseudo-R^2
2018-19			
Frontenac	-12.583	878.704	0.816
Marquette	-23.474	737.323	0.489
Petite Pearl	-7.262	819.018	0.622
2019-20			
Brianna	-6.479	559.116	0.977
Frontenac	-8.434	617.557	0.940
La Crescent	-7.000	589.817	0.926
Marquette	-8.000	558.346	0.895
Petite Pearl	-5.046	493.341	0.785

Table 3. Calculations for critical chill quantities, including $chill_{thr}$, $chill_{sat}$, and *active chill range* and the relationship with deacclimation potential (Ψ_{deacc}). Chill quantities are listed in 'North Carolina' (NC) chill units and were calculated separately for each cultivar and between years.

Cultivar	slope at inflection point[a]	$chill_{thr}$ (NC chill-units)[b]	$chill_{sat}$ (NC chill-units)[c]	*active chill range* (NC chill-units)[d]	Ψ_{deacc} at $chill_{thr}$ (%)[e]	Ψ_{deacc} at $chill_{sat}$ (%)[f]	Ψ_{deacc} within *active chill range* (%)[g]
2018-19							
Frontenac	0.0036	739	1018	279	10.2	86.5	76.3
Marquette	0.0080	675	800	126	11.0	87.2	76.2
Petite Pearl	0.0022	593	1045	451	8.8	85.4	76.6
2019-20							
Brianna	0.0029	387	732	345	8.4	85.1	76.7
Frontenac	0.0034	471	764	293	9.3	85.8	76.5
La Crescent	0.0030	421	758	337	8.7	85.3	76.6
Marquette	0.0036	419	698	279	9.1	85.6	76.5
Petite Pearl	0.0026	298	689	391	7.3	84.4	77.1

[a] Slope of the line tangent to Ψ_{deacc} inflection point.
[b] Chill quantity where line tangent to Ψ_{deacc} inflection point equals zero deacclimation potential (Ψ_{deacc} = 0%).
[c] Chill quantity where line tangent to Ψ_{deacc} inflection point equals maximum deacclimation potential (Ψ_{deacc} = 100%).
[d] Difference between $chill_{sat}$ and $chill_{thr}$.
[e] Percent Ψ_{deacc} that corresponds with $chill_{thr}$.
[f] Percent Ψ_{deacc} that corresponds with $chill_{sat}$.
[g] Proportion of Ψ_{deacc} within $chill_{thr}$ and $chill_{sat}$.

Table 4. Statistical fit and logistic parameters for relative thermal contribution (H_{deacc}) models calculated at each level of chill with cultivars pooled. Linear, quadratic, cubic are based on R^2 whereas logistic is based on Effron's Pseudo-R^2. The logistic model parameters were calculated using the nls() function including parameter *a* (y-intercept), parameter *g* (steepness of curve), parameter *h* (inflection point). Parameter *h* is represented in units of temperature (°C).

Relative Thermal Contribution (H_{deacc})								
		Linear	Quadratic	Cubic	Logistic			
Cultivar	Chill	Fit	Fit	Fit	Fit	*a*	*g*	*h*
2018-19								
pooled	689	0.38	0.44	0.43	0.57	0.079	-9.971	21.016
	776	0.65	0.63	0.60	0.67	0.183	-2.229	18.244
	972	0.79	0.82	0.80	0.86	0.286	-3.177	16.830
	1023	0.90	0.93	0.93	0.95	0.623	-2.957	16.186
	1357	0.82	0.91	0.93	0.92	0.205	-1.722	9.064
2019-20								
pooled	527	0.65	0.65	0.63	0.68	0.238	-4.217	23.389
	1057	0.46	0.44	0.41	0.50	0.143	-1.400	10.358
	1289	0.19	0.17	0.13	0.23	0.000	-1.000	9.412

Table 5. Parameters estimated for the model with combined chill unit accumulation effects and temperature effects using the nls() function. Chill unit accumulation effects are represented by parameter *b* (steepness of curve) and parameter *c* (inflection point). Temperature effects are represented by parameter *a* (y-intercept), parameter *g* (steepness of curve), and parameter *h* (inflection point). Fitness of the model is reported using Effron's Pseudo-R^2.

Combined Effect for Chill Unit Accumulation and Temperature						
Cultivar	*b*	*c*	*a*	*g*	*h*	Pseudo-R^2
2018-19						
Frontenac	-14.576	815.248	0.388	-1.872	17.021	0.815
Marquette	-10.837	707.790	0.266	-2.569	13.107	0.854
Petite Pearl	-8.179	793.095	0.505	-2.364	16.848	0.837
2019-20						
Brianna	-3.367	623.331	0.619	-2.596	16.196	0.984
Frontenac	-6.870	634.702	0.000	-5.685	7.511	0.943
La Crescent	-6.000	594.643	0.000	-2.104	6.531	0.924
Marquette	-6.000	560.566	0.388	-1.128	12.000	0.893
Petite Pearl	-2.629	476.848	0.294	-1.786	11.000	0.848

Table 6. Linear model for evaluating accuracy of the model with combined chill unit accumulation effects (Ψ_{deacc}) and temperature effects, following the formula:

$$\Delta LTE_{(T,Chill)} = \beta \times k_{deacc} \times time,$$

where β is the regression coefficient, R^2 is coefficient of determination, N is the number of LTEs included in the model, n is the percent of LTEs included after removing outliers. Estimates were calculated separately for each cultivar and between years.

Cultivar	β	R^2	N (LTEs)	n (%)
2018-19				
Frontenac	0.891	0.231	1429	0.995
Marquette	1.006	0.335	1446	0.999
Petite Pearl	0.824	0.249	1386	0.996
2019-20				
Brianna	0.915	0.849	613	0.997
Frontenac	0.932	0.872	635	0.989
La Crescent	0.987	0.825	613	0.998
Marquette	0.983	0.833	592	0.998
Petite Pearl	0.978	0.812	594	0.992

Figures

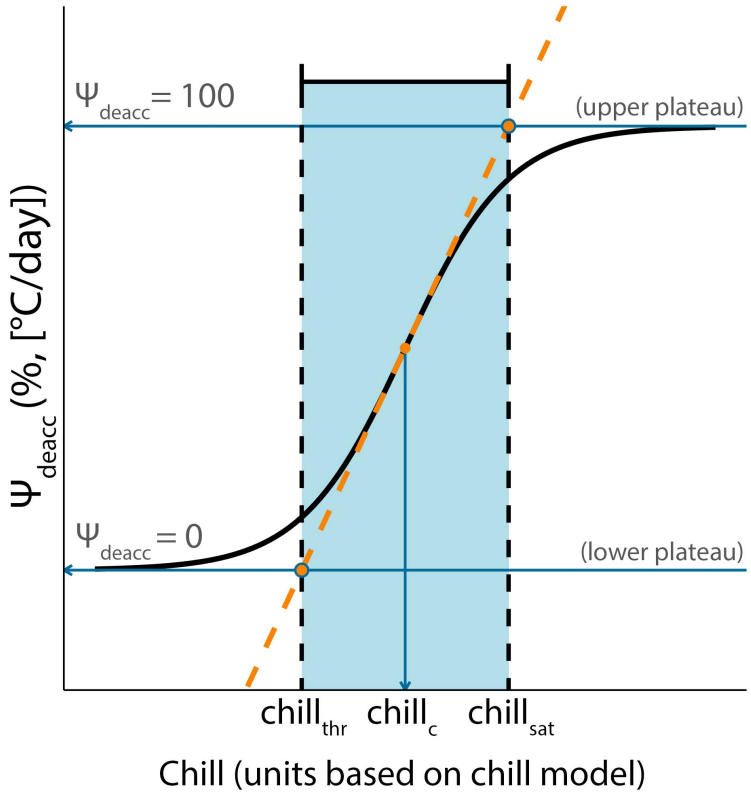

Figure 1. Conceptual diagram for the relationship between Ψ_{deacc} curve, $chill_{thr}$, $chill_{sat}$, and *active chill range*. The slope of the tangent line at Ψ_{deacc} inflection point ($chill_c$) is equal to the first derivative of Ψ_{deacc} at $chill_c$, following the equation:

$$\left(\frac{d\Psi_{deacc}}{dchill}\Big|_{chill=c} = \frac{-b}{(4\times c)}\right), ^{*}$$

where parameter *b* and parameter *c* are estimated by the nls() model. $Chill_{thr}$ is equal to chill where the line tangent to the inflection point is equal to 0 and $chill_{sat}$ is equal to chill where the line tangent to the inflection point is equal to 100. The difference between $chill_{sat}$ and $chill_{thr}$ is the *active chill range*.

*This equation is a reduced form of the first derivative specifically at $chill_c$. The full derivative equation for the slope of a line tangent to any point of Ψ_{deacc} is:

$$\frac{d\Psi_{deacc}}{dchill}\Big| = -e^{(b\times(\ln chill - \ln c)} \times \frac{(b\times(\frac{1}{chill})}{\left[1+e^{(b\times(\ln chill - \ln c)}\right]^2}$$

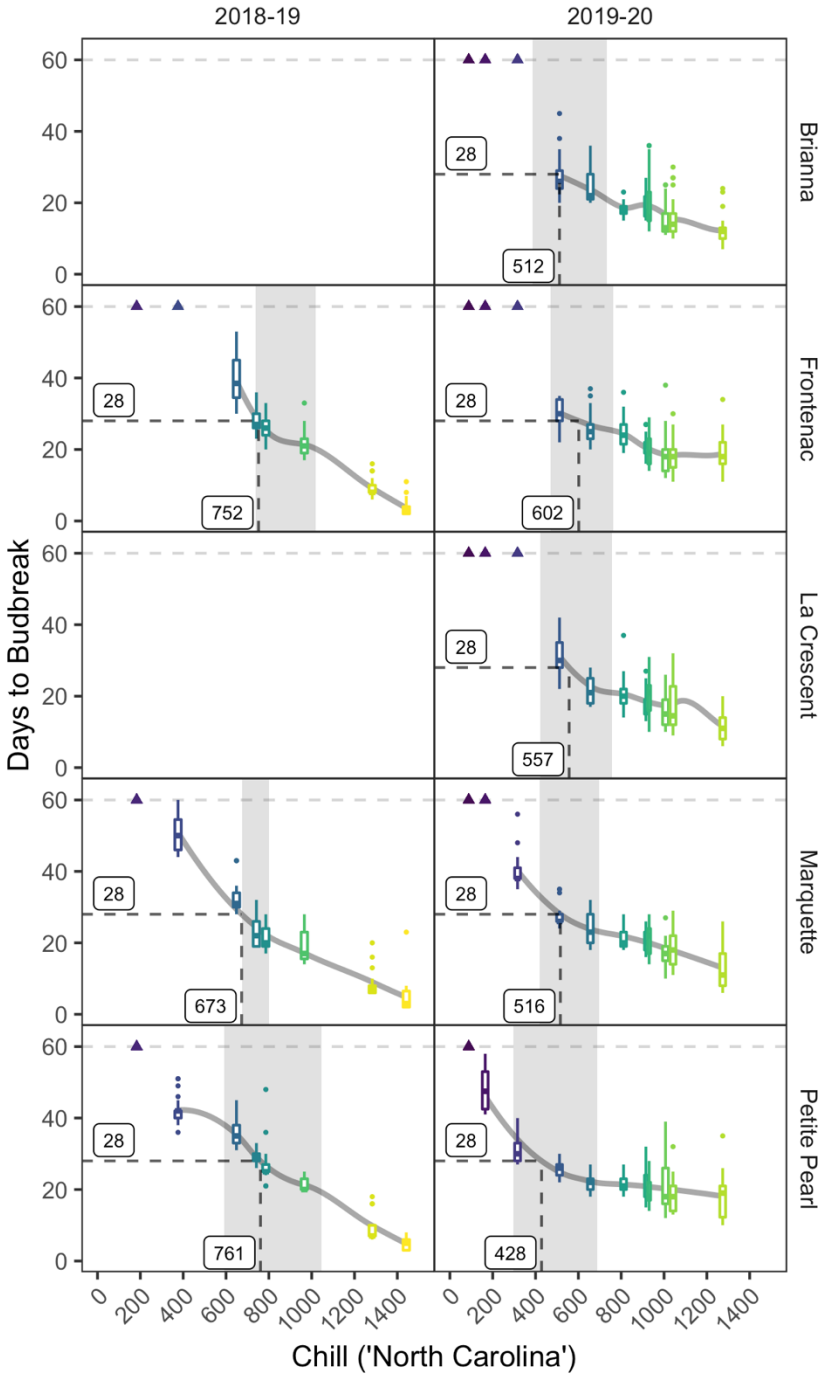

Figure 2. Days to budbreak across chill unit accumulation. Each box-and-whisker represents one bud forcing assay with 25 single-node cuttings, which are colored based on chill. A trend line fit was with "loess" method of non-parametric regression (grey curves). Chill requirements based on a 28-day threshold are labeled (intersecting, black, dashed lines). Assays were concluded after 60 days (horizontal, grey, dashed lines). Assays where less than 50% of buds grew are labeled (colored triangles). The *active chill range* based on deacclimation potential (Ψ_{deacc}) models is represented by shaded grey rectangles.

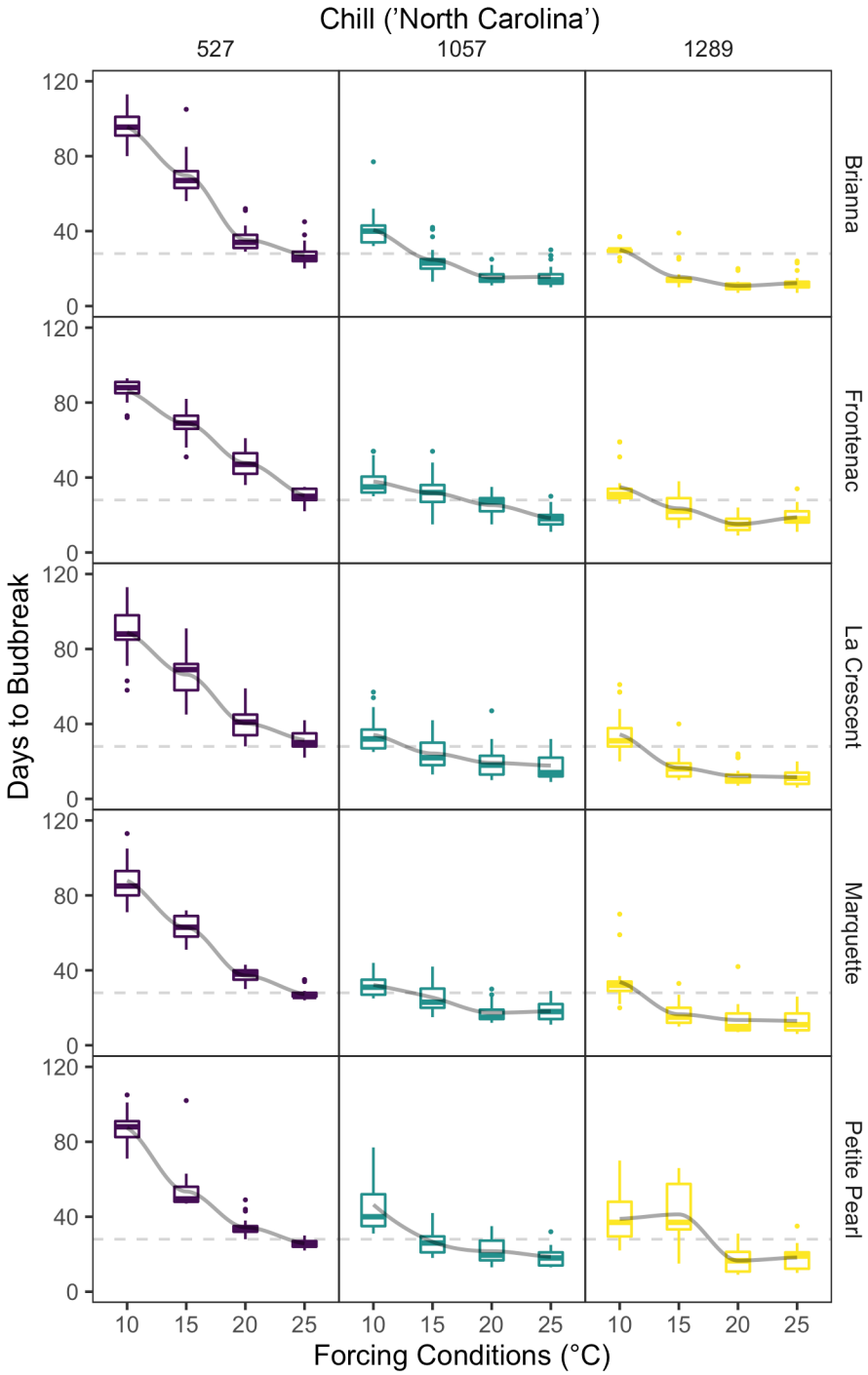

Figure 3. Days to budbreak in forcing conditions at four temperatures across three amounts of chill unit accumulation (separated by column) in 2019-20. A trend line was fit with "loess" method of non-parametric regression (grey curves). The horizontal grey, dashed line designates 28 days.

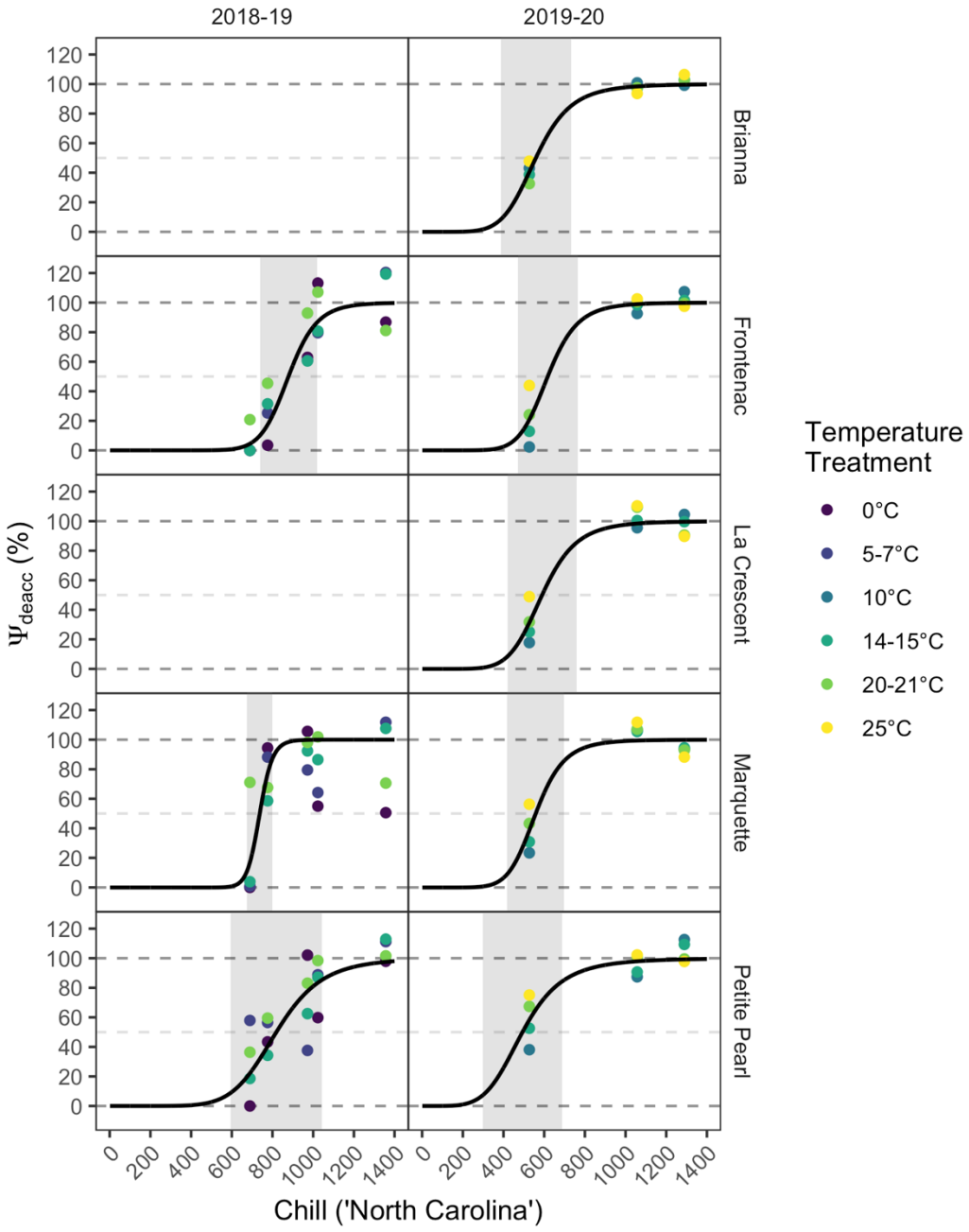

Figure 4. Deacclimation potential (Ψ_{deacc}) model predictions (black curves) and observed deacclimation potential at different temperatures (colored points) plotted across chill unit accumulation. Deacclimation potential at 0%, 50%, and 100% are indicated by horizontal, grey, dashed lines. The *active chill range* is represented by the grey shaded rectangles.

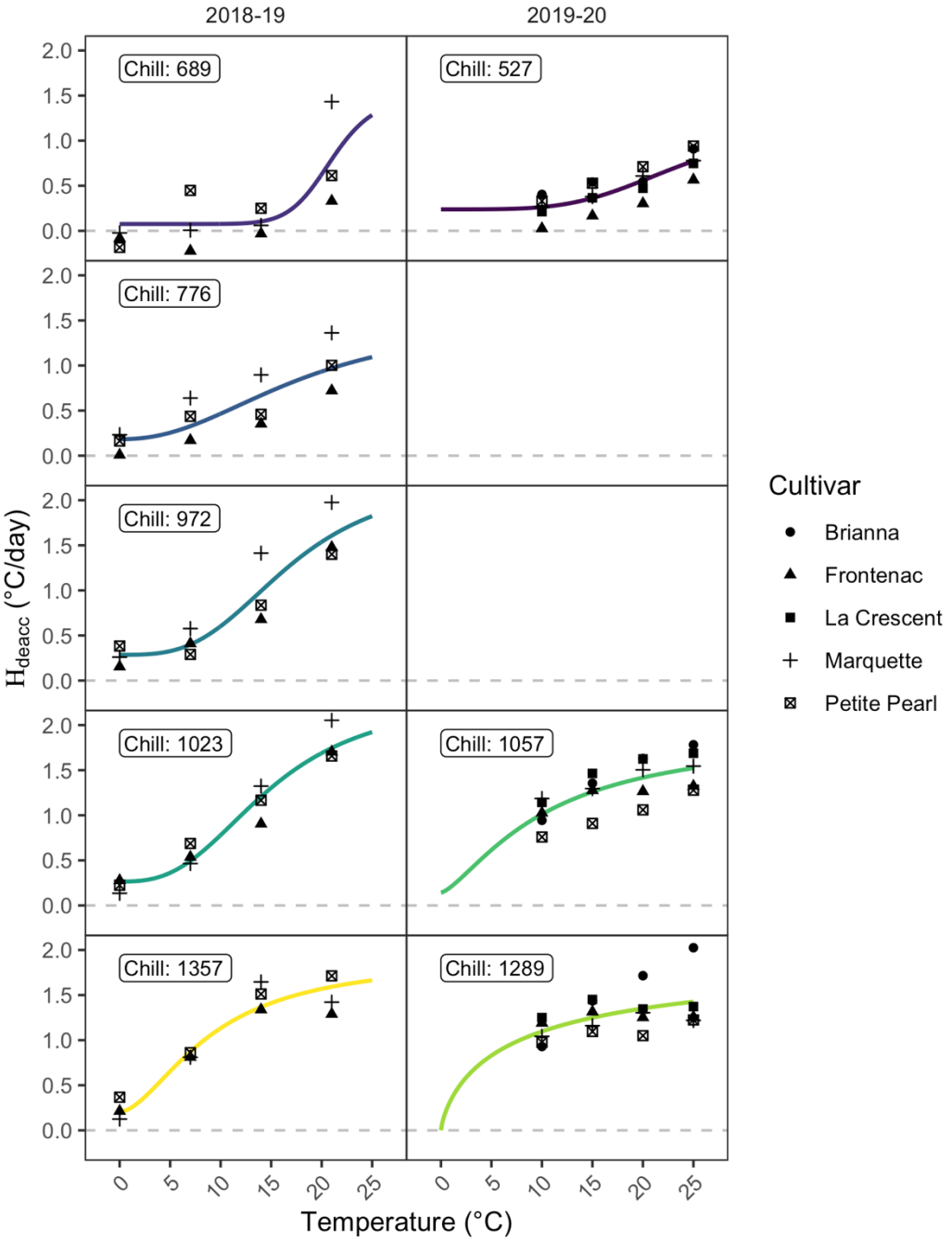

Figure 5. Relative thermal contribution (H_{deacc}) model prediction (colored curves) and observed deacclimation rate (black symbols) plotted across temperature. Predictions for each year are separated by column. Predictions for each level of chill unit accumulation are separated by row and chill unit accumulation is labeled inside the panel. Deacclimation rate minimum (0°C/day) is indicated by horizontal, grey, dashed lines.

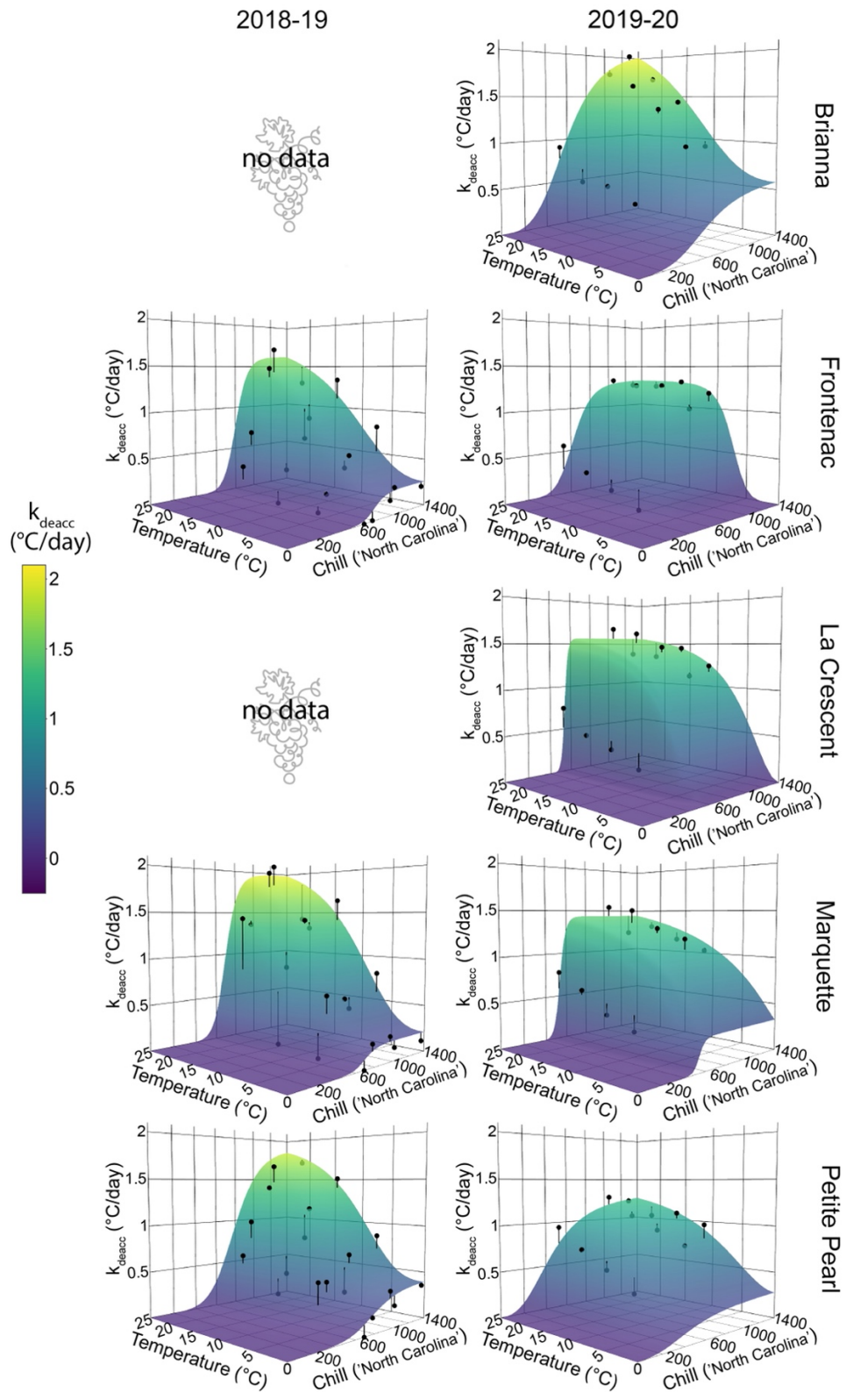

Figure 6. See caption on following page.

Figure 6. Predicted deacclimation rates (colored surface) plotted with observed deacclimation rates (black points). The difference between predicted and observed deacclimation rate is represented by vertical black lines. Predictions were calculated using the model that combined chill unit accumulation effects and temperature effects.

Chapter 4: Dormancy completion in cold-climate hybrid grapevines: considering the role of freezing temperatures and contextual implications of cold hardiness evaluation

Abstract

Dormancy is an essential adaptation for woody perennials like grapevine (*Vitis* spp.) to survive in temperate climates. Prolonged exposure to chilling temperatures gradually overcomes growth inhibiting mechanisms associated with dormancy. Chilling is often considered to be cool, above freezing temperatures and chilling requirements are defined as the duration of chilling hours needed for endodormancy completion. The aims of this study were (1) determine the contribution of freezing temperatures towards endodormancy completion and (2) to determine chilling requirements for five cold-climate hybrid grapevine cultivars. To address these aims, we evaluated endodormancy completion using two criteria: time to budbreak and percent budbreak. These criteria were measured in buds exposed to three different chill treatments, including field-based chill, experimental chill at constant 5°C, and experimental chill fluctuating diurnally from 6.5 to -3.5°C. We also measured cold hardiness changes under field conditions to contrast with budbreak criteria. For cold-climate hybrid grapevine cultivars in this study, freezing temperatures were effective in promoting endodormancy completion. However, many chill models do not include chill unit calculations for freezing temperatures. Therefore, chill models will need to be adapted to include freezing temperatures in order to accurately estimate chill requirements and characterize endodormancy completion. Furthermore, we observed budbreak at a similar number of days and within the endodormancy threshold for buds exposed to different chill treatments, while their cold hardiness levels differed by approximately twofold (i.e., buds in

the field were twice as cold hardy as buds in constant chill). This contextual evidence provided by cold hardiness evaluation contradicts the traditional interpretation of dormancy assessed by bud forcing assay. Therefore, estimated chill requirements reported in this study do not represent an absolute chill requirement that is transferrable across regions or from year-to-year. Instead, estimated chill requirements likely represent a combination of traits involved in both dormancy status and deacclimation capacity. Future research that characterizes dormancy transitions should complement bud forcing assays with cold hardiness evaluation to guide interpretation of results.

Introduction

To survive in temperate climates, grapevines (*Vitis* spp.) must harmonize bud growth and bud dormancy with the annual rhythm of seasons (Chuine and Régnière 2017, Lang 1987, Weiser 1970). There are two sequential dormancy phases that occur during winter, endodormancy and ecodormancy, which are separated based on internal (endo-) versus environmental (eco-) mechanisms inhibiting growth (Lang et al. 1987). Endodormancy is initiated in the fall and buds gradually overcome endodormancy through prolonged exposure to cool (i.e., chilling) temperatures (Coville 1920). Different genotypes are known to require specific amounts of chilling temperature to fully overcome endodormancy (Samish 1954). Once the chilling requirement is "fulfilled", buds are ecodormant and have the capacity to grow but fail to do so because of unfavorable environmental conditions. With enough time in warm temperatures, ecodormant buds will resume growth and development.

If chilling requirements are not fulfilled during winter, budbreak synchronicity, shoot number, cluster number, and fruit ripening are all thought to be negatively impacted (Dokoozlian 1999, Dokoozlian et al. 1995, Lavee and May 1997). However, buds also gain the capacity to lose cold hardiness, i.e., deacclimate, once chilling requirements are fulfilled (Arora and Taulavuori 2016). When buds deacclimate in response to unseasonal, warm winter weather they are more vulnerable to freezing injury. In horticultural production settings, both genetic adaptations and environmental conditions are often modified, which increases the likelihood for insufficient chilling or early fulfillment of chilling requirements (Winkler et al. 1974). Cold-climate grapevine cultivars have complex genetic backgrounds and consequently exhibit diverse phenotypes (Atucha et al. 2018). In addition, cold-climate grapevine cultivars have propelled

production industries in new growing regions that regularly experience very low winter temperatures, extreme winter weather, and late spring frosts (Tuck et al. 2017). Thus, phenotyping chilling requirements for cold-climate cultivars will provide insights into winter survival, spring phenology, summer productivity and guide improvement of relevant management practices.

There are two important challenges to defining chilling requirements. One is the generally limited understanding of chilling perception and related mechanisms in dormant woody perennials (Fadón et al. 2020). The second is the lack of validated molecular markers or non-destructive physiological markers to define dormancy status (Cooke et al. 2012). Therefore, studies that focus on phenology modeling, relating temperature to phenological events such as budbreak, have been the main source of information regarding the most effective temperature range to overcome dormancy (Chuine and Régnière 2017). A typical approach in these studies involves artificially conditioning dormant samples in chilling temperatures at progressively longer intervals. At each interval, a set of samples are removed from the chilling treatment for analysis via bud forcing assays. Visual observation of percent budbreak and time to (50%) budbreak under favorable growing conditions are the primary criteria measured in bud forcing assays.

It is important to note that buds lose their cold hardiness before budbreak occurs (Kovaleski et al. 2018a) and the time it takes to lose cold hardiness is determined by deacclimation rate (Kalberer et al. 2006). This means observations made in bud forcing assays are dependent on a bud's cold hardiness and deacclimation rate. Despite this, the standard dormancy assessment procedure through bud forcing assays does not include cold hardiness or deacclimation evaluation.

Based on previous phenology research, chill models have been developed to quantify effective chilling temperatures as chill units (Fishman et al. 1987b, 1987a, Richardson et al. 1974, Shaltout and Unrath 1983, Weinberger 1950). Each model calculates chill units for different ranges of temperatures that are thought to contribute to endodormancy completion. Many models calculate varying magnitudes of chill units for each chilling temperature. Chill requirements are reported as cumulative chill, which is the summation of chill units across time. Chill models are often calibrated for specific species, cultivars, and/or production regions (Seeley 1996).

In grapevine, optimum chilling temperatures for dormancy completion and deacclimation are thought to be between 0 and 7.2°C but there is likely variation among cultivars in the most effective chill temperatures (Cragin et al. 2017, Dokoozlian 1999, Weaver and Iwasaki 1977, Weaver et al. 1961). There is also evidence that temperatures outside of this range contribute to chill requirements for some cultivars (Cragin et al. 2017). Furthermore, chill requirements are thought to vary highly across species and between genotypes (Anzanello et al. 2018, Londo and Johnson 2014). Therefore, the objectives of this research were (1) test the contribution of freezing temperatures towards meeting the chilling requirement for endodormancy completion and (2) to determine chilling requirements for five cold-climate hybrid grapevine cultivars.

Materials and Methods

Site description. This study was conducted throughout two winter seasons, 2018-2019 and 2019-2020 in a vineyard at the West Madison Agricultural Research Station in Verona, WI (lat.

43° 03’ 37” N, long. 89° 31’ 54” W). The vineyard is in U.S. Department of Agriculture Plant Hardiness Zone 5a (USDA, 2019).

Weather data. Weather data were collected from September 1 to April 30 using a Network for Environment and Weather Applications (NEWA; http://www.newa.cornell.edu/) participating station (Model MK-III SP running IP-100 software; Rainwise, Trenton, ME). Hourly weather data were used to compute chill units using the ‘North Carolina’ model (Shaltout and Unrath 1983). Cumulative chill was calculated in two steps to determine the start date for each season (Richardson et al. 1974). First, the cumulative chill was calculated starting from September 1. The time with the most negative chill was identified and cumulative chill was re-calculated with this as the start date (i.e., new date for 0 chill unit accumulation). For each season, these dates were (1) September 21, 2018, and (2) October 2, 2019.

Vineyard design and sampling plant material. The vineyard is arranged as a randomized complete block design with four replications. Each block is comprised of two rows of vines that include six, four-vine panels per row. Buds from node positions three to ten (at most) were sampled (maximum of 10 buds per vine) from canes with green phloem and xylem. Buds were sampled evenly across vineyard blocks and vines within vineyard blocks (16 vines total for each cultivar). Canes were cut several centimeters away from the bud. Buds were collected in plastics bags, stored on ice during transportation, and prepped immediately upon returning to the lab.

Chill treatments. Buds were conditioned under three chill treatments, including (1) field-based chill, (2) constant experimental chill and (3) fluctuating experimental chill. There was no

manipulation introduced for the field chill treatment. Buds were exposed to seasonal varying air temperatures. The constant chill treatment held temperatures at 5±0.5°C. The fluctuating chill treatment included 6 hours at -3.5±0.5°C, ramped up to 6.5°C over 1-hour, maintained 6.5±0.5°C for 16 hours, then ramped down to -3.5°C over 1-hour. This cycle repeated every 24-hours.

Buds were sampled for experimental chill treatments on October 11, 2018 and October 15, 2019. Canes were cut into single-node cuttings and randomized across vines and blocks. The randomized cuttings were then grouped into bundles, wrapped at either end of the bundle with moist paper towels, and sealed in a plastic bag. The bagged bundles were placed in dark growth chambers programmed for the constant and fluctuating chill treatments.

Bud forcing assays. For each bud forcing assay, 25 single-node cuttings were placed in square 8-cm pots that were arranged in plastic seedling trays filled with deionized water. The trays were maintained at 22±1.5 °C with a 16-hour photoperiod using LED fixtures (Model: HY-MD-D169-S, Roleandro, Shenzhen, China). The LED fixtures include blue (460-465 nm) and red (620-740 nm) lights with 150 μmol m-2s-1 photon flux. The growth stage of the bud on each single-node cutting was evaluated daily for up to 60 days, and the date of budbreak was recorded. Budbreak was defined as stage 3 (wooly bud) of the modified E-L system (Coombe 1995). Buds that had no visible change by the end of the assay were dissected with a razor blade to determine if the bud was viable (green) or dead (brown). Dead buds were removed from the sample size for data analysis.

Cold hardiness evaluation. Differential thermal analysis (DTA) was used to estimate the cold hardiness of individual buds by measuring their low temperature exotherms (LTE) (Mills et al.

2006). The DTA equipment and sample preparation used in this study was the same as described in Chapter 2. To summarize, the equipment used includes thermoelectric modules (TEMs) (model HP-127-1.4-1.5-74 and model SP-254-1.0-1.3, TE Technology, Traverse City, MI) to detect exothermic freezing reactions. A copper-constantan (Type T) thermocouple (22 AWG) was positioned in proximity to the TEM units to monitor temperature. Trays with TEMs and thermocouples were loaded in a Tenney Model T2C programmable freezing chamber (Thermal Product Solutions, New Columbia, PA) connected to a Keithley 2700-DAQ-40 multimeter data acquisition system (Keithley Instruments, Cleveland, OH). TEM voltage and thermocouple temperature readings were collected at 6- or 15-second intervals via a Keithley add-in for Microsoft Excel (Microsoft Corp., Redmond, WA) or Keithley KickStart software.

Each DTA included 30 buds per cultivar. To prepare samples for DTA, buds including the bud cushion were excised from the cane. The cut surface of the bud was covered with a moistened piece of Kimwipe (Kimberly Clark, Roswell, GA) to provide an extrinsic ice nucleator source and to prevent dehydration prior to bud freezing. A group of five buds were wrapped in aluminum foil and placed on a TEM. The trays were cooled to 4 °C and conditioned for an hour, cooled to 0 °C and conditioned for an hour, then cooled to -44 °C at a rate of -4 °C per hour. DTA was performed approximately biweekly between October and April.

Data analysis. All data analysis was performed using R (ver. 4.0.5; R Core Team 2021). The Kaplan-Meier method with "survival curves" was used to compare budbreak between cultivars and chill treatments (Camargo Alvarez et al. 2018, Cragin et al. 2017, Londo and Johnson 2014). Survival curves represent the probability that budbreak will occur based on chill unit accumulation in each chill treatment. Statistical differences among survival curves were

evaluated by estimated marginal means analysis and complementary log–log models that were fit using the glm() function. The response variable was days to budbreak and the explanatory variable included cultivar, chill treatment, chill duration, year, and interactions. Collectively, there are 235 separate survival curves across all cultivars and all treatments. Therefore, we present a visualized summary of budbreak using box-and-whisker plots.

To define chill requirements, a third-degree polynomial for chill unit accumulation was fit using linear regression and days to budbreak as a response variable. Chilling requirements were considered fulfilled when the fitted regression line crossed 28 days, i.e., 50% of buds reached budbreak within 28 days of exposure to bud forcing assay conditions (Londo and Johnson 2014).

There were bud forcing assays where no viable buds grew within the timeframe of the assay (right-censored observations). The most that can be said about (unobserved) budbreak in these assays is that time to budbreak was greater than 60 days. There were also bud forcing assays where some viable buds grew but cumulative budbreak was less than 50%. Observations in these assays were included in Kaplan-Meier analysis. However, assays where less than 50% of viable buds grew were excluded from datasets used to estimate chill requirements by linear regression.

Results

Days to budbreak decreased (Figure 1) and percent budbreak increased (Panel 1 in Figure 2) as buds were exposed to longer chill duration in all chill treatments. Accordingly, all chill treatments were able to overcome endodormancy for each cultivar (based on 50% budbreak

within 28 days). However, estimated chill requirements were different among cultivars and across chill treatments.

Differences across chill treatments. Estimated chill requirements were different across the chill treatments (Table 1). In general, chill requirements were lowest for field chill, intermediate for fluctuating chill, and highest for constant chill. A similar pattern across chill treatments was observed in the minimum amount of chill need to reach 100% budbreak (field < fluctuating < constant, Figure 2). Field chill was also more effective at promoting budbreak than both experimental chill treatments (Panel 2 in Figure 2 and Figure 3). Between experimental chill treatments, the fluctuating chill (diurnal fluctuation between -3.5 and 6.5 °C) increased the probability of budbreak more than the constant chill (5°C).

Differences across cultivars. Overall, Petite Pearl had the lowest chill requirements and Frontenac had the highest chill requirements, while Brianna, La Crescent, and Marquette had intermediate chill requirements. Based on estimated marginal means analysis, Petite Pearl buds reached budbreak most often, even at low levels of cumulative chill. In contrast, Frontenac required high levels of cumulative chill in order to reach budbreak within the timeframe of the bud forcing assay.

Cold hardiness evaluation. Cold hardiness for each cultivar followed the standard U-shaped curve, with acclimation in the fall and early winter, maintenance of cold hardiness throughout winter, and deacclimation in late winter/ and spring (Panel 2 in Figure 4). Buds overcame endodormancy at approximately the end of the acclimation period (endodormancy completion

dates in Table 2; cold hardiness pattern in Panel 2 of Figure 4). After this point, the median cold hardiness (LT_{50}) curve fluctuates throughout winter. However, buds maintained a deep level of cold hardiness until early March when consistent deacclimation began.

Summary of winter weather. Some chilling occurred in the field before buds were sampled to initiate experimental chill treatments. Therefore, cumulative chill for experimental chill treatments were adjusted to include this portion of field-based chill (183 chill units in 2018-19 and 180 chill units in 2019-20). Coincidentally, the first date ambient temperatures were below 0°C occurred on October 12 in both 2018 and 2019.

Discussion

Dormancy is an essential phenological stage for woody perennials to survive in cool, temperate climates. The objectives in this study were (1) evaluate the contribution of freezing temperature towards chill unit accumulation and subsequent dormancy completion and (2) estimate chill requirements for five cold-climate hybrid grapevine cultivars. While not defined in our original objectives, we also contrasted bud forcing results related to our objectives with cold hardiness evaluation and a recently described dormancy assessment using deacclimation kinetics (Chapter 3 in this thesis).

Dormancy completion varied based on temperature range of chill treatment

Bud dormancy responses were different across the three chill treatments. Based on percent budbreak and survival curve analysis, buds in the field have the highest likelihood of

reaching budbreak, followed by fluctuating chill, and lastly constant chill (Panel 2 in Figure 2). The same pattern is illustrated in estimated chill requirements based on time to budbreak (Table 1). Chill requirements were lowest for field chill, followed by fluctuating chill, and were highest for experimental chill (across columns with different colors; Figure 1). Discrepancies in the number of chill units required to overcome endodormancy across chill treatments are in part due to limitations in chill models that define temperature ranges that contribute effective chill. Most chill models (e.g., Erez et al. 1990, Fishman et al. 1987a, 1987b, Richardson et al. 1974) do not calculate chill units for freezing temperatures or calculate small chill units for freezing temperatures. The 'North Carolina' model (Shaltout and Unrath 1983), reported throughout this study, calculates less than 0.5 chill units for temperatures between -1.1 and 1.6 °C and zero chill units for temperatures less than -1.1°C. During the time from initiation of chill unit accumulation and endodormancy completion, buds were exposed to ambient temperatures below -1.1°C for ~24% of time in the field and ~33% of the time in fluctuating experimental chill. More specifically, for the time below -1.1 in the field, temperatures were also occasionally lower than the fluctuating chill treatment (less than -3≈58%; -3.5 to -1.1≈42%). In contrast, no time in the constant chill conditions were below 0°C. Previous studies have demonstrated freezing temperatures promote endodormancy completion in other crops, including apple (Guak and Neilsen 2013), black currant (Rose and Cameron 2009), grapevine ('Chardonnay', Cragin et al. 2017), and sweet cherry (Guak and Neilsen 2013, Mahmood et al. 2000).

Freezing temperatures might stimulate mechanisms that promote endodormancy completion. Some research suggests grapevine endodormancy release involves molecular mechanisms that resemble oxidative stress conditions, i.e., increased calcium signaling, hypoxia, and altered ABA and ethylene metabolism (Halaly et al. 2008, Keilin et al. 2007, Meitha et al.

2015, Ophir et al. 2009, Pang et al. 2007, Zheng et al. 2015). Previous studies have observed endodormancy release after treating endodormant buds with sublethal heat shock or hydrogen cyanamide (Halaly et al. 2008, Ophir et al. 2009, Or et al. 2002). Both treatments were characterized by increased levels stress-related enzyme transcripts. These conditions also impaired mitochondrial function thereby leading to increased glycolysis and fermentation, both of which may be involved in activating downstream genes that regulate endodormancy release. Other research suggests that endodormancy release may occur after opening symplastic cell-to-cell communication and restoring the supply of growth-promoting signals in the shoot apical meristem (van der Schoot and Rinne 2011). Prolonged exposure to chilling temperature opened plasmodesmata by removing 1,3-β-d-glucan plugs at plasmodesmata in birch and hybrid aspen (Rinne et al. 2011). In addition to the hydrogen cyanamide treatment effects described above, hydrogen cyanamide also activated the expression of 1,3-β-d-glucanase, which may breakdown glucan plugs at plasmodesmata and subsequently promote endodormancy release (Pérez et al. 2009). Freezing temperatures and/or chill treatments that include freeze-thaw cycling are forms of sublethal stress that may lead to endodormancy release by stimulating stress conditions similar to those described above (Gusta and Wisniewski 2013). This may even occur more effectively under freezing conditions than under cool but above freezing conditions (Arora 2018). Therefore, it possible that not only are chill units for freezing temperatures unaccounted for in chill models but also chilling at freezing temperatures is more effective than at above freezing temperatures.

Comparing cold hardiness and bud forcing assays

Budbreak can only happen after buds have lost their cold hardiness (Ferguson et al. 2014, Kovaleski et al. 2018a, Salazar-Gutiérrez et al. 2014) and the time it takes for a bud to lose cold

hardiness is determined by deacclimation rate (Kalberer et al. 2006). Therefore, the time to budbreak is a function of both a bud's initial cold hardiness status and its deacclimation rate. We have previously described a positive correlation between deacclimation rates and the transition from endo- to ecodormancy (Chapter 3 in this thesis). Based on this, changes in deacclimation rates during the dormant period can be used to quantitively assess transitions from endo- to ecodormancy (Kovaleski et al. 2018a).

While evaluating buds in field-based chill and constant experimental chill, we compared results from bud forcing assays with deacclimation rates and cold hardiness. By late November, the average days to 50% budbreak was near or below the 28-day endodormancy threshold for both field-based chill and constant experimental chill (average for each year listed in Table 3; individual cultivar differences labeled in Panel 1 of Figure 4). A reasonable interpretation of these data would conclude that the buds in both treatments have completed endodormancy since they similarly reached 50% budbreak within dormancy threshold. However, buds in each treatment had very different levels of cold hardiness at the start of the bud forcing assays. When buds were sampled to begin experimental chill, the average LT_{50} across cultivars was -12.5 °C and -14.2 °C in 2018-19 and 2019-20 respectively (Table 3). Endodormant buds held at constant low temperatures do not gain cold hardiness but actually lose cold hardiness slowly (~ 0–0.1 °C/day; Chapter 3 of this thesis). Therefore, as buds were moved from the constant chill treatment into bud forcing conditions, they were as cold hardy or less cold hardy than when they were sampled to begin chill treatments. In contrast, buds that received field-based chill gained cold hardiness throughout October and December. By late-November, the average LT_{50} across cultivars was -24.0 °C and -23.1 °C in 2018-19 and 2019-20 respectively (Table 3). This means buds with field-based chill were approximately twice as cold hardy as buds with constant

experimental chill (LT_{50} for individual cultivars labeled in Panel 2 of Figure 4). Taking into consideration that buds deacclimate before growing, the buds in each chill treatment have deacclimated at different rates in order to reach budbreak at a similar time.

This example highlights an important discrepancy between dormancy assessed by bud forcing assays versus cold hardiness/deacclimation. That is, buds in each chill treatment similarly reached 50% budbreak within the defined dormancy threshold. Concurrently, buds in each chill treatment had cold hardiness that was different by twofold (i.e., buds in the field were twice as cold hardy as buds in constant chill). According to bud forcing assays, buds in both treatments had completed the transition from endo- to ecodormancy. Whereas according to cold hardiness and deacclimation rates, buds in the field-based chill treatment were twice as advanced into the transition from endo- to ecodormancy.

This example also has implications for chill model optimization and chill requirements estimation. Cumulative chill was different for each chill treatment in late November, the time period described in the example above (Panel 3 in Figure 4). The constant experimental chill had accumulated more chill units than the field-based chill (~500 and ~375 additional chill units in 2018-19 and 2019-20 respectively). Likewise, chilling requirements were estimated higher for experimental constant chill as compared to field-based chill (Figure 1). Based on the bud forcing assay dormancy assessment, a future research objective might aim to adjust the range of temperatures that confer chill units and/or adjust the relative magnitude of chill units at specific temperatures. However, based on the cold hardiness dormancy assessment, chill model adjustments would need to be even more severe. Therefore, an accurate assessment of dormancy status will be essential to advance research objectives aiming to optimize or calibrate chill models and define chill requirements.

Estimated chill requirement variation

Defining chill requirements for cold-climate hybrid cultivars was a primary objective in this study. Chill requirements for grapevine are thought to vary among *Vitis* species and cultivars (Londo and Johnson 2014). Since hybrid cultivars have complex genetic backgrounds that include several different species (Atucha et al. 2018), we believed it was important to phenotype cultivar-specific chill requirements. However, estimated chill requirements varied across treatments and between years. This is likely due shortcomings in the chill model (e.g., neglecting chill unit calculations for freezing temperatures) and the confounding effect of cold hardiness on budbreak assays for dormancy assessment that are described above. Therefore, estimated chill requirements reported in this study do not represent an absolute chill requirement that is transferrable across regions or from year-to-year. Instead, estimated chill requirements likely represent a combination of traits involved in both dormancy status and deacclimation capacity.

Conclusion

Research that characterizes when dormancy transitions occur can improve our understanding of the factors regulating dormancy and concomitant development. This, in turn, can be used to improve models predicting cold hardiness changes throughout winter and phenological development in spring. Accurate chill models and dormancy release assessments are fundamental to advance these research objectives. In this study, we observed higher increases in budbreak probability and greater decreases in time to budbreak for chill treatments that included below freezing temperatures as compared to constant above freezing temperatures.

Adjustments to chill models will be needed to integrate chill unit calculations at freezing temperatures for cold-climate hybrid grapevine cultivars. Furthermore, cold hardiness evaluation provided underlying contextual evidence that bud forcing assays are not an appropriate methodology to evaluate endodormancy completion. We observed budbreak within the endodormancy threshold for two chill treatments, but cold hardiness levels differed by approximately twofold (i.e., buds in the field were twice as cold hardy as buds in constant chill). Consequently, the interpretation of endodormancy completion is not aligned between bud forcing assays and deacclimation potential. Future research aiming to characterize dormancy transitions should complement bud forcing assays with cold hardiness evaluation to guide interpretation of results.

Literature Cited

Anzanello R, Fialho FB, dos Santos HP. 2018. Chilling requirements and dormancy evolution in grapevine buds. Cienc e Agrotecnologia 42:364–371.

Arora R. 2018. Mechanism of freeze-thaw injury and recovery: A cool retrospective and warming up to new ideas. Plant Sci 270:301–313.

Arora R, Taulavuori K. 2016. Increased risk of freeze damage in woody perennials VIS-À-VIS climate change: Importance of deacclimation and dormancy response. Front Environ Sci 4:1–7.

Atucha A, Hedtcke J, Workmaster BA. 2018. Evaluation of cold-climate interspecific hybrid wine grape cultivars for the upper midwest. J Am Pomol Soc 72:80–93.

Camargo Alvarez H, Salazar-Gutiérrez M, Zapata D, Keller M, Hoogenboom G. 2018. Time-to-event analysis to evaluate dormancy status of single-bud cuttings: An example for grapevines. Plant Methods 14:1–13.

Chuine I, Régnière J. 2017. Process-Based Models of Phenology for Plants and Animals. Annu Rev Ecol Evol Syst 48:159–182.

Cooke JEK, Eriksson ME, Junttila O. 2012. The dynamic nature of bud dormancy in trees: Environmental control and molecular mechanisms. Plant, Cell Environ 35:1707–1728.

Coombe BG. 1995. Growth Stages of the Grapevine: Adoption of a system for identifying grapevine growth stages. Aust J Grape Wine Res 1:104–110.

Coville F. 1920. The influence of cold in stimulating the growth of plants. Proc Natl Acad Sci USA 6:434–435.

Cragin J, Serpe M, Keller M, Shellie K. 2017. Dormancy and cold hardiness transitions in winegrape cultivars chardonnay and cabernet sauvignon. Am J Enol Vitic 68:195–202.

Dokoozlian NK. 1999. Chilling temperature and duration interact on the budbreak of "Perlette" grapevine cuttings. HortScience 34:1054–1056.

Dokoozlian NK, Williams LE, Neja RA. 1995. Chilling exposure and hydrogen cyanamide interact in breaking dormancy of grape buds. HortScience 30:1244–1247.

Erez A, Fishman S, Linsley-Noakes GC, Allan P. 1990. the Dynamic Model for Rest Completion in Peach Buds. Acta Hortic:165–174.

Fadón E, Fernandez E, Behn H, Luedeling E. 2020. A conceptual framework for winter dormancy in deciduous trees. Agronomy 10.

Ferguson JC, Moyer MM, Mills LJ, Hoogenboom G, Keller M. 2014. Modeling dormant bud cold hardiness and Budbreak in twenty-three Vitis genotypes reveals variation by region of

origin. Am J Enol Vitic 65:59–71.

Fishman S, Erez A, Couvillon GA. 1987a. The temperature dependence of dormancy breaking in plants: Computer simulation of processes studied under controlled temperatures. J Theor Biol 126:309–321.

Fishman S, Erez A, Couvillon GA. 1987b. The Temperature Dependence of Dormancy Breaking in Plants: Mathematical Analysis of a Two-Step Model Involving a Cooperative Transition. J Theor Biol 124:473–483.

Guak S, Neilsen D. 2013. Chill unit models for predicting dormancy completion of floral buds in apple and sweet cherry. Hortic Environ Biotechnol 54:29–36.

Gusta L V., Wisniewski M. 2013. Understanding plant cold hardiness: An opinion. Physiol Plant 147:4–14.

Halaly T, Pang X, Batikoff T, Crane O, Keren A, Venkateswari J, Ogrodovitch A, Sadka A, Lavee S, Or E. 2008. Similar mechanisms might be triggered by alternative external stimuli that induce dormancy release in grape buds. Planta 228:79–88.

Kalberer SR, Wisniewski M, Arora R. 2006. Deacclimation and reacclimation of cold-hardy plants: Current understanding and emerging concepts. Plant Sci 171:3–16.

Keilin T, Pang X, Venkateswari J, Halaly T, Crane O, Keren A, Ogrodovitch A, Ophir R, Volpin H, Galbraith D, et al. 2007. Digital expression profiling of a grape-bud EST collection leads to new insight into molecular events during grape-bud dormancy release. Plant Sci 173:446–457.

Kovaleski AP, Reisch BI, Londo JP. 2018. Deacclimation kinetics as a quantitative phenotype for delineating the dormancy transition and thermal efficiency for budbreak in Vitis species. AoB Plants 10:1–12.

Lang GA. 1987. Dormancy: A New Universal Terminology. HortScience 22:817–820.

Lang GA, Early JD, Martin GC, Darnell RL. 1987. Endo-, para-, and Ecodormancy: Physiological Terminology and Classification for Dormancy Research. HortScience 22:371–377.

Lavee S, May P. 1997. Dormancy of grapevine buds - facts and speculation. Aust J Grape Wine Res 3:31–46.

Londo JP, Johnson LM. 2014. Variation in the chilling requirement and budburst rate of wild Vitis species. Environ Exp Bot 106:138–147.

Mahmood K, Carew JG, Hadley P, Battey NH. 2000. Chill unit models for the sweet cherry cvs Stella, Sunburst and Summit. J Hortic Sci Biotechnol 75:602–606.

Meitha K, Konnerup D, Colmer TD, Considine JA, Foyer CH, Considine MJ. 2015. Spatio-

temporal relief from hypoxia and production of reactive oxygen species during bud burst in grapevine (Vitis vinifera). Ann Bot 116:703–711.

Mills LJ, Ferguson JC, Keller M. 2006. Cold-hardiness evaluation of grapevine buds and cane tissues. Am J Enol Vitic 57:194–200.

Ophir R, Pang X, Halaly T, Venkateswari J, Lavee S, Galbraith D, Or E. 2009. Gene-expression profiling of grape bud response to two alternative dormancy-release stimuli expose possible links between impaired mitochondrial activity, hypoxia, ethylene-ABA interplay and cell enlargement. Plant Mol Biol 71:403–423.

Or E, Vilozny I, Fennell A, Eyal Y, Ogrodovitch A. 2002. Dormancy in grape buds: Isolation and characterization of catalase cDNA and analysis of its expression following chemical induction of bud dormancy release. Plant Sci 162:121–130.

Pang X, Halaly T, Crane O, Keilin T, Keren-Keiserman A, Ogrodovitch A, Galbraith D, Or E. 2007. Involvement of calcium signalling in dormancy release of grape buds. J Exp Bot 58:3249–3262.

Pérez FJ, Vergara R, Or E. 2009. On the mechanism of dormancy release in grapevine buds: A comparative study between hydrogen cyanamide and sodium azide. Plant Growth Regul 59:145–152.

Richardson EA, Sceley SD, Walker DR. 1974. A Model for Estimating the Completion of Rest for "Redhaven" and "Elberta" Peach Trees. HortScience 9:331–332.

Rinne PLH, Welling A, Vahala J, Ripel L, Ruonala R, Kangasjärvi J, van der Schoot C. 2011. Chilling of dormant buds hyperinduces FLOWERING LOCUS T and recruits GA-inducible 1,3-β-glucanases to reopen signal conduits and release dormancy in Populus. Plant Cell 23:130–146.

Rose GA, Cameron RW. 2009. Chill unit models for blackcurrant (Ribes nigrum L.) cultivars "Ben Gairn", "Ben Hope" and "Ben Tirran." Sci Hortic (Amsterdam) 122:654–657.

Salazar-Gutiérrez MR, Chaves B, Anothai J, Whiting M, Hoogenboom G. 2014. Variation in cold hardiness of sweet cherry flower buds through different phenological stages. Sci Hortic (Amsterdam) 172:161–167.

Samish RM. 1954. Dormancy in Woody Plants. Annu Rev Plant Physiol:183–204.

van der Schoot C, Rinne PLH. 2011. Dormancy cycling at the shoot apical meristem: Transitioning between self-organization and self-arrest. Plant Sci 180:120–131.

Seeley S. 1996. Modelling climatic regulation of bud dormancy. *In* Plant dormancy: Physiology, biochemistry, and molecular biology. GA Lang (ed.), pp. 361–376. CAB Intl., Wallingford, Oxon, U.K.

Shaltout AD, Unrath CR. 1983. Rest Completion Prediction Model for "Starkrimson

Delicious" Apples. J Am Soc Hortic Sci 108:957–961.

Tuck B, Gartner W, Appiah G. 2017. Economic Contribution of Vineyards and Wineries of the North, 2015. University of Minnesota Extension.

Weaver RJ, Iwasaki K. 1977. Effect of temperature and length of storage, rooth growth and termination of bud rest on "Zinfandel" grapes. Am J Enol Vitic 28:149–151.

Weaver RJ, McCune SB, Coombe BG. 1961. Treatments on Rest Period of Grape Buds. Am J Enol Vitic 12:131–142.

Weinberger JH. 1950. Chilling Requirements of Peach Varieties. Proc Amer Soc Hort Sci 56:122–128.

Weiser C. 1970. Cold Resistance and Injury in Woody Plants. 169:1269–1278.

Winkler AJ, Cook JA, Kliewer WM, Lider LA. 1974. General Viticulture. University of California Press, San Diego, CA, USA.

Zheng C, Halaly T, Acheampong AK, Takebayashi Y, Jikumaru Y, Kamiya Y, Or E. 2015. Abscisic acid (ABA) regulates grape bud dormancy, and dormancy release stimuli may act through modification of ABA metabolism. J Exp Bot 66:1527–1542.

Tables

Table 1. Estimated chill requirements to overcome endodormancy for five hybrid grapevine cultivars in three chill treatments and in two years. Chill treatments include field-based chill (field), experimental chill at constant 5°C (constant), and experimental chill fluctuating daily from -3.5 to 6.5°C (fluctuating). Chill requirements are based on 50% budbreak within 28-days. Ranks are ordered numerically (1=lowest, 5=highest). Range is difference between the maximum and minimum chill requirements within a chill treatment.

Chill treatment	Cultivar	Chill requirement ('North Carolina')	Rank within chill treatment	Range within chill treatment
2018-19				
field-based	Brianna	690	2	111
	Frontenac	771	4	
	La Crescent	741	3	
	Marquette	679	1	
	Petite Pearl	790	5	
constant (5°C)	Brianna	1093	3	513
	Frontenac	1284	5	
	La Crescent	1136	4	
	Marquette	961	2	
	Petite Pearl	771	1	
2019-20				
field-based	Brianna	508	2	204
	Frontenac	637	5	
	La Crescent	571	4	
	Marquette	531	3	
	Petite Pearl	433	1	
constant (5°C)	Brianna	1148	5	449
	Frontenac	1014	3	
	La Crescent	1074	4	
	Marquette	952	2	
	Petite Pearl	699	1	
fluctuating (-3.5 to 6.5°C)	Brianna	853	4	365
	Frontenac	996	5	
	La Crescent	852	3	
	Marquette	845	2	
	Petite Pearl	631	1	

Table 2. Estimated date of endodormancy completion for five hybrid grapevine cultivars under field-based chill in two years. Endodormancy completion is based on 50% budbreak within 28-days.

	2018-19	2019-20
Brianna	November 18	November 18
Frontenac	November 30	November 28
La Crescent	November 24	November 23
Marquette	November 16	November 19
Petite Pearl	November 30	November 12

Table 3. Contrasting **(1)** time to budbreak, **(2)** cold hardiness evaluation, and **(3)** chill unit accumulation in two chill treatments averaged across five hybrid grapevine cultivars. Chill treatments include field-based chill (field), experimental chill at constant 5°C (constant).

	A: constant chill	B: field chill
2018-19		
average time to 50% budbreak (days)	21.3	25.4
average cold hardiness (°C)	≥ -12.5	-24.0
chill accumulation ('North Carolina')	1257.0	742.0
2019-20		
average time to 50% budbreak (days)	29.6	27.6
average cold hardiness (°C)	≥ -14.2	-23.1
chill accumulation ('North Carolina')	899.0	527.0

Figures

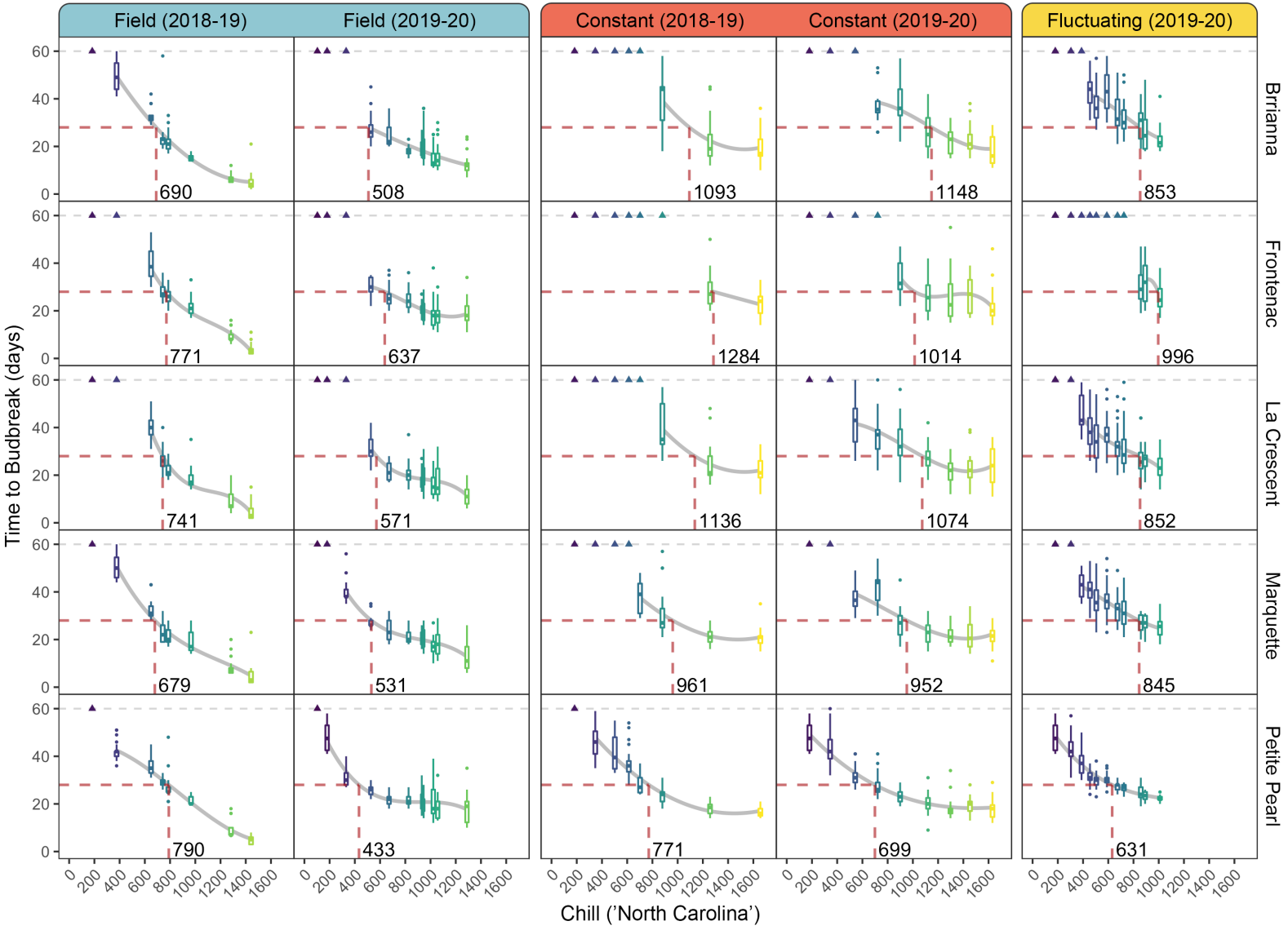

Figure 1. See caption on next page.

Figure 1. Time to budbreak for five hybrid grapevine cultivars under three chill treatments during two years. Buds were conditioned in field-based chill (field; blue columns), experimental chill at constant 5°C (constant; red columns), and experimental chill fluctuating daily from -3.5 to 6.5°C (fluctuating; yellow column). Each box-and-whisker represents one bud forcing assay with 25 single-node cuttings, which are colored based on a continuous chill scale. A trend line fit was with a cubic linear regression (grey curves). Chill requirements based on a 28-day threshold are identified (intersecting, red, dashed lines) and labeled (number along internal x-axis). Assays were concluded after 60 days (horizontal, grey, dashed lines). Assays where less than 50% of buds grew are labeled (colored triangles).

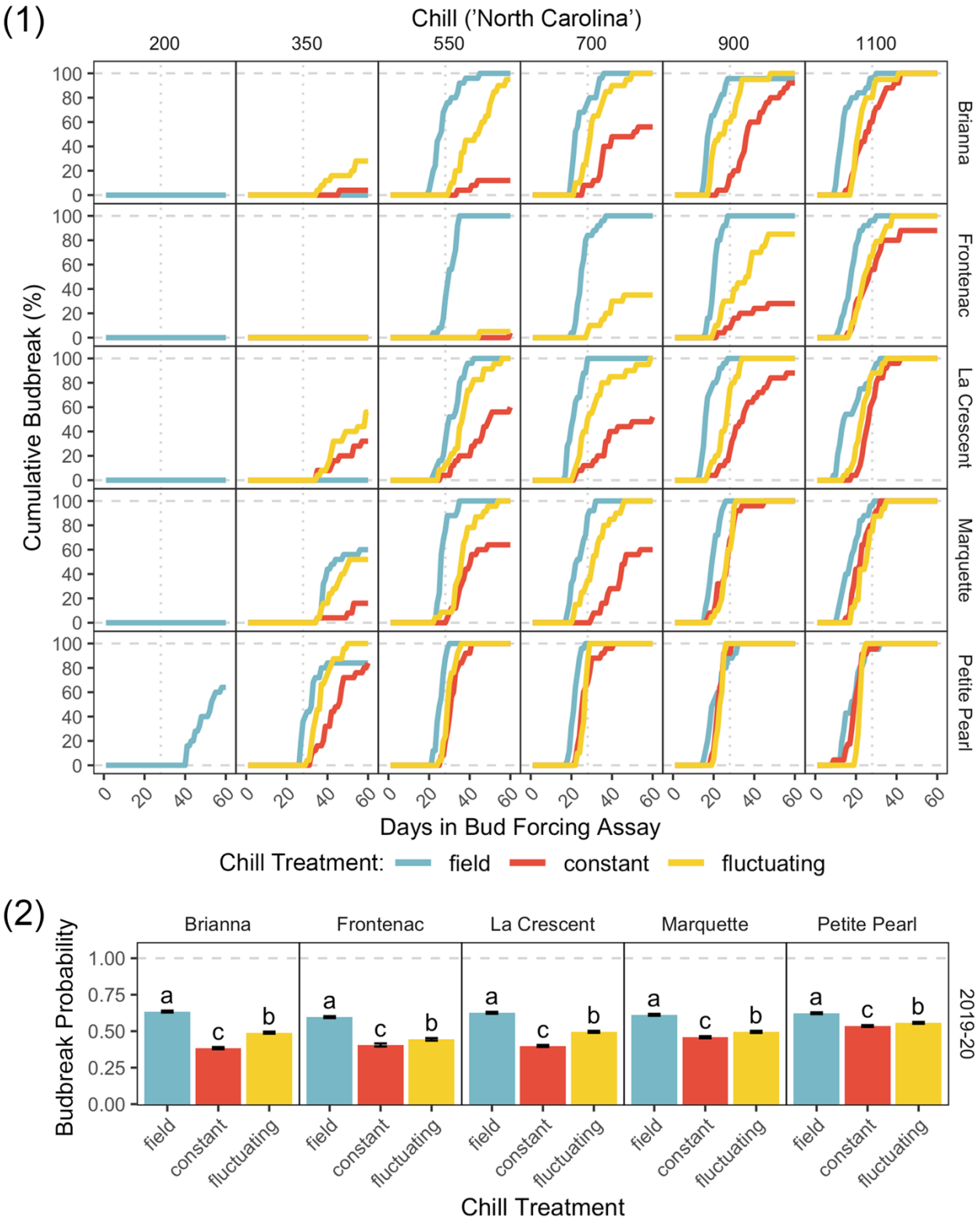

Figure 2. See caption on the following page.

Figure 2. (1) Cumulative budbreak and **(2)** budbreak probability calculated by estimated marginal means analysis for five hybrid grapevine cultivars and three chill treatments in 2019-20. Buds were conditioned in field-based chill (field), experimental chill at constant 5°C (constant), and experimental chill fluctuating daily from -3.5 to 6.5°C (fluctuating). **(1)** Cumulative budbreak is represented by colored lines that make 1-day "steps" based on daily observation for up to 60 days. Each chill treatment is sorted into columns based on the approximate chill units ('North Carolina') at the time of the assay. Only "field" chill occurs in the "200" column because experimental chill treatments were initiated at that time. Grey, dashed lines at zero (0%) and maximum (100%) budbreak. Grey, dotted line at 28 days for a visual reference to days to budbreak criteria. **(2)** Budbreak probability is represented by colored bars. Lowercase letters within a panel designate statistical difference using 95% confidence interval and Tukey HSD with significance level α=0.05.

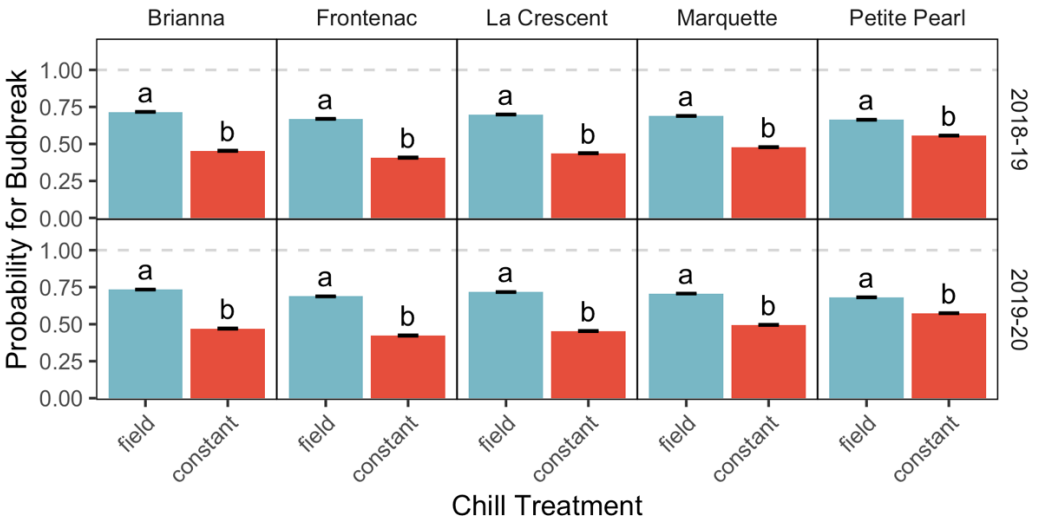

Figure 3. Budbreak probability calculated by estimated marginal means analysis for five hybrid grapevine cultivars in two chill treatments and in two years. Budbreak probability is represented by colored bars for both chill treatments including field-based chill (field; blue) and experimental chill at constant 5°C (constant; red). Lowercase letters within a panel designate statistical difference using 95% confidence interval and Tukey HSD with significance level α=0.05.

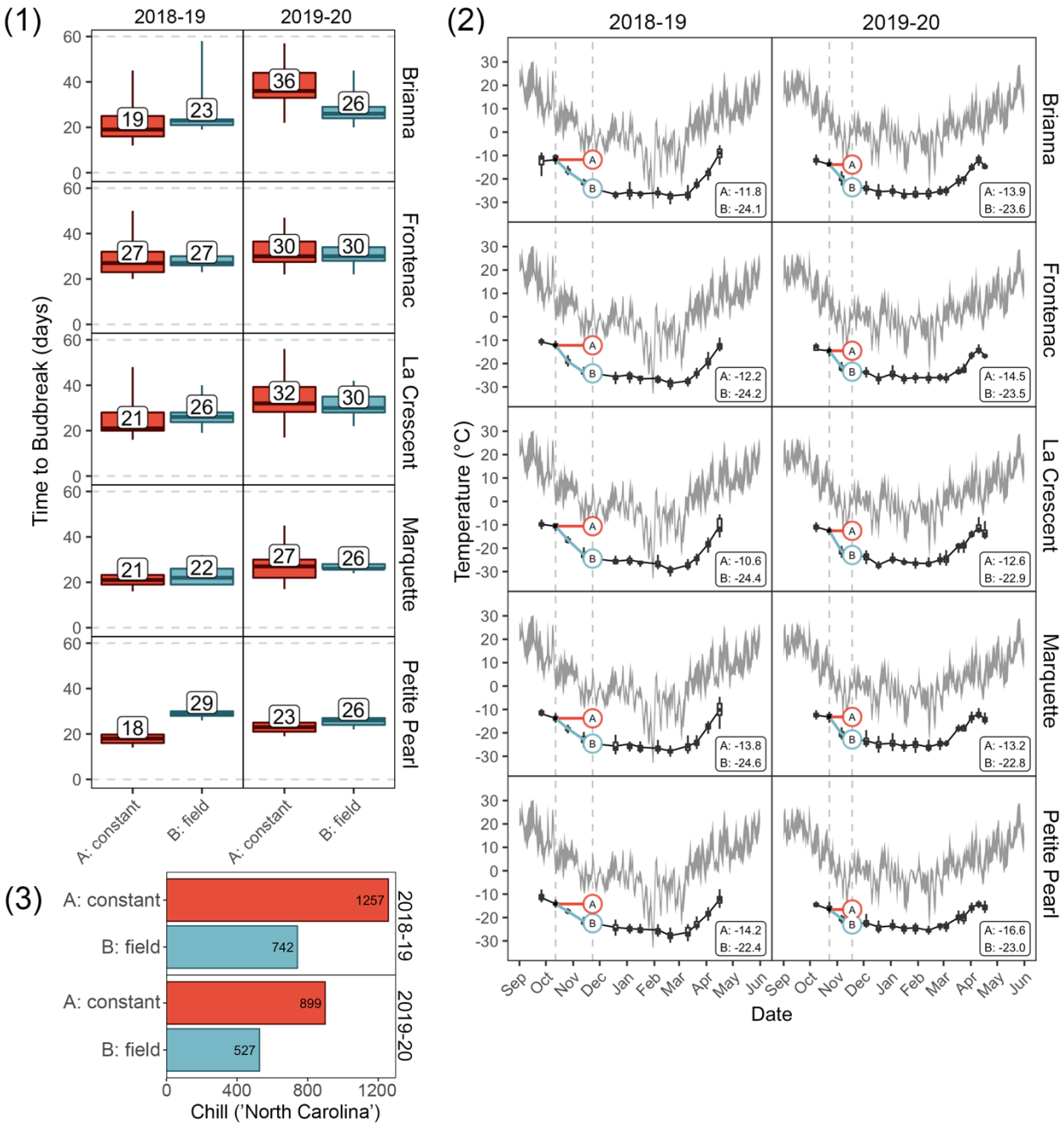

Figure 4. See caption on the following page.

Figure 4. Contrasting **(1)** time to budbreak, **(2)** cold hardiness evaluation, and **(3)** chill unit accumulation for five hybrid grapevine cultivars in two chill treatments during two years. Chill treatments include field-based chill (field; blue), experimental chill at constant 5°C (constant; red). **(1)** Median time to budbreak is labeled in each panel. Box-and-whisker illustrates 25% and 75% quantiles (bottom and top of boxes) as well as minimum and maximum observations (whiskers). **(2)** Cold hardiness at points A (constant) and B (field) are labeled in the lower right corner of each panel. Seasonal cold hardiness changes are represented by black lines and box-and-whiskers. Daily maximum and minimum temperatures are represented by the grey ribbon. Vertical dashed, grey lines indicate the date experimental chill started (left) and date of contrasting data (right). **(3)** Cumulative chill on the date of contrasting data in 'North Carolina' chill-units for each year.

Chapter 5: General conclusions

Cold hardiness and dormancy adaptations are among the most important traits that define plant geographical distribution and prevent freeze injury-related economic losses in cultivated crops. Cold hardiness and dormancy in woody plants, such as grapevine, are complex and dynamic processes. Descriptions of the mechanisms by which plants develop cold hardiness and the factors regulating cold hardiness changes are necessary to understand the freeze injury risks that grapevines face, especially in cold-climate growing regions. Furthermore, characterization of dormancy transitions can improve our understanding of the factors regulating dormancy and concomitant development. Despite the importance of these processes, we have a fairly basic understanding of cold hardiness, dormancy, and to what extent they are interdependent. This dissertation explored cold hardiness and dormancy in five cold-climate hybrid grapevine cultivars as described in the following studies.

In our first study, we used seasonal cold hardiness data in multiple years to characterize cold hardiness patterns with an explanatory model and predicted daily cold hardiness changes with a predictive model. We determined temperature is an important factor that regulates hybrid grapevine cold hardiness changes, and it seems cultivars respond to temperature signals at varying degrees. We calculated highly accurate cold hardiness predictions after we reparametrized a prediction model for each cold-climate hybrid grapevine cultivar. Future research could further optimize and test the prediction model for cold-climate hybrid cultivars and new or other important hybrid cultivars through continued collection of longitudinal cold hardiness datasets. Compared to the studies that originally developed the predictive model, ecodormant temperature threshold ($T_{eco,th}$), needed additional, lower levels to improve prediction accuracy for hybrids during spring deacclimation. Deacclimation at low temperatures in

preparation for budbreak could be an important ecological trait for cold-climate hybrids to maximize their use of shorter growing seasons. However, it simultaneously increases the risk of freeze injury and crop loss during spring. During this study, we also observed a unique cold hardiness response to extreme winter weather conditions during the polar vortex in January 2019. The response presumably leveraged mechanisms related to both deep supercooling and freeze dehydration, which allowed hybrids to achieve a deeper level of freeze injury resistance than previously evaluated. Future research that explores the physiological mechanism underlying the interplay between deep supercooling and freeze dehydration could provide critical information regarding deep supercooling species survival in extreme winter conditions.

In our deacclimation study, we described the effects of two factors, chill unit accumulation and temperature, on deacclimation responses. Deacclimation responses increased continuously as chill units accumulated rather than categorically based on dormancy status. This continuum of deacclimation responses was quantified as a rate ratio, referred to as deacclimation potential (Ψ_{deacc}). Deacclimation potential quantifies a bud growth phenotype that proceeds externally visible bud growth, which is the observation that is necessary in bud forcing assays. Future studies aiming to describe dormancy transitions and chilling requirements should include assessment of deacclimation potential in their experimental designs because it provides an advantageous alternative to bud forcing assays for quantifying dormancy transitions. Furthermore, deacclimation potential characterizes a chill range where bud growth responses continuously increase until they reach their maximum potential. This introduces an opportunity to identify the most effective temperatures that contribute to dormancy transition and thereby improve chill models. Deacclimation rates also increased along a logistic trend as temperatures increase, referred to as the relative thermal contribution (H_{deacc}). Relative thermal contribution

demonstrates that temperature, as a variable in predictive models, needs to be integrated in total units rather than units of change (ΔT). Furthermore, deacclimation occurred at low temperatures (as low as 0 °C), which has not been reported for grapevine before. Future studies are necessary to evaluate the potential for deacclimation at low temperatures in other woody plants. This could inform adjustments to base temperatures in models predicting phenological development for plants that deacclimate at low temperatures. We also demonstrated that the effects of chill unit accumulation and ambient temperature can be combined in a predictive model that accurately describes changes in deacclimation responses across the dormant period. This deacclimation model can guide development of new cold hardiness prediction models or improvements to existing models.

In our dormancy study, we described bud endodormancy completion variability in different temperature profiles of three chill treatments. We demonstrated freezing temperatures are effectively contributing to endodormancy completion in cold-climate grapevine cultivars. Chill models will need adjustments that incorporate chill unit calculations at freezing temperatures in order to accurately estimate chill requirements and characterize endodormancy completion. We also aimed to define individual chill requirements for each cold-climate cultivar. However, cold hardiness evaluation (and consideration of deacclimation potential) provided underlying contextual evidence that contradicted standard interpretation of dormancy assessed by bud forcing assays. That is, while budbreak occurred after a similar number of forcing days and within the endodormancy threshold for buds exposed to different chill treatments, cold hardiness levels differed by approximately two times. Consequently, the interpretation of endodormancy completion is not aligned between bud forcing assays and deacclimation potential. Estimated chill requirements reported in this study do not represent an absolute chill requirement that is

transferrable across regions or from year-to-year but rather represent a combination of traits involved in both dormancy status and deacclimation capacity. Future research aiming to characterize endodormancy completion should complement bud forcing assays with cold hardiness evaluation to guide dormancy status interpretations.

The research presented in this dissertation provides insights into two aspects of cold-climate hybrid grapevine winter survival, cold hardiness and dormancy, as well as the role temperature plays in regulating both. We have shown it is possible to adapt an existing cold hardiness prediction model for new cultivars and for cold-climate growing regions. We have also verified a quantitative phenotype for both endodormancy completion and cold hardiness loss. This provided context to demonstrate chill requirements estimated by bud forcing assays may be inaccurate. Collectively, the studies in this thesis provide framework for future research aiming to model seasonal cold hardiness changes, spring phenology, or grapevine winter responses to a changing climate.

Appendix A: Supplemental material – Chapter 3

Table 1. Linear regression statistics for models used to calculate deacclimation rates. Linear models were fit separately for each cultivar and year using chill unit accumulation and temperature as factors.

Cultivar	Chill[1]	T[2]	Intercept[3]		Slope[3]		Adjusted R^2	P-value
2018-19								
Frontenac	689	0	-20.7±0.7	***[4]	0.018±0.251	NS[4]	0.7936	< 0.001
	689	7	-20.2±0.7	***	-0.223±0.250	NS		
	689	14	-20.0±0.7	***	-0.032±0.260	NS		
	689	21	-20.3±0.7	***	0.331±0.254	.		
	776	0	-24.6±0.7	***	0.009±0.266	NS		
	776	7	-24.1±0.7	***	0.171±0.255	NS		
	776	14	-23.9±0.7	***	0.353±0.260	**		
	776	21	-24.2±0.7	***	0.722±0.251	***		
	972	0	-25.7±0.7	***	0.154±0.252	NS		
	972	7	-25.2±0.7	***	0.411±0.252	**		
	972	14	-25.0±0.7	***	0.679±0.255	***		
	972	21	-25.3±0.7	***	1.478±0.255	***		
	1023	0	-27.4±0.7	***	0.747±0.260	***		
	1023	7	-26.8±0.7	***	1.055±0.261	***		
	1023	14	-26.6±0.7	***	1.583±0.254	***		
	1023	21	-27.0±0.7	***	2.212±0.263	***		
	1357	0	-19.2±0.7	***	0.213±0.251	NS		
	1357	7	-18.7±0.7	***	0.812±0.250	***		
	1357	14	-18.5±0.7	***	1.338±0.251	***		
	1357	21	-18.9±0.7	***	1.289±0.249	***		
Marquette	689	0	-20.6±0.6	***	-0.023±0.231	NS	0.8748	< 0.001
	689	7	-20.5±0.6	***	0.006±0.222	NS		
	689	14	-20.6±0.6	***	0.059±0.226	NS		
	689	21	-20.4±0.6	***	1.432±0.222	***		
	776	0	-25.5±0.6	***	0.232±0.229	.		
	776	7	-25.4±0.6	***	0.639±0.226	***		
	776	14	-25.5±0.6	***	0.896±0.231	***		
	776	21	-25.3±0.6	***	1.362±0.227	***		
	972	0	-26.6±0.6	***	0.260±0.227	.		
	972	7	-26.4±0.6	***	0.576±0.222	***		

Marquette (continued)	972	14	-26.5±0.6	***	1.413±0.222	***	0.8748	< 0.001
	972	21	-26.3±0.6	***	1.975±0.223	***		
	1023	0	-27.2±0.6	***	0.423±0.228	***		
	1023	7	-27.1±0.6	***	0.465±0.227	***		
	1023	14	-27.2±0.6	***	1.589±0.232	***		
	1023	21	-26.9±0.6	***	2.197±0.234	***		
	1357	0	-17.5±0.6	***	0.125±0.224	NS		
	1357	7	-17.3±0.6	***	0.810±0.225	***		
	1357	14	-17.4±0.6	***	1.646±0.222	***		
	1357	21	-17.2±0.6	***	1.422±0.222	***		
Petite Pearl	689	0	-19.0±0.6	***	-0.184±0.211	NS	0.8489	< 0.001
	689	7	-19.6±0.6	***	0.448±0.219	***		
	689	14	-19.0±0.6	***	0.250±0.212	.		
	689	21	-19.1±0.6	***	0.613±0.217	***		
	776	0	-23.7±0.6	***	0.163±0.218	NS		
	776	7	-24.4±0.6	***	0.437±0.224	***		
	776	14	-23.8±0.6	***	0.460±0.222	***		
	776	21	-23.9±0.6	***	1.002±0.223	***		
	972	0	-25.3±0.6	***	0.383±0.217	***		
	972	7	-26.0±0.6	***	0.291±0.220	**		
	972	14	-25.4±0.6	***	0.836±0.221	***		
	972	21	-25.5±0.6	***	1.401±0.212	***		
	1023	0	-27.2±0.6	***	0.642±0.223	***		
	1023	7	-27.9±0.6	***	0.974±0.212	***		
	1023	14	-27.2±0.6	***	1.450±0.216	***		
	1023	21	-27.4±0.6	***	2.378±0.215	***		
	1357	0	-18.7±0.6	***	0.368±0.231	**		
	1357	7	-19.4±0.6	***	0.866±0.213	***		
	1357	14	-18.7±0.6	***	1.511±0.228	***		
	1357	21	-18.9±0.6	***	1.713±0.228	***		

Cultivar	Chill[1]	T[2]	Intercept[3]		Slope[3]		Adjusted R^2	P-value
2019-20								
Brianna	527	10	-23.5±0.6	***[4]	0.404±0.146	***[4]	0.9212	< 0.001
	527	15	-23.5±0.6	***	0.540±0.146	***		
	527	20	-23.5±0.6	***	0.545±0.151	***		
	527	25	-23.4±0.6	***	0.909±0.157	***		

Brianna (continued)	1057	10	-24.9±0.6	***	0.944±0.081	***	0.9212	< 0.001
	1057	15	-24.9±0.6	***	1.355±0.081	***		
	1057	20	-24.9±0.6	***	1.630±0.088	***		
	1057	25	-24.8±0.6	***	1.782±0.100	***		
	1289	10	-19.8±0.6	***	0.929±0.119	***		
	1289	15	-19.8±0.6	***	1.436±0.124	***		
	1289	20	-19.9±0.6	***	1.715±0.163	***		
	1289	25	-19.7±0.6	***	2.025±0.239	***		
Frontenac	527	10	-23.4±0.6	***	0.026±0.156	NS	0.9207	< 0.001
	527	15	-23.4±0.6	***	0.167±0.156	.		
	527	20	-23.4±0.6	***	0.303±0.156	***		
	527	25	-23.4±0.6	***	0.566±0.151	***		
	1057	10	-26.4±0.6	***	1.026±0.083	***		
	1057	15	-26.4±0.6	***	1.276±0.083	***		
	1057	20	-26.4±0.6	***	1.265±0.082	***		
	1057	25	-26.4±0.6	***	1.323±0.084	***		
	1289	10	-22.4±0.6	***	1.190±0.120	***		
	1289	15	-22.4±0.6	***	1.314±0.120	***		
	1289	20	-22.4±0.6	***	1.252±0.120	***		
	1289	25	-22.3±0.6	***	1.258±0.120	***		
La Crescent	527	10	-22.8±0.8	***	0.213±0.189	.	0.8888	< 0.001
	527	15	-22.8±0.8	***	0.366±0.189	***		
	527	20	-22.7±0.8	***	0.472±0.196	***		
	527	25	-22.8±0.8	***	0.748±0.189	***		
	1057	10	-24.8±0.8	***	1.143±0.106	***		
	1057	15	-24.7±0.8	***	1.464±0.106	***		
	1057	20	-24.7±0.8	***	1.624±0.125	***		
	1057	25	-24.8±0.8	***	1.688±0.121	***		
	1289	10	-19.0±0.8	***	1.250±0.152	***		
	1289	15	-18.9±0.8	***	1.451±0.157	***		
	1289	20	-18.9±0.8	***	1.345±0.170	***		
	1289	25	-19.0±0.8	***	1.372±0.163	***		
Marquette	527	10	-22.9±0.7	***	0.261±0.161	**	0.9151	< 0.001
	527	15	-22.9±0.7	***	0.380±0.161	***		
	527	20	-22.8±0.7	***	0.608±0.180	***		
	527	25	-22.7±0.7	***	0.778±0.166	***		
	1057	10	-24.4±0.7	***	1.186±0.087	***		
	1057	15	-24.3±0.7	***	1.296±0.087	***		

Marquette (continued)	1057	20	-24.3±0.7	***	1.504±0.087	***	0.9151	< 0.001
	1057	25	-24.2±0.7	***	1.545±0.096	***		
	1289	10	-18.2±0.7	***	1.042±0.123	***		
	1289	15	-18.1±0.7	***	1.160±0.128	***		
	1289	20	-18.1±0.7	***	1.304±0.143	***		
	1289	25	-18.0±0.7	***	1.219±0.143	***		
Petite Pearl	527	10	-22.8±0.7	***	0.331±0.183	***	0.8563	< 0.001
	527	15	-22.9±0.7	***	0.528±0.183	***		
	527	20	-22.9±0.7	***	0.711±0.183	***		
	527	25	-22.9±0.7	***	0.940±0.183	***		
	1057	10	-23.4±0.7	***	0.759±0.095	***		
	1057	15	-23.4±0.7	***	0.910±0.097	***		
	1057	20	-23.4±0.7	***	1.060±0.094	***		
	1057	25	-23.5±0.7	***	1.278±0.099	***		
	1289	10	-20.0±0.7	***	0.977±0.162	***		
	1289	15	-20.1±0.7	***	1.096±0.138	***		
	1289	20	-20.0±0.7	***	1.050±0.139	***		
	1289	25	-20.1±0.7	***	1.224±0.138	***		

[a] Chill accumulation calculated using the 'North Carolina' model (Shaltout and Unrath, 1983).
[b] T = temperature (°C) that buds were incubated at during deacclimation experiments.
[c] Intercept (°C) and slope (°C/day) and associated standard errors from linear models of deacclimation for each level of chill unit accumulation and temperature.
[d] Significance designations for estimates from linear models:
"NS" not significant
"." significant at α=0.05
"*" significant at α=0.01
"***" significant at α=0.001

Appendix B: Imaging callose at plasmodesmata in the apex of dormant bud meristems with confocal microscopy

Background

This project was based on a dormancy model proposed by Rinne and van der Schoot (2004) that defines cell-to-cell communication as a key factor in dormancy cycling. Specifically, they proposed that endodormancy can be depicted as the state of the meristem in which cell-to-cell communication via plasmodesmata is suspended by an innate mechanism. During the onset of endodormancy, 1,3-β-D-glucan (callose) is deposited, both as an external sphincter ring around plasmodesmal entrances and as an internal plasmodesmal plug. The simultaneous formation of a ring and a plug stabilizes the plasmodesmal neck region and could also develop a hermetic seal as the external sphincter-ring expands inwardly, thereby closing on the internal canal-plug.

We followed a protocol described by Zavaliev and Epel (2014) to stain and image callose at plasmodesmata. In comparison to callose associated with other tissues (Furch et al. 2007, Zhou et al. 2012), the levels of callose at plasmodesmata are significantly low. Therefore, callose detection and quantification at plasmodesmata require higher resolution fluorescent images. Consequently, these images also contain high background signal and often include nonspecific fluorescence, which are major obstacles in subsequent image analysis. The protocol described by Zavaliev and Epel (2014) also includes a procedure for image analysis. However, this project focused on steps for sectioning, staining, and imaging.

Materials and Methods

Dormant buds were collected from Frontenac vines following the same methods described in Chapters 2-4. Buds were collected for ultramicrotome sectioning in October, December, and April and for hand sectioning in November, December, and March.

Ultramicrotome section preparation and staining; fixed sections. The outermost bud scales were removed before buds were excised into vials containing fixation solution on ice. Two fixation solutions were used, including (1) 4% (v/v) glutaraldehyde (Sigma-Aldrich) in 0.1 M KPO_4 buffer (pH 7.2) and (2) 3% (v/v) paraformaldehyde (Sigma-Aldrich) with 2% (v/v) glutaraldehyde in 0.1 M KPO_4 buffer (pH 7.2). While samples were on ice with vials loosely capped, a vacuum was applied three times for ~5 minutes each time and slowly releasing pressure between. A vacuum was applied one more time for ~15 minutes and samples were stored overnight under vacuum pressure at 4 °C. The following day, samples were rinsed with 0.05 KPO_4 buffer (pH 7.2). Samples were then dehydrated in a series of solutions with increasing ethanol concentration, allowing 24 hours for each ethanol solution. Following dehydration, samples were infiltrated gradually with medium-grade LR White (Ted Pella Inc.), also allowing 24 hours for each increased concentration of LR White. The LR White was polymerized by heating samples to 60 °C for 28 hours. Samples were mounted on stubs for longitudinal sectioning (2 µm sections) on a Sorvall MT-2 ultramicrotome (Ivan Sorvall). Sections were annealed to Fisher Probe-On-Plus slides (Fisher Scientific) and stained with 0.0025% (w/v) aniline blue fluorochrome (Biosupplies) in double distilled water for ~1 hour. Slides and sections were rinsed with double distilled water and mounted with Citifluor AF1 (EMS). Some sections were reserved for staining with 0.05% (w/v) Toluidine Blue O (Sigma Aldrich).

Hand section preparation and staining; fresh sections. Stem tissue at the base of the bud was pruned away at an angle in order to section longitudinally by cutting from the proximal end towards the distal end of the bud. Cutting in this direction seemed to help prevent crushing the bud tissue as sections were cut. Buds were cut using a double-sided razor blade while submerged in 10 mM 2-deoxy-D-glucose (2-DDG; Fisher Scientific) to limit wound induced callose production (Rinne et al. 2005, 2016). Subsequently, the sections were incubated for ~3 hours in 96% ethanol. Sections were then transferred to double distilled water with 0.01% (v/v) Tween-20. Sections were placed in a vacuum desiccator and a vacuum was applied twice for ~5 minutes each time, slowly releasing pressure afterwards. Sections were then incubated for ~1 hour on a slow shaker (~ 20 rpm). Lastly, sections were transferred to glass vials wrapped in aluminum foil containing 0.1 M K_2HPO_4 buffer (pH 12) with 0.01% (w/v) aniline blue and 5 mM 2-DDG. Some sections were kept in double distilled water for an unstained control. A vacuum was applied again, twice for ~5 minutes each time, slowly releasing pressure afterwards. Sections were then incubated for ~5 hours on a shaker (~80 rpm). Sections were mounted in double distilled water between two large-size cover glasses for just before imaging.

Imaging with confocal. Sections were imaged using a Zeiss LSM 710 confocal microscope with 40× water immersion objective. A 405 nm diode laser was used for excitation with 475-525 nm band-pass emission filter. The scanning parameters were set to 1,024 × 1,024, 12-bit pixel depth, line sequential scanning, scan average 4, and 1× zoom. The laser intensity, detector gain, detector off-set, and detector digital gain were configured first using unstained sections. Settings were adjusted until the image was dark. These same settings were then used with stained sections.

Summary

Dormant buds were successfully fixed and sectioned with the ultramicrotome (Figure 1). However, there were high amounts of autofluorescence in the fixed sections (Figure 2). There may have also been limited stain penetration on fixed sections. Future work using fixed sections could explore other stains, other staining procedures to improve stain penetration, narrower band-pass emission filters to minimize autofluorescence, and/or linear unmixing to separate autofluorescence. Callose at plasmodesmata was visible in fresh sections (Figure 3). Since the sections were not completely flat, z-stack imaging was needed to capture portions of a larger area in focus. This could complicate automation of subsequent image analysis. There were varying patterns of callose at plasmodesmata for buds sampled in March as compared to buds sampled in November and December. Differences between spring and winter samples were not explored in detail because this project was interrupted by COVID-19 restrictions. Future work using fresh sections will need to standardize the procedure for imaging z-stacks and adapt the image analysis protocol described by Zavaliev and Epel (2014) for use with z-stacks.

Literature Cited

Furch ACU, Hafke JB, Schulz A, Van Bel AJE. 2007. Ca2+-mediated remote control of reversible sieve tube occlusion in Vicia faba. J Exp Bot 58:2827–2838.

Rinne PLH, van der Schoot C. 2004. Cell-cell communication as a key factor in dormancy cycling. J Crop Improv 10:113–156.

Rinne PLH, Boogaard R Van Den, Mensink MGJ, Kopperud C, Kormelink R, Goldbach R, Schoot C Van Der. 2005. Tobacco plants respond to the constitutive expression of the tospovirus movement protein NSM with a heat-reversible sealing of plasmodesmata that impairs development. Plant J 43:688–707.

Rinne PLH, Paul LK, Vahala J, Kangasjärvi J, Van Der Schoot C. 2016. Axillary buds are dwarfed shoots that tightly regulate GA pathway and GA-inducible 1,3-β-glucanase genes during branching in hybrid aspen. J Exp Bot 67:5975–5991.

Zavaliev R, Epel BL. 2014. Imaging Callose at Plasmodesmata Using Aniline Blue: Quantitative Confocal Microscopy. Plasmodesmata Methods Protoc:105–119.

Zhou J, Spallek T, Faulkner C, Robatzek S. 2012. CalloseMeasurer: A novel software solution to measure callose deposition and recognise spreading callose patterns. Plant Methods 8.

Figures

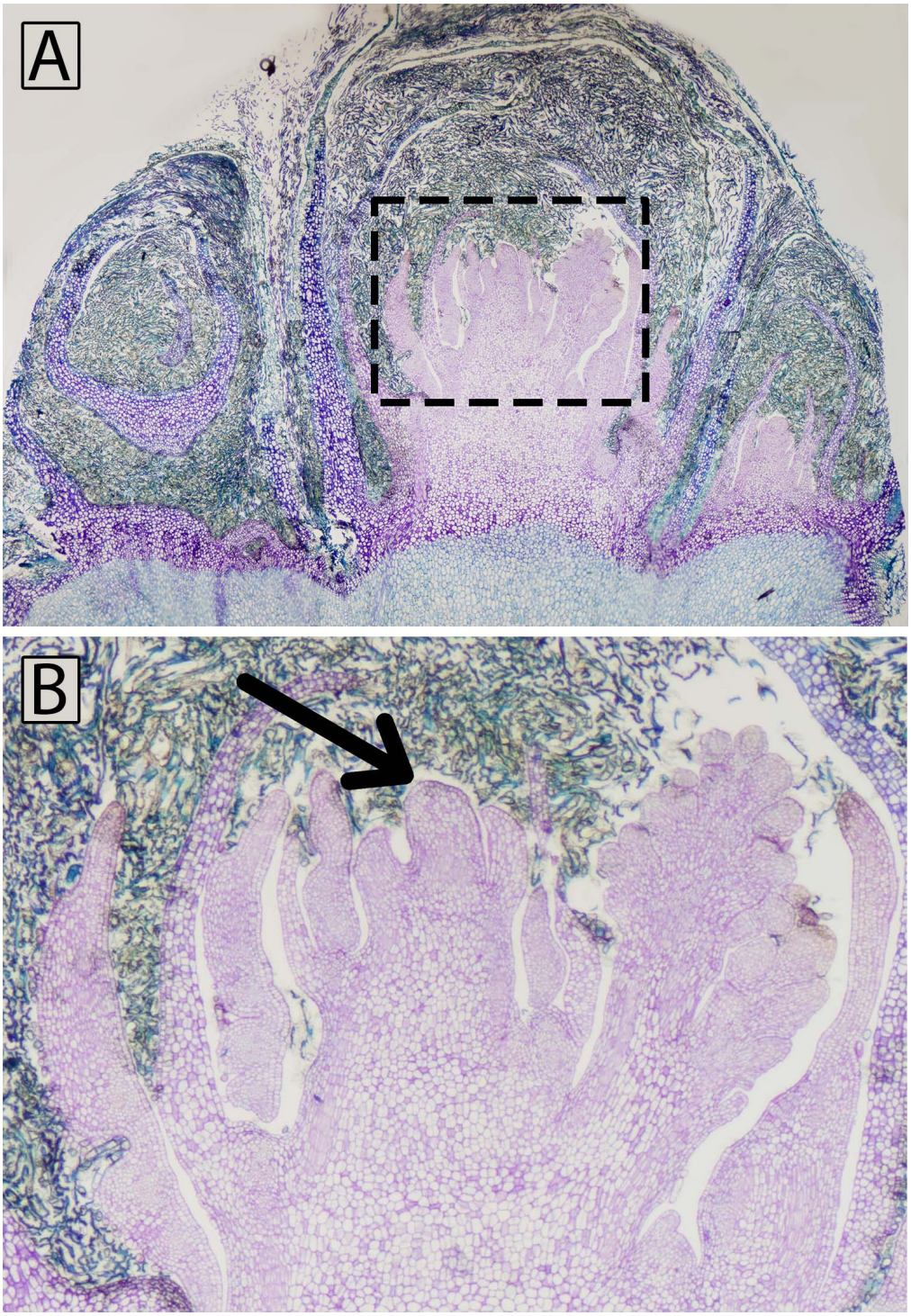

Figure 1. Fixed, longitudinal sections stained with Toluidine Blue O and imaged with a bright-field Olympus BX50 microscope (Olympus Optical Company). Morphology of entire grapevine bud (**A**). Close-up of primary meristem outlined with by the dashed rectangle (**B**). Arrow identifies the region imaged with confocal microscopy.

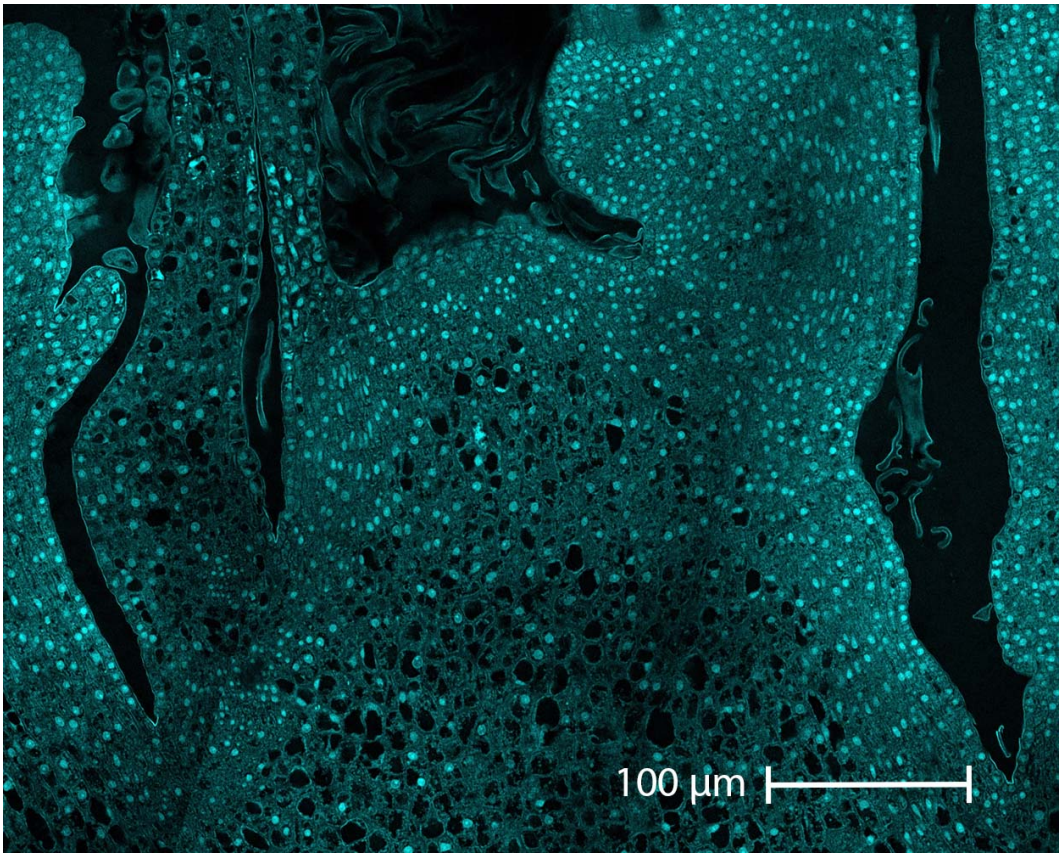

Figure 2. Autofluorescence of a fixed section imaged with confocal microscopy.

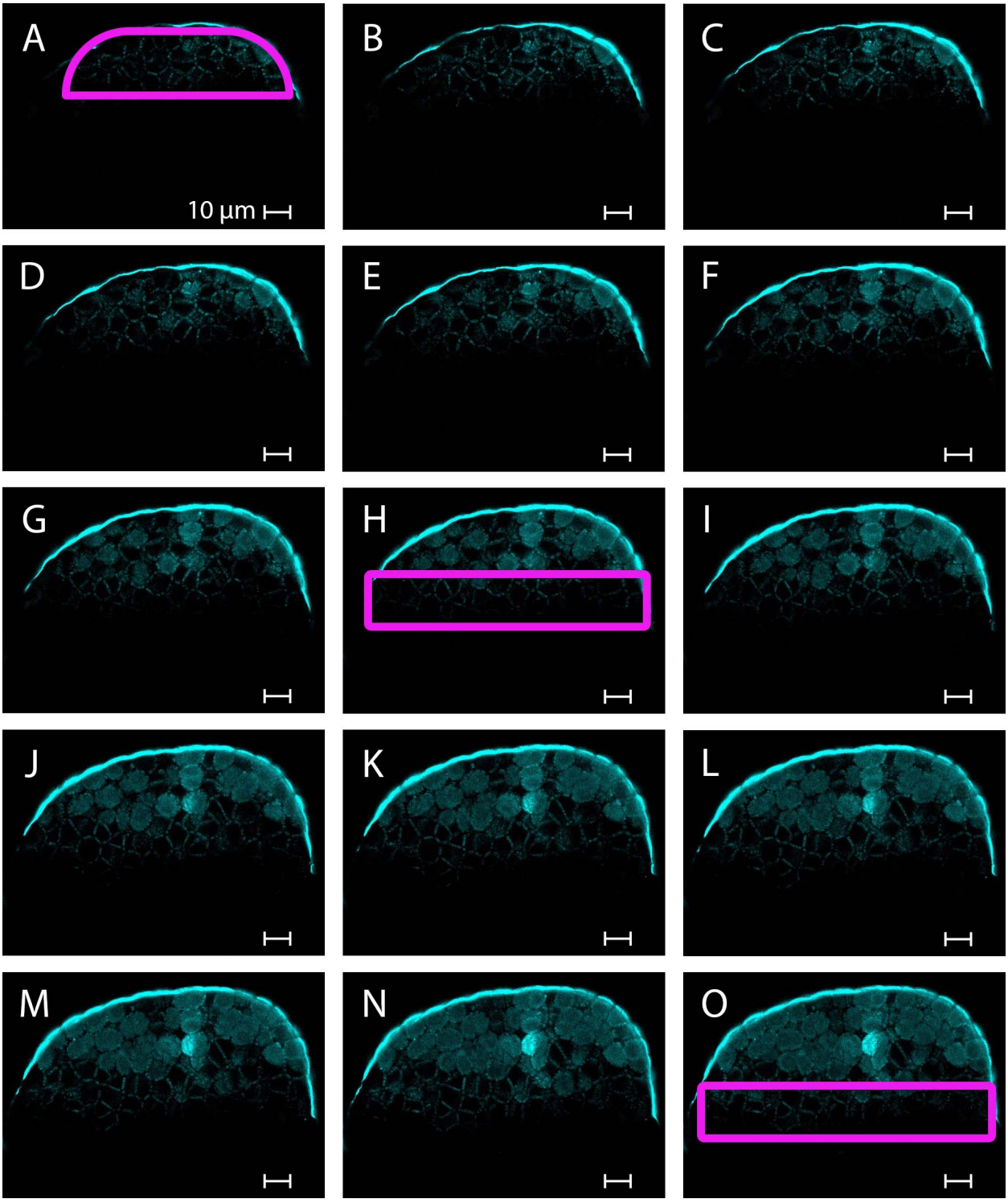

Figure 3. Fresh section stained with aniline blue and imaged with confocal microscopy as a z-stack. Section was cut from a bud sampled in December. The area where callose at plasmodesmata is in focus shifts since the section is not completely flat. Some example areas in focus are outlined in pink (**A**, **H**, **O**).